

Arbitrary Boundary Conditions and Constraints in Quantum Algorithms for Differential Equations via Penalty Projections

Philipp Schleich,^{1,2,*} Tyler Kharazi,^{3,4} Xiangyu Li,⁵ Jin-Peng Liu,^{6,7}
 Alán Aspuru-Guzik,^{1,2,8,9,10,11,12,13,14} and Nathan Wiebe^{1,5,15,†}

¹*Department of Computer Science, University of Toronto, Canada.*

²*Vector Institute for Artificial Intelligence, Toronto, Canada.*

³*Department of Chemistry, University of California, Berkeley*

⁴*Berkeley Quantum Information and Computation Center, University of California, Berkeley*

⁵*Pacific Northwest National Laboratory, Richland, USA*

⁶*Yau Mathematical Sciences Center and Department of Mathematics, Tsinghua University, Beijing, China*

⁷*Yanqi Lake Beijing Institute of Mathematical Sciences and Applications, Beijing, China*

⁸*Department of Chemistry, University of Toronto, Canada*

⁹*Canadian Institute for Advanced Research, Toronto, Canada.*

¹⁰*Acceleration Consortium, Toronto, Canada.*

¹¹*Department of Chemical Engineering & Applied Chemistry, University of Toronto, Toronto, Canada.*

¹²*Department of Materials Science & Engineering, University of Toronto, Toronto, Canada.*

¹³*Lebovic Fellow, Canadian Institute for Advanced Research, Toronto, Canada.*

¹⁴*NVIDIA, Toronto, Canada.*

¹⁵*Canadian Institute for Advanced Studies, Toronto, Canada*

(Dated: Monday 30th June, 2025)

Complicated boundary conditions are essential to accurately describe phenomena arising in nature and engineering. Recently, the investigation of a potential speedup through quantum algorithms in simulating the governing ordinary and partial differential equations of such phenomena has gained increasing attention. We design an efficient quantum algorithms for solving differential equations with arbitrary boundary conditions. Specifically, we propose an approach to enforce arbitrary boundary conditions and constraints through adding a penalty projection to the governing equations. Assuming a fast-forwardable representation of the projection to ensure an efficient interaction picture simulation, the cost of to enforce the constraints is at most $O(\log \lambda)$ in the strength of the penalty λ in the gate complexity; in the worst case, this goes as $O(\|v(0)\|^2 \|A_0\| + \|b\|_{L^1[0;t]}^2) t^2 / \varepsilon$, for precision ε and a dynamical system $\frac{d}{dt} v(t) = A_0(t)v(t) + b(t)$ with negative semidefinite $A_0(t)$ of size $n^d \times n^d$. E.g., for the heat equation, this leads to a gate complexity overhead of $\tilde{O}(d \log n + \log t)$. We show constraint error bounds for the penalty approach and provide validating numerical experiments, and estimate the circuit complexity using the Linear Combination of Hamiltonian Simulation.

CONTENTS

I. Introduction	3
A. Notation	4
B. Problem Setting	5

* philipps@cs.toronto.edu

† nawiebe@cs.toronto.edu

	2
II. Approximating Boundary Conditions with a Projection	8
A. Motivation	8
B. Approximation Guarantees	11
1. Constant dynamics	12
2. Time-dependent dynamics	16
C. Application to Discretized Partial Differential Equations	21
1. Non-zero Dirichlet boundaries	21
2. Neumann boundary conditions	23
D. Input Model of Constraint Projections for Quantum Implementation	24
1. Projections for Dirichlet conditions and value constraints	25
2. Projectors for Neumann conditions and derivative constraints	26
3. Input Model for Robin Boundary Conditions	31
E. Hamiltonian simulation of combined projections	32
III. Numerical Experiments	32
A. Setup	33
B. Simulation results	33
1. Heat equation with Dirichlet and Neumann boundary conditions	33
2. Wave equation with Dirichlet boundary conditions	34
3. Discussion	39
IV. Quantum Algorithm via Interaction-Picture simulation	40
A. Time Evolution by LCHS	41
1. Oracles	42
B. Complexity	43
1. Final Result	43
2. Analysis of smoothness factors	44
3. Implications for the solution of discretized PDEs with boundary conditions	48
V. Conclusion and Outlook	48
Code and Data Availability	49
Acknowledgements	49
References	50
A. Proof of Lemma 15	53
B. Derivatives for conjugated generators	53
C. Proof of Proposition 6	55

I. INTRODUCTION

Ordinary and partial differential equations (ODEs, PDEs) describe many processes and phenomena in science and engineering. The modelling of these phenomena typically involves describing interactions of the system studied with its environment through ‘boundaries’, which imposes constraints on the solution of these equations. Hence, for a meaningful numerical solution it is crucial to represent such constraints and boundary conditions. In addition, solving DEs on classical computers is cursed by dimensionality. Quantum algorithms for differential equations have been developed in order to mitigate exponential cost in the dimension. Such algorithms are based on, e.g., encoding the solution in a linear system [1–6], performing explicit ‘time-marching’ [7, 8], or making use of integral identities [9–14]. Recently, algorithms that map the ODE to a Lindblad evolution has been explored in [15], drawing from quantum algorithms that are able to simulate open quantum systems. Particular systems studied are mostly focused around popular models from classical differential equations courses such as the Poisson equation [16] or more general elliptic equations [6, 17], the advection equation [18] or the wave equation [19] and also the Maxwell equations [20] or nonlinear equations such as reaction diffusion equations [4, 21–23] or fluid dynamics [24–26]. Most studies so far focus on input models that assume a structured geometry with no (or, periodic) boundary conditions which limits applicability. Imposing the boundaries in the encoding of the generator of the dynamics is possible for several techniques [6, 22, 27, 28], based on other classical techniques such as complex absorbing potentials, perfect matched layers or Dirichlet-to-Neumann maps [29] or analytic continuation [30]. However, there are some practical limitations to this in the way it can affect the respective access model of the system matrix, e.g. the complexity of a circuit construction of a specific block-encoding. Additionally, it is not immediately obvious how to approach boundary conditions in the recently popular Linear Combination of Hamiltonian Simulations (LCHS) algorithm [11, 12], which is promising due to (near-)optimal scaling both in the number of state-preparation queries as well as the system matrix queries. Furthermore, [31] considers the implementation of complex absorbing potentials, where the main underlying dynamics are unitary. Beyond the specific concept of boundary conditions, we may be interested in more general constraints.

In this work, we implement boundary values or constraints on evolution equations by separating the dynamics into unconstrained and constrained dynamics using perturbation theory. Our method is also capable to model interface conditions, which was also explored in the context of quantum algorithms in [28], as well as Robin boundary conditions. Conceptually, shows connections to a wide range of existing approaches that relate to perturbation methods and penalty methods [32]. Primarily, there are ties to ‘complex absorbing potentials’ for quantum dynamics [33], as previously used in quantum algorithms for non-unitary dynamics [11, 34]. Another interesting study in the simulation of acoustic waves uses counter-acting waves to annihilate the solution [35] – imagine numerical noise-cancelling headphones. Specifically, our approach adds a projection scaled by $i\lambda$ to the generator of a dynamical system. A physical interpretation of this may be seen as measurement with (very fast) frequency λ on the domain of the projector, similar to the quantum Zeno effect. Thereby, our bounds also closely resemble respective bounds related to the Zeno effect, generalized adiabatic dynamics and the rotating-wave approximation [36, 37]. General results from perturbation theory suggest what we are looking for is a small signal-to-noise ratio [38]. For an ODE $\frac{d}{dt}v(t) = A_0v(t)$, this can be envisioned as the systems ‘energy’ divided by the strength of the perturbation, $\frac{|\langle v(0), A_0v(0) \rangle|}{\lambda}$; this gives us intuition about what necessary frequency in the perturbation to expect. Our bounds in Section II B confirm this intuition. Using interaction-picture simulation, which is possible if the projection is chosen to be fast-forwardable as will be the case as we demonstrate later, we can expect a modest overhead of $O(\log(\lambda))$ to solving differential equations (DEs) when adding constraints in this manner.

Within this work, we focus on ordinary differential equations under constraints. This is equivalent to readily discretized partial differential equations under boundary conditions. We further focus on evolution equations of the kind $\frac{d}{dt}v(t) = A(t)v(t) + b(t)$ and a “time” parameter $t \geq 0$ and will consider stationary boundary value problems in future work. Fig. 1 depicts the general approach: When evolving an ODE, the addition of the penalty projection allows us to produce a final state that satisfies a set of constraints, as represented by the projection onto an infeasible space, up to some accuracy ε .

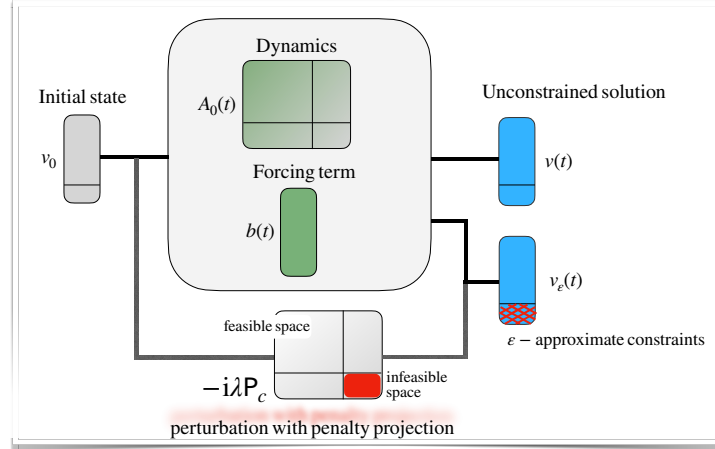


FIG. 1: Enforcing constraints in solution $v(t)$ to an ordinary differential equation defined by $A_0(t)$ and source term $b(t)$, by adding a penalty function defined by a projection operation P_c that projects onto the infeasible, constraint space. By appropriately choosing the penalty strength λ , this approach leads can enforce constraints that are efficiently representable by a projection up to arbitrarily small accuracy $\varepsilon > 0$.

A. Notation

Throughout this work we assume operators as finite-dimensional representations, typically as n^d -dimensional complex matrices, where n is the spatial grid number in each coordinate and d is the spatial dimension. Results reported pertaining to partial differential equations thus assume suitable numerical discretization. We often use bracket notation for inner products with a comma for non-normalized (non-quantum states) vectors, $\langle a, b \rangle \equiv a^\dagger b$. Whenever we do not specify the type of norm, we use the spectral or operator norm for matrices and $\|A\|$ and the ℓ_2 -norm for vectors $\|v\| = \|v\|_{\ell_2}$. Bold notation \mathbf{j} denotes multi-indices so that $\mathbf{j} \in \mathbb{N}^d$, or quantities after spatial discretization. When we say “stable” in this work in the context of a differential equation, we mean that for an ODE $\frac{d}{dt}v = Av$, $\text{Re}(A) \leq 0$, which is a sufficient condition for numerical stability. We use square-bracket notation for ordered sets of integers: $[n, m] = \{n, n+1, \dots, m\}$ for any $n < m \in \mathbb{Z}$. Most commonly, for $n > 0$, $[n] \equiv [1, n]$, $[n]_0 \equiv [0, n]$. With \mathbb{I} we denote the identity matrix; if dimensionality is not clear from context, \mathbb{I}_N acts on N qubits, i.e., on \mathbb{C}^{2^N} . Some operators/matrices are denoted by sans-serif font, e.g., P for projections. The relations $\approx, \gtrsim, \lesssim$ are used to denote the relations up to a constant or asymptotically similar/greater/smaller.

B. Problem Setting

Within this work, we consider the solution of ODEs given constraints, using a quantum algorithm. To motivate the setting, let A be an operator on continuously differentiable functions on some finite-dimensional vector space, let $v(t) : [0, T] \rightarrow \mathbb{C}^{n^d}$, and let $P : \mathbb{C}^{n^d} \rightarrow \mathbb{C}^{n^d}$ be a linear constraint function, so that $P(v_{\text{bad}}) = \lambda v_{\text{bad}}$ with some penalty $\lambda > 0$ if the constraint is not satisfied and $P(v_{\text{good}}) = 0$ if it is. Then, the kernel of P spanned by v_{good} makes up the constraint-admissible subspace a degenerate eigenspace of P with eigenvalue $\lambda > 0$ spanned by v_{bad} forms the constraint-inadmissible subspace. We seek a solution $v(t)$ to the constrained ODE such that $v(t)$ satisfies

$$\begin{aligned} \frac{d}{dt}v(t) &= A(v(t)) \\ P(v(t)) &= 0, \end{aligned} \tag{1}$$

which implies that we want $v_{\text{bad}}(t) = 0$. Our nomenclature follows penalty methods in constrained optimization [32]: A penalty function is a function that satisfies (i) P is continuous, (ii) $P(x) \geq 0$ for any valid input x , and (iii) $P(x) = 0$ if and only if x is in the feasible region, i.e., it satisfies the constraint. Then, an optimization problem via such a penalty function has as limit point the solution to the constrained optimization problem. Later on, we outline that the problem setup in Problem 7 indeed satisfies these requirements. Moreover, there is an equivalence between stationary solutions of a dynamical system and optimization. Quantum algorithms for this purpose exist, as in [39], and could be extended by the penalty projections in our work to satisfy constraints.

We are particularly interested in settings where the constraint arises from boundary conditions on spatially discretized PDEs. In this case, P can take the form of a projector being applied to either the solution or its derivative to enforce Dirichlet or Neumann boundary conditions respectively on a subset of grid points. Dirichlet boundary conditions are conditions that constrain the solution to follow specific values, whereas Neumann conditions constrain the derivative (within domains in 3D space, typically the surface normal derivative). Linear combination of Dirichlet and Neumann condition leads to what is typically called Robin boundary conditions.

Definition 1 (Computational domain). *We consider a problem over a n^d -dimensional finite space \mathbb{C}^{n^d} . This can be expressed in terms of basis elements $\{\mathbf{j}\}$ where each label $\mathbf{j} = (j_1, \dots, j_d) \in ([n-1]_0)^d$ is a d -dimensional tuple indexing a basis element; there are $n \in \mathbb{N}$ elements per dimension, such as representing each spatial dimension of the problem domain. The following definitions are used throughout the paper to describe the relevant subsets of the problem domain that appear in our work.*

1. We first define the index set \mathcal{I}_Ω making up the unconstrained space, or “inside the domain”, consisting of all basis elements

$$\mathcal{I}_\Omega = \{\mathbf{j} \in [n-1]_0^d \mid \mathbf{j} \text{ is unconstrained}\}.$$

This corresponds to points inside a domain, i.e. the set of all points where the constraint operation in Eq. (1) acts trivially on.

2. Further, there is the set with value constraints

$$\mathcal{I}_{\Gamma_D} = \{\mathbf{j} \in [n-1]_0^d \mid \mathbf{j} \text{ has a constraint on the value}\}$$

as the case for a Dirichlet boundary and the set spanning the derivate constraint

$$\mathcal{I}_{\Gamma_N} = \{\mathbf{j} \in [n-1]_0^d \mid \mathbf{j} \text{ has a derivative constraint}\}$$

such as on a Neumann boundary.

3. For every $\mathbf{j} \in \mathcal{I}_{\Gamma_N}$, we have the neighbour set

$$\zeta_{\mathbf{j}} = \{\mathbf{k} \in [n-1]_0 \mid \mathbf{k} \text{ neighbours } \mathbf{j} \text{ in a discretized directional derivative}\}.$$

By neighbouring we mean at most distance one per each coordinate $1 \leq l \leq d$.

For now, we do not pose additional constraints on neighbouring points but will do so when we discuss implementing derivative constraints.

4. We call the constrained set, or boundary set, $\mathcal{I}_{\Gamma} = \mathcal{I}_{\Gamma_D} \sqcup \mathcal{I}_{\Gamma_N}$,
5. We require mutual satisfiability of the constraints; formally, $\mathcal{I}_{\Gamma_D} \cap \mathcal{I}_{\Gamma_N} = \emptyset$, $\mathcal{I}_{\Omega} \cap \mathcal{I}_{\Gamma} = \emptyset$. This ensures orthogonality of all subspaces spanned by the basis vectors coming from the index sets.

Definition 2 (Linear space associated to computational domain). *Given bases indexed according to Definition 1, call the space associated to the index set \mathcal{I}_{Ω} feasible or unconstrained space*

$$S = \text{span}\{|\mathbf{j}\rangle \mid \mathbf{j} \in \mathcal{I}_{\Omega}\} \subseteq \mathbb{C}^{n^d}$$

and the constrained space associated to \mathcal{I}_{Γ} we call $S_c \subseteq \mathbb{C}^{n^d}$, which again is split into the two orthogonal subspaces S_c^D and S_c^N for \mathcal{I}_{Γ_D} and \mathcal{I}_{Γ_N} , respectively. The solutions we consider live in the space $\bar{S} = S \oplus S_c$.

We further define the following projections.

Definition 3 (Projection on constrained space). *Consider a feasible (unconstrained) space S and infeasible (constrained) spaces S_c , S_c^D , S_c^N as defined in Definition 1. Then, for $v \in \bar{S}$, we have the following projections,*

$$\mathbf{P}_c v = \begin{cases} v, & v \in S_c \\ 0, & v \in S \end{cases}, \quad (2)$$

$$\mathbf{P}_c^\perp = \mathbb{I} - \mathbf{P}_c, \quad (3)$$

so that \mathbf{P}_c projects onto the constrained space S_c and \mathbf{P}_c to its complement S . Here, \mathbb{I} is the identity on \bar{S} . We can further decompose $\mathbf{P}_c = \mathbf{P}_c^D + \mathbf{P}_c^N$ so that $(S_c^D)^\perp = S \oplus S_c^N = \ker(\mathbf{P}_c^D)$ and $(S_c^N)^\perp = S \oplus S_c^D = \ker(\mathbf{P}_c^N)$.

Definition 4 (ℓ_2 -norms over computational spaces). *Given the computational spaces from Definition 2 and projectors onto the spaces from Definition 3, we define the ℓ_2 -norms over the feasible and infeasible spaces. Let $a \in \bar{S}$, then*

$$\|a\|_{\ell_2, S_c} = \left(\sum_{\mathbf{j} \in \mathcal{I}_{\Gamma}} a_{\mathbf{j}}^2 \right)^{1/2} = \|\mathbf{P}_c a\|_{\ell_2} \quad (4)$$

This is equivalent to the notion of a \mathbf{P}_c -inner product so that

$$\langle a, \mathbf{P}_c a \rangle = \langle a, \mathbf{P}_c^2 a \rangle = \langle \mathbf{P}_c a, \mathbf{P}_c a \rangle = \|a\|_{\ell_2, S_c}^2. \quad (5)$$

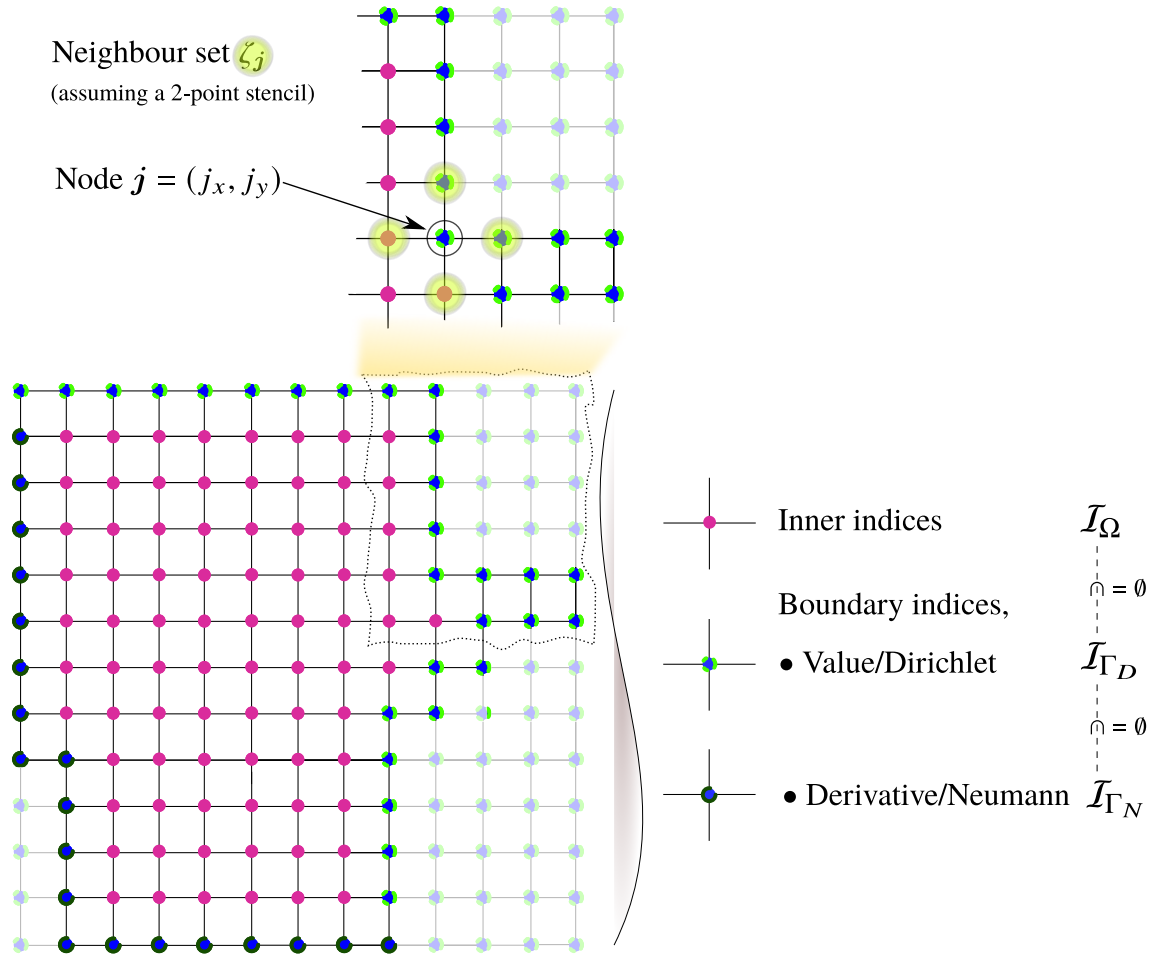


FIG. 2: Visualization of relevant index sets as a graph depicted as a uniform grid. Recall that “inner” points span the unconstrained space S . The boundary, i.e., the constrained space, is composed by $S_c = S_c^D \oplus S_c^N$.

$A \|\cdot\|_{\ell_2, S}$ -norm can be defined equivalently through a P_c^\perp -inner product.

Next, we define the problem setting we generally consider in this work.

Problem 5 (Constrained Discrete Initial Value Problem). *We consider a finite-dimensional initial value problem with solution vector $v(t) : \mathbb{R}_+ \rightarrow \bar{S}$ and a matrix $A : \bar{S} \rightarrow \bar{S}$ as dynamical generator. We seek*

approximate solutions to the constrained dynamics

$$\frac{d}{dt}v(t) = Av(t) + b(t), \quad t \geq 0 \quad (6)$$

$$\begin{aligned} \mathbf{P}_c^D v(t) &= g \quad \text{and } t \geq 0, \\ \mathbf{P}_c^N v(t) &= h \quad \text{and } t \geq 0, \\ v(0) &= v_0, \quad \mathbf{P}_c^D v_0 = v_0 \text{ and } \mathbf{P}_c^N v_0 = v_0. \end{aligned} \quad (7)$$

That means there is initial data $v(t=0)|_S = v_0$ on the feasible space S and satisfies the constraints on the constrained space S_c , i.e., $v(t=0)|_{S_c^D} = g$ and $v(t=0)|_{S_c^N} = h$.

Remark 1 (Projection matrices as constraint functions are penalty functions). Recall that, following [32], penalty functions need to satisfy (i) continuity, (ii) non-negativity and (iii) they evaluate to zero if and only if the preimage is element of the feasible region. Therefore the penalty projections in Problem 5 satisfy these requirements, as (i) they are matrices (bounded linear operators are continuous), (ii) projections have eigenvalues 0, 1 and (iii) by Definition 3.

Remark 2. For the derivative constraint in Eq. (7), \mathbf{P}_c^N already embodies the notion of a finite difference approximation of a derivative constraint. Given a proper construction of \mathbf{P}_c^D and \mathbf{P}_c^N , we can expect that the treatment of Dirichlet and Neumann conditions will be mostly equivalent. Later on, we will assume \mathbf{P}_c^D and \mathbf{P}_c^D commute and are orthogonal projections for efficient simulation. One way to ensure is by assuming that every point can only fall under one constraint, $\mathcal{I}_{\Gamma_D} \cap \mathcal{I}_{\Gamma_N} = \emptyset$. Then, the (nontrivial) domains of the corresponding projections commute by construction as they do not overlap.

II. APPROXIMATING BOUNDARY CONDITIONS WITH A PROJECTION

$$\begin{aligned} & \begin{matrix} A_0 & & -i\lambda P_c & & A \end{matrix} \\ & \left[\begin{array}{cc} \mathbf{P}_c^\perp A_0 \mathbf{P}_c^\perp & \mathbf{P}_c^\perp A_0 \mathbf{P}_c \\ \mathbf{P}_c A_0 \mathbf{P}_c^\perp & \mathbf{P}_c A_0 \mathbf{P}_c \end{array} \right] + \left[\begin{array}{cc} & \\ & -i\lambda \mathbf{P}_c \end{array} \right] = \left[\begin{array}{cc} \text{grid with pink dots} & \text{grid with pink and blue dots} \\ \text{bullet points:} & \text{bullet points:} \end{array} \right] \\ & \text{bullet points:} \quad \begin{aligned} & \bullet \text{ leave } \mathbf{P}_c^\perp \text{ invariant} \\ & \bullet \text{ suppress on } \mathbf{P}_c \\ & \bullet \text{ suppress "boundary interaction"} \\ & \text{(nonzero constraint values: shift solution)} \end{aligned} \end{aligned}$$

FIG. 3: Inducing a constraint subspace via a penalty projection $-i\lambda P_c$ with $\lambda > 0$ and P_c the projection onto the constraint subspace. Then, dynamical evolution of $A = A_0 - i\lambda P_c$ leaves the \mathbf{P}_c^\perp -subspace invariant (pink vertices as in Fig. 2) and suppresses the solution on P_c (blue vertices).

A. Motivation

Now, we discuss a method to efficiently implement the solution of such boundary problems on a quantum computer. To that end, we take inspiration from the so-called complex absorbing potentials in quantum

physics and chemistry [33]. Note that for the case when Eq. (6) has $A = -iH$ anti-Hermitian and operator and a normalized initial state, the dynamics of $\psi(t, x)$ follows the Schrödinger equation, i.e.,

$$-i\frac{\partial}{\partial t}\psi(t, x) = H\psi(t, x). \quad (8)$$

Then, a modification of the Hamiltonian with $\lambda > 0$

$$H \rightarrow H - i\lambda P_c \quad (9)$$

leads to enforcing that $\psi(t, x') \rightarrow 0$ for all $x' \in \Gamma$ on the boundary in the limit of $\lambda \rightarrow \infty$ if $P_c = \int_{\Gamma} d|x'\rangle\langle x'|$. In particular, we want $\lambda \gg \|H\|$. This is easy to see, as then in the solution

$$\psi(t, x) = e^{-i(H - i\lambda P_c)t} \psi(0, x), \quad (10)$$

components of the solution $\psi(t, x)$ on Γ are suppressed to zero. The rest of $\psi(t, x)$ remains unchanged.

In what follows, we will show that the modification in Eq. (9) in the case for boundary conditions over more general, not necessarily quantum dynamics such as in Eq. (6) can work the same way. In a general setting, we consider the following modified dynamics governed by a (potentially time-dependent) system matrix $A_0(t)$ and a forcing term $b(t)$,

$$\frac{d}{dt}v(t) = (A_0(t) - i\lambda P_c)v(t) + b(t). \quad (11)$$

Compared to the case of complex absorbing potentials in Eq. (9), $A_0(t)$ need not be Hermitian. As we will be working with orthogonal projections P_c, P_c^\perp exclusively, this implies their Hermiticity; a more careful analysis could relax the assumptions to non-Hermitian penalty functions in future work. Additionally, a time-dependent constraint region can be thought of via a $P_c(t)$.

We make the following observation here. In the case of quantum dynamics, Eqs. (8) and (9), a perturbation of the form $i\lambda$ as in complex absorbing potentials “dissipates” the wavefunction on the boundaries. Our approach in Eq. (11) with positive λ does not add dissipation per se. Rather, we can understand this e.g. under the realm of the rotating-wave approximation, where the evolution under a Hamiltonian $H = H_0 + H_1$ shows a separation of time-scales with respect to dynamics generated by H_0 and H_1 , respectively. Then, one can say that the solution coming from the perturbative generator is negligible with respect to the initial dynamics in the sense that the on the unperturbed system’s time-scale, the highly oscillatory perturbation averages to zero. In other words, the solution on the infeasible region then is perceived negligible compared to the solution on the feasible region.

Our analysis follows perturbation theoretic arguments, which is reasonable given the perturbation strength λ is chosen to be much larger than the system $\|A_0\|$ and forcing $\|b(t)\|$. For the following arguments, we change the point-of-view to strong perturbation, in the sense that we consider the system dynamics generated by A_0 as a perturbation of the constraint projection $-iP_c$ with perturbation parameter $\frac{1}{\lambda}$. Then, a natural way to estimate the error is to consider ‘transition elements’ with respect to the projections P_c^\perp, P_c , as expectations $\langle v(t'), P v(t) \rangle$. For $t = t'$, the Kubo formula [40] gives a natural pathway to find an estimate. We are interested in a non-Hermitian formulation, which was developed in [41] and further discussed in [42]. Building on this, we provide a generalization that also covers time-dependent generators for the unperturbed dynamics, and a forcing term. This enables the remainder of our analysis enforce the constraints.

Before stating the result, we introduce some context and notation. We are looking at a dynamical system $\frac{d}{dt}v(t) = A(t)v(t) + b(t)$, where $A(t) = H(t) + \zeta V(t)$ so that $V(t)$ is a perturbation of the original dynamics $H(t)$ in the sense that $\zeta\|V(t')\| \ll \|H(t')\|$ at all times. For now, $A(t), H(t), V(t)$ are arbitrary complex,

square matrices and we take $1 \gg \zeta > 0$ and note that this can also be simply reformulated to cases of where the scaling term is time-dependent. The Kubo formula allows to estimate the difference between the expectation of an observable P with respect to a perturbed compared to an unperturbed solution vector – in our more general case, the quadratic form of a matrix. We will use the following quantities:

- Let $\bar{V}(t, t')$ be the cumulative perturbation in the interval $[t'; t]$ for $t' \leq t$, $\bar{V}(t, t') := \int_{t'}^t d\tau V(\tau)$.
- We denote by $T_t(\cdot)$ the time propagation of the argument (borrowing notation from dynamical semi-groups). In Proposition 6, this relates to the unperturbed dynamics, $T_t := \mathcal{T} \int_0^t ds \exp\left(\int_s^t ds' H(s')\right)$. Then, the solution to the inhomogeneous problem is given by $T_t(v(0)\delta(t) + b(t))$ with the Dirac-delta distribution $\delta(t)$.
- We use $\sigma(t', t)$ for the outer product of solutions at times t', t , i.e., $\sigma(t', t) := v(t')v(t)^\dagger$. This notion is similar to the density matrix of pure quantum states, however with non-normalized complex vectors $v(t)$.

Proposition 6 (A non-Hermitian, time-dependent, inhomogeneous Kubo formula). *Let $A(t) = H(t) + \zeta V(t)$ be a perturbed dynamical generator with $\zeta \|V(t')\| \ll \|H(t')\|$ for any $t \geq t' \geq 0$ and $A(t), H(t), V(t)$ complex matrices. Let $v(t)$ be the solution to $\frac{d}{dt}v(t) = A(t)v(t) + b(t)$ with initial data $v(0)$. Further, suppose we are interested in measuring the expectation value of a matrix P . Then, the effect due to perturbation $\zeta V(t)$ on the expectation of P up to first order in the strength of the perturbation*

$$\langle P(t) \rangle - \langle P \rangle_0 = \zeta \int_0^t dt' \frac{\text{tr} \left[\left\{ P, \bar{V}(t, t') \sigma(t', t) \right\}_\sim \right]}{\text{tr} [\sigma(t, t)]} + O(\zeta^2) \quad (12)$$

where $\langle P(t) \rangle$ is the perturbed expectation and $\langle P \rangle_0$ is the expectation due to the unperturbed dynamics generated by $H(t)$. Further, there is the modified anticommutator $\{X, Y\}_\sim = XY + Y^\dagger X$, a density augmented by the forcing term $b(t)$ through $\sigma(t', t) = T_{t'}(v(0)\delta(t') + b(t'))(T_t(v(0)\delta(t) + b(t)))^\dagger$ where $T_t(u) = \int_0^t ds \mathcal{T} \exp\left(\int_s^t dt' H(t')\right)u(s)$ and $\bar{V}(t, t') = \int_{t'}^t d\tau V(\tau)$.

Remark 3 (Original Kubo formula). *For completeness, we briefly restate the original Kubo formula, as derived in [40], with adapted notation. We are given Hermitian $H, V(t)$ as well as a Hermitian observable P , so the dynamics of a Schrödinger equation through the Hamiltonian H is perturbed by time-dependent $V(t)$. Then, with $P(t)$ the observable evolved in the Heisenberg picture,*

$$\langle P \rangle_t - \langle P \rangle_0 = -i \int_0^t ds \langle [P(t), V(s)] \rangle_0, \quad (13)$$

where $\langle \cdot \rangle_0$ denotes the expectation with respect to the unperturbed dynamics and $P(t)$ is the Heisenberg-evolved observable with respect to the perturbed dynamics.

We point out the following differences compared to Proposition 6. Non-Hermitian original dynamics lead to a necessary re-normalization (as observed in [41, 42]), as well as replacing the commutator by a (modified) anticommutator. Additionally, time-dependence of the original dynamics induce the time-cumulative perturbation \bar{V} and the definition of σ allows to add inhomogeneities to the solution.

The proof of Proposition 6 is given in Appendix C. In the next section, we obtain tighter bounds on the error for special cases – such as time-independent A_0 or $b(t) = 0$ – with less general technique than Proposition 6. Therefore, we are looking into specific bounds under different sets of assumptions.

B. Approximation Guarantees

In the upcoming section, we provide error bounds on the approximation of constraints such as given in Problem 5. We will structure this argumentation as follows. First, we consider the case of only one type of constraint, i.e., we do not split S_c into S_c^D and S_c^N using only the projective properties of P_c . This is sufficient, as we will show how to construct the projections so that the constraints on the different boundary strips will not affect each other, and $[P_c^D, P_c^N]$, aligning with our assumption in Definition 2 that $S_c^D \perp S_c^N$. Once we have derived guarantees for general constraints, we then proceed to connect this to the case of Dirichlet and Neumann boundary conditions in discretized PDEs in Section II C.

First, we consider the more general problem of

Problem 7 (Projection-Constrained Discrete Initial Value Problem). *Under the same assumptions as in Problem 5, we define*

$$\frac{d}{dt}v(t) = (A_0(t) - i\lambda P_c)v(t) + b(t), \quad t \geq 0, \quad (14)$$

where P_c is a Hermitian projection and $\lambda > 0$ is a penalty term that needs to be chosen. Then, given $\varepsilon > 0$, we seek λ such that

$$\|v(t)\|_{\ell_2, S_c} \leq \varepsilon, \quad (15)$$

where $v(t)$ is understood to satisfy a constraint with respect to a projection P_c if $P_c v(t) = 0$ (Definition 3).

To verify that Problem 7 using the modified dynamics shows the sought-after behaviour, we need to show the following:

1. The solution error within the feasible space S is small.
2. We can find λ so that the approximation error on the boundary quantified by Eq. (4) is small.

Let us start by showing that Item 1 holds true under the problem setup in Problem 7.

Lemma 8 (Error within the feasible space). *The solution $v(t)$ to Problem 7 within the feasible space S and the one to Problem 5 are equivalent.*

Proof. Let $u(t)$ follow the unconstrained dynamics $\frac{d}{dt}u = Au(t)$ and $v(t)$ the constrained dynamics, $\frac{d}{dt}v(t) = (A - i\lambda P_c)v(t)$ with the same initial conditions, $u(0) = v(0) = w$. Then, consider

$$\|u(t) - v(t)\|_{\ell_2, S}^2 = \|(e^{At} - e^{A - i\lambda P_c}t)w\|_{\ell_2, S}^2. \quad (16)$$

Now we use the definition of $\|\cdot\|_{\ell_2, S}$ from Definition 4 to see that P_c^\perp leaves the norm over this space invariant and

$$\|(e^{At} - e^{A - i\lambda P_c}t)w\|_{\ell_2, S}^2 \leq \|P_c^\perp e^{At} - P_c^\perp e^{A - i\lambda P_c}t\|_{\ell_2, S}^2 \|w\|_{\ell_2, S}^2. \quad (17)$$

We want to show that the difference between the time propagators in the $\|\cdot\|_{\ell_2, S}$ -norm vanishes. To that end, use a Taylor series expansion of the matrix exponential and use that P_c^\perp is a projection to see that

$$P_c^\perp e^{(A - i\lambda P_c)t} = P_c^\perp \left(\sum_{k \geq 0} \frac{((A - i\lambda P_c)t)^k}{k!} \right) = \sum_{k \geq 0} \frac{t^k}{k!} (P_c^\perp A - i\lambda P_c^\perp P_c)^k. \quad (18)$$

Observe that $P_c^\perp P_c = 0$ by definition, so $P_c^\perp e^{At} = P_c^\perp e^{A - i\lambda P_c} t$. This means Eq. (17) can be upper-bounded by zero and $\|u(t) - v(t)\|_{\ell_2, S} = 0$ for any $t \geq 0$. \square

Remark 4. For time-independent P_c , Lemma 8 holds equivalently for time-dependent $A(t)$ and constant P_c by expanding a time-ordered exponential in Eq. (18) with a Dyson series. Furthermore, this statement is independent of whether the initial condition satisfies the constraint exactly or $\exists 1 > \varsigma \geq 0, \|P_c w\|_{\ell_2} < \varsigma$ (implying that $\|P_c^\perp w\|_{\ell_2} \geq 1 - \varsigma$).

In what follows, we look at the approximation of different constraints in order to show Item 2. More specifically,

- A is stable, i.e., its real part is negative semi-definite: $\text{Re}(A) \leq 0$. Often, this is also denoted as A having non-positive logarithmic norm (discussion in [4]).
- Given final time $T > 0$, $\exists C_T > 0$, $\sup_{t \in [0; T]} \|\exp(At)\| \leq C_T$ (a similar assumption as Krovi [4] makes). This can be generally achieved by scaling λ by an additional factor of C_T .
- Time-dependent $A(t)$.

Generally, we assume that initial data satisfies the constraints. For the quantum implementation this can be ensured by the approach outlined in Eq. (154).

1. Constant dynamics

Lemma 9 (Error in the infeasible space under stable dynamics). *We consider a system as in Problem 5 with dynamics generated by $A = A_0 - i\lambda P_c$, the real part of A_0 is negative semi-definite, $\lambda > 0$ and P_c the projector on the infeasible space as defined in Definition 3. Further, we require that the initial data $v(0)$ satisfies $\|P_c v(0)\|_{\ell_2}^2 = 0$. Then, the solution error at time $t > 0$ in the infeasible space is bounded as follows,*

$$\|v(t)\|_{\ell_2, S_c}^2 \leq \varepsilon \quad (19)$$

for $\lambda \geq \frac{2v_{\max}^2 \|A_0\|}{\varepsilon}$.

Proof. We have ODE and solution as

$$\frac{d}{dt} v(t) = A v(t), \quad v(t) = \exp(At) v(0) \quad (20)$$

with initial condition $v(0)$. Moreover,

$$|\langle v(0), A v(0) \rangle| \leq |\langle v(0), A_0 v(0) \rangle| + \lambda |\langle v(0), P_c v(0) \rangle| \leq \|v(0)\|^2 \|A_0\|. \quad (21)$$

We thus define $E_0 = \|v(0)\|^2 \|A_0\|$. Using the assumptions that $\text{Re}(A) \leq 0$, we have that $\|v(0)\| = \max_{0 \leq t' \leq t} \|v(t')\| =: v_{\max}$, then, for all times $t > 0$,

$$\langle v(t), A v(t) \rangle = \langle v(0), \exp(At)^\dagger A \exp(At) v(0) \rangle = \langle v(0), \exp(At)^\dagger \exp(At) A v(0) \rangle, \quad (22)$$

and we want to argue that

$$\left| \langle v(0), \exp(At)^\dagger \exp(At) A v(0) \rangle \right| \leq E_0 \quad (23)$$

under the assumption that A_0 is stable, i.e., $\text{Re}(A_0) \leq 0$. First, notice that $|\langle v(0), \exp(At)^\dagger \exp(At) A v(0) \rangle| \leq \|\exp(At)^\dagger \exp(At)\| |\langle v(0), A v(0) \rangle|$. Then, $\|\exp(At)^\dagger\| \|\exp(At)\| \leq \exp(\|\text{Re}(A_0)\|t) \exp(\|\text{Re}(A_0)\|t) = \exp(2\|\text{Re}(A_0)\|t) \leq 1$. This shows the boundedness of the “initial energy” E_0 in the stable case.

Carrying on with

$$|\langle v(t), A_0 v(t) \rangle - i\lambda \langle v(t), P_c v(t) \rangle| \geq 0, \quad (24)$$

we can apply the reverse triangle inequality to obtain a bound on the other side

$$|\langle v(t), A_0 v(t) \rangle - i\lambda \langle v(t), P_c v(t) \rangle| \geq \|\langle v(t), A_0 v(t) \rangle\| - \lambda \|\langle v(t), P_c v(t) \rangle\| \quad (25)$$

$$\geq -|\langle v(t), A_0 v(t) \rangle| + \lambda \|\langle v(t), P_c v(t) \rangle\|. \quad (26)$$

Thus we can conclude, under the assumption of $\text{Re}(A_0) \leq 0$, that

$$|\langle v(t), P_c v(t) \rangle| \leq \frac{E_0 + |\langle v(t), A_0 v(t) \rangle|}{\lambda} \leq v_{\max}^2 \frac{2\|A_0\|}{\lambda}, \quad (27)$$

where we used that $P_c \geq 0$. Note that $\langle v(t), P_c v(t) \rangle$ corresponds to the 2-norm of $v(t)$ over the region S_c . This means that for stable DEs, we can choose λ so that the solution norm in the infeasible space is small. \square

Lemma 10 (Error in the infeasible space under dissipative and normal dynamics with an inhomogeneity). *We consider a system as in Problem 5 with dynamics generated by $A = A_0 - i\lambda P_c$, where the real parts of the eigenvalues of A_0 are non-positive, $\lambda > 0$ and P_c the projector on the infeasible space as defined in Definition 3. Here, we further consider an inhomogeneity $b(t') : [0, t] \rightarrow \mathbb{C}^{n_d}$ so that $\max_{0 \leq t' \leq t} \|b(t')\|_{\ell_2} \leq B$. We require the initial condition $v(0)$ and $b(t')$ to be adapted to the constraints at all times $0 \leq t' \leq t$, so that vanish under the action of P_c . Then, the solution error at time $t > 0$ in the infeasible space with Dirichlet condition $g = 0$ is bounded as follows,*

$$\|v(t)\|_{\ell_2, S_c}^2 \leq \varepsilon \quad (28)$$

for $\lambda \geq \frac{2\|A_0\|}{\varepsilon} (v_{\max}^2 + 2v_{\max}tB + t^2B^2)$ and where $v_{\max} \geq \max_{0 \leq t' \leq t} \|v(t')\| = \|v(0)\|$.

Proof. We have ODE and solution as

$$\frac{d}{dt}v(t) = Av(t) + b(t), \quad v(t) = \underbrace{e^{At}v(0)}_{v_h(t)} + \underbrace{\int_0^t ds e^{As}b(t-s)}_{v_p(t)} \quad (29)$$

with initial condition $v(0)$. This allows us to express a quantity $\langle v(t), Av(t) \rangle$ $t > 0$ as a sum of those expressed by the homogeneous and particular solution,

$$\langle v(t), Av(t) \rangle = \underbrace{\langle v_h(t), Av_h(t) \rangle}_{=: (i)} + \underbrace{\langle v_h(t), Av_p(t) \rangle + \langle v_p(t), Av_h(t) \rangle}_{=: (ii)} + \underbrace{\langle v_p(t), Av_p(t) \rangle}_{=: (iii)}. \quad (30)$$

The purely homogeneous term follows from Lemma 9. We briefly recall that, thanks to the negative-semidefiniteness of $\text{Re}(A_0)$,

$$|(i)| = |\langle v_h(t), Av_h(t) \rangle| \leq v_{\max}^2 \|A_0\|. \quad (31)$$

Now, we bound the second and third term for the case of time-dependent $b(t)$. Recall that the particular solution is

$$v_p(t) = \int_0^t ds e^{As} b(t-s).$$

By assumption, $\exists B > 0, \max_t \|b(t)\|_{\ell_2} \leq B$ which implies that $|\langle b(t), Ab(t) \rangle| \leq B^2 \|A\| \forall t > 0$. Next, we consider the third term that comes only from the particular solution,

$$\begin{aligned} |(iii)| &= |\langle v_p(t), Av_p(t) \rangle| = \left| \left\langle \int_0^t ds_1 e^{As_1} b(t-s_1), A \int_0^t ds_2 e^{As_2} b(t-s_2) \right\rangle \right| \\ &= \left| \int_0^t ds_1 \int_0^t ds_2 \langle b(t-s_1), e^{A^\dagger s_1} e^{As_1+A(s_2-s_1)} Ab(t-s_2) \rangle \right| \\ &\leq B^2 \|A_0\| \int_0^t ds_1 \int_0^t ds_2 \left\| e^{A^\dagger s_1} e^{As_1+A(s_2-s_1)} \right\| \\ &\leq B^2 \|A_0\| \int_0^t ds_1 \|e^{As_1}\|^2 \int_0^t ds_2 \|e^{A(s_2-s_1)}\| \end{aligned} \quad (32)$$

The appearance of only $\|A_0\|$ in the second-last inequality is due to $P_c b(s) = 0 \forall s$. We can start by bounding the norms of the exponentials through their maximum eigenvalues:

$$\|e^{As}\| = \|e^{\text{Re}(A)s}\| \leq e^{\hat{\mu}_R(A)s}, \quad (33)$$

with $\hat{\mu}_R(A) = \max_j \text{Re}(\mu_j(A))$; and we recall that $\hat{\mu}_R(A) \leq 0$. This can be used to bound both exponentials in Eq. (32) and obtain

$$|\langle v_p(t), Av_p(t) \rangle| \leq B^2 \|A_0\| \int_0^t ds_1 e^{2\hat{\mu}_R(A)s_1} \int_0^t ds_2 e^{\hat{\mu}_R(A)(s_2-s_1)}. \quad (34)$$

The solution to an integral of the form above for any non-zero L is

$$\int_0^t ds_1 e^{2Ls_1} \int_0^t ds_2 e^{L(s_2-s_1)} = \frac{(1-e^{Lt})^2}{L^2}. \quad (35)$$

Thus, we make a case distinction here regarding $\hat{\mu}_R(A) = 0$ or $\hat{\mu}_R(A) < 0$. If $\hat{\mu}_R(A) = 0$, the upper bound is $|\langle v_p(t), Av_p(t) \rangle| \leq B^2 \|A_0\|$. If $\hat{\mu}_R(A) < 0$, we choose $L = \hat{\mu}_R(A)$ in Eq. (35), and overall

$$|\langle v_p(t), Av_p(t) \rangle| \leq B^2 \|A_0\| \cdot \begin{cases} \frac{(1-e^{\hat{\mu}_R(A)t})^2}{(\hat{\mu}_R(A))^2}, & \hat{\mu}_R(A) < 0, \\ t^2, & \hat{\mu}_R(A) = 0. \end{cases} \quad (36)$$

For the second term, which depends both on the homogeneous and the particular solution, we obtain using

the same techniques as for the previous terms,

$$\begin{aligned}
|(ii)| &= |\langle v_h(t), Av_p(t) \rangle + \langle v_p(t), Av_h(t) \rangle| \\
&= \left| \int_0^t ds \left[\langle e^{At} v(0), A e^{As} b(t-s) \rangle + \langle e^{As} b(t-s), A e^{At} v(0) \rangle \right] \right| \\
&= \left| \int_0^t ds \left[\langle v(0), e^{A^\dagger t} e^{As} A_0 b(t-s) \rangle + \langle b(t-s), e^{A^\dagger s} e^{At} A_0 v(0) \rangle \right] \right| \\
&\leq \|A_0\| \int_0^t ds \left(|\langle e^{At} v(0), e^{As} b(t-s) \rangle| + |\langle e^{As} b(t-s), e^{At} v(0) \rangle| \right) \\
&\leq \|A_0\| e^{\hat{\mu}_R(A)t} \int_0^t ds \left(|\langle v(0), e^{As} b(t-s) \rangle| + |\langle e^{As} b(t-s), v(0) \rangle| \right) \\
&\leq \|A_0\| e^{\hat{\mu}_R(A)t} \int_0^t ds \left(2v_{\max} B e^{\hat{\mu}_R(A)s} \right) \\
&\leq 2v_{\max} B \|A_0\| \cdot \begin{cases} \frac{e^{\hat{\mu}_R(A)t} - 1}{\hat{\mu}_R(A)}, & \hat{\mu}_R(A) < 0 \\ t, & \hat{\mu}_R(A) = 0. \end{cases} \tag{37}
\end{aligned}$$

Now we proceed as in Lemma 9 where we applied the reverse triangle inequality in Eq. (26) to obtain a situation where we can express a bound on $|\langle v(t), P_c v(t) \rangle|$,

$$\lambda |\langle v(t), P_c v(t) \rangle| - |\langle v(t), A_0 v(t) \rangle| \leq |\langle v(t), Av(t) \rangle|. \tag{38}$$

Moreover, we can identify that the upper bound we obtained on the $|\langle v(t), Av(t) \rangle|$ holds equivalently for the terms without the constraint projection, $|\langle v(t), A_0 v(t) \rangle|$, which is easy to see as all the matrix norm dependencies in the bound on the former simplify to $\|A_0\|$ thanks to initial conditions and forcing terms satisfying the constraint and the constraint term being purely imaginary, thus $\hat{\mu}_R(A) = \hat{\mu}_R(A_0)$. Hence, we can assemble the final bound using Eqs. (31), (36) and (37) and get

$$|\langle v(t), P_c v(t) \rangle| \leq \frac{2\|A_0\|}{\lambda} \left(v_{\max}^2 + 2v_{\max} B \begin{cases} \frac{e^{\hat{\mu}_R(A)t} - 1}{\hat{\mu}_R(A)}, & \hat{\mu}_R(A) < 0 \\ t, & \hat{\mu}_R(A) = 0 \end{cases} + B^2 \begin{cases} \frac{(e^{\hat{\mu}_R(A)t} - 1)^2}{(\hat{\mu}_R(A))^2}, & \hat{\mu}_R(A) < 0 \\ t^2, & \hat{\mu}_R(A) = 0 \end{cases} \right) \tag{39}$$

We can simplify this by using the bound considering $\hat{\mu}_R(A) = 0$, as $\frac{e^{tL} - 1}{L}$ is monotonously increasing on $L \in (-\infty, 0)$ and $\lim_{L \nearrow 0} \frac{e^{tL} - 1}{L} = t$. \square

Furthermore, we study the case of A_0 that are not stable, i.e., the eigenvalues of A_0 are not all non-positive. Here, we consider two cases. Case (I), A_0 has positive eigenvalues but $A_0 v(0) v(0)^\dagger$ does not (as discussed in [12, Eq. (10)]). Then, the analysis follows equivalently to the other Lemmas presented.

For Case (II), we have the following Lemma.

Lemma 11 (Error in the infeasible space under non-stable dynamics). *Under the same assumptions as Lemma 9, however there is a $0 < \hat{\mu}_{R,0} < \infty$ as the maximum real part eigenvalue of A_0 , $\hat{\mu}_{R,0} = \max_j \text{Re}(\mu_j(A_0))$. Then, we have*

$$\|v(t)\|_{\ell_2, S_c}^2 \leq \epsilon \tag{40}$$

for $\lambda \geq v_{\max}^2 \|A_0\| \frac{1 + \exp(2\hat{\mu}_{R,0}t)}{\epsilon}$.

Proof. The proof follows the same structure as the one for Lemma 9. We can define an initial “energy” as in Eq. (21). Further on in Eq. (27), instead of bounding $\langle v(t), A_0 v(t) \rangle$ by the bound from Eq. (21), we use that

$$\left\| e^{A^\dagger t} e^{At} \right\| \leq e^{2\hat{\mu}_{R,0}t}. \quad (41)$$

Hence we conclude with

$$|\langle v(t), P_c v(t) \rangle| \leq \|A_0\| \frac{1 + e^{2\hat{\mu}_{R,0}t}}{\lambda}. \quad (42)$$

□

2. Time-dependent dynamics

Next, we look into enforcing constraints under time-dependent dynamics. These considerations are mostly based on the Kubo formula [40], which allows us to estimate the difference in an expectation value – such as the projection onto the infeasible domain as a notion of constraint error – under a perturbation. As mentioned previously, we consider a strong perturbation, so that $iP_c \rightarrow iP_c + \frac{1}{\lambda}A_0(t)$ with $\frac{\|A_0(t)\|}{\lambda} \ll 1$. We consider the homogeneous case with $b = 0$ in Lemma 12, where we can make use of existing results from Sticlet *et al.* [41], Geier and Hauke [42] and an inhomogeneous case, where we use the result in Proposition 6. We note that while our penalty projections are both constant in time and Hermitian, Proposition 6 is able to cover time-dependent and non-Hermitian projections as well.

Lemma 12 (Error in the infeasible space under stable dynamics with a time-dependent generator). *Here, we have the same assumptions as in Lemma 9, however with a time-dependent generator of the dynamics in the sense that $A(t) = A_0(t) - i\lambda P_c$. Furthermore, the solution to Problem 5 in case of a time-dependent generator is given by the time-ordered operator exponential using the time-ordering operator \mathcal{T} ,*

$$v(t) = \mathcal{T} e^{\int_0^t A(\tau) d\tau} v(0). \quad (43)$$

This leads to the following error bound in the infeasible space,

$$\|v(t)\|_{\ell_2, S_c}^2 \leq \varepsilon \quad (44)$$

for $\lambda \geq \frac{t v_{\max}^2}{\varepsilon} \max_{0 \leq t' \leq t} \|[P_c, A_0(t')]\|$, where $[P, Q] \sim \equiv PQ - Q^\dagger P$.

Proof. For the time-dependent case, we make use of Kubo’s formula. Kubo’s formula was first introduced for Hamiltonian dynamics as a linear response result given an expectation value of an operator P ,

$$\delta \langle P(\tau) \rangle = - \int_{\tau_0}^{\tau} d\tau' \langle [P(\tau), V(\tau')] \rangle_0 \quad (45)$$

for an a constant term $H_0 = H(0)$ and a time-dependent perturbation $V(t)$ so that the time-dependent generator is

$$iH(t) = i(H_0 + V(t)). \quad (46)$$

Expectations are defined with respect to the current state (referring to the time of the operator), $\langle \cdot \rangle_t \sim$

$\langle v(t), (\cdot)v(t) \rangle$ or the unperturbed expectation $\langle \cdot \rangle_0 \sim \langle (e^{-iP_c t} v(0)), (\cdot)(e^{-iP_c t} v(0)) \rangle$ and are normalized with respect to the unperturbed evolution $v^{(0)}(t) = e^{-iP_c t} v(0)$, so that

$$\langle P(t) \rangle \approx \langle P(t) \rangle_0 + \delta \langle P(t) \rangle. \quad (47)$$

Using a correction as in Eq. (45), this is an identity due to the fundamental theorem of calculus and not a first-order approximation. The dynamics we are interested in stem from

$$A(\tau) = -i\lambda P_c + A_0(\tau); \quad (48)$$

note that P_c takes the role of H_0 above in Eq. (46). We have a constant constraint projection and a time-dependent $A_0(t)$. There exist generalizations of Kubo's result for non-Hermitian systems [43] and including time-dependency [41]. Then, we need to express Eq. (45) more generally using a linear response function $\chi_{PQ}(t, t')$ for an operator P whose expectation we are interested in and a perturbation term Q ,

$$\delta \langle P(\tau) \rangle = -i \int_{\tau_0}^{\tau} d\tau' \chi_{PQ}(\tau, \tau'), \quad (49)$$

and neither the original generator nor the perturbation need to be Hermitian. Note that compared to [41], we do not separate the perturbation into constant operator and time-dependent forcing that can be pulled out of the response function. In our case, the constraint projection is Hermitian however, which will lead to a simplification of the general response function form [41, Eq. (4)] that resembles Eq. (45) up to a modified commutator $[P, Q]_{\sim} := PQ - Q^\dagger P$, and does not require constant re-normalization. Note that in [41], the generator corresponding to Eq. (48) is expressed as $-i\lambda P_c + iA_0(\tau)$, leading to the commutator expression. Hence, in our case and corresponding to what we will be seeing in Proposition 6, the commutator needs to be replaced with an anticommutator $\{P, Q\}_{\sim} := PQ + Q^\dagger P$. This results in $\chi_{PQ}(\tau, \tau') = -i \mathbf{1}_{[\tau \geq \tau']} \langle \{P(\tau), Q(\tau')\}_{\sim} \rangle_0$, or when the dynamics are defined without the imaginary unit in front of $A_0(t)$, then $\chi_{PQ}(\tau, \tau') = \mathbf{1}_{[\tau \geq \tau']} \langle \{P(\tau), Q(\tau')\}_{\sim} \rangle_0$ so that

$$\delta \langle P(\tau) \rangle = \int_{\tau_0}^{\tau} d\tau' \langle \{P(\tau), Q(\tau')\}_{\sim} \rangle_0 \quad (50)$$

Then, we rephrase the setup as strong perturbation with small $\zeta = \frac{1}{\lambda}$,

$$A(t) = -iP_c + \zeta A_0(t), \quad (51)$$

that we can treat with the Kubo formula. We look for

$$|\langle P(t) \rangle_t - \langle P(t) \rangle_0| = \left| \int_0^t d\tau \langle [P(t), \zeta A_0(\tau)]_{\sim} \rangle_0 \right|. \quad (52)$$

Now, recall that expectations are normalized with respect to unperturbed *unitary* evolution $e^{-iP_c \tau} v(0)$, so that

$$\langle P(\tau) \rangle_\tau = \frac{\langle v^{(0)}(\tau), P(\tau) v^{(0)}(\tau) \rangle}{\langle v^{(0)}(\tau), v^{(0)}(\tau) \rangle} = \frac{\langle e^{-iP_c \tau} v(0), P(\tau) e^{-iP_c \tau} v(0) \rangle}{\langle e^{-iP_c \tau} v(0), e^{-iP_c \tau} v(0) \rangle}. \quad (53)$$

This is less straightforward if the original dynamics are not unitary, as e.g. would be the case if P_c is *not*

orthogonal. We can use this to continue with Eq. (52),

$$\begin{aligned} |\langle P(t) \rangle_t - \langle P(t) \rangle_0| &= \text{Eq. (52)} \leq \zeta \int_0^t d\tau \left| \frac{\langle e^{-iP_c t} v(0), \{P(t), A_0(\tau)\}_{\sim} e^{-iP_c t} v(0) \rangle}{\langle e^{-iP_c t} v(0), e^{-iP_c t} v(0) \rangle} \right| \\ &\stackrel{\text{by Eq. (53)}}{\leq} \zeta \int_0^t d\tau \|\{P(t), A_0(\tau)\}_{\sim}\|. \end{aligned} \quad (54)$$

which satisfies the inequality,

$$|\langle P(t) \rangle_t - \langle P(t) \rangle_0| \leq \zeta t \max_{0 \leq t' \leq t} \|\{P(t), A_0(t')\}_{\sim}\|. \quad (55)$$

Next, we can use that the observable of choice is $P(t) = P_c$, which is constant over time. Furthermore, the initial conditions are adapted to the constraint and $\langle P_c \rangle_0 = 0$ consequently. The expectation $\langle P_c \rangle$ is normalized with respect unperturbed dynamics, thus

$$|\langle P_c(t) \rangle - \langle P_c \rangle_0| = \left| \frac{\langle v(t), P_c v(t) \rangle}{\langle v^{(0)}(t), v^{(0)}(t) \rangle} \right| \leq (\cdot) \Leftrightarrow |\langle v(t), P_c v(t) \rangle| \leq (\cdot) v_{\max}^2.$$

Remembering that $\zeta = \lambda^{-1}$, we can conclude that the final error is given by

$$|\langle v(t), P_c v(t) \rangle| \leq \frac{1}{\lambda} t v_{\max}^2 \max_{0 \leq t' \leq t} \|\{P_c, A_0(t')\}_{\sim}\|. \quad (56)$$

□

We point out that the framework of Kubo's formula would also allow us to look at time-dependent strengths of the projection, which may allow to make the overall choice more optimal, and also time-dependent forms of the constraint projection P_c . This is left up to future research.

Lemma 13 (Error in the infeasible space under stable dynamics with a time-dependent generator and inhomogeneity with a generalized non-Hermitian, inhomogeneous Kubo formula formula). *Under the same assumptions as in Lemma 12, however with a time-dependent generator of the dynamics $A(t) = A_0(t) - i\lambda P_c$ and a time-dependent inhomogeneous term $b(t)$ so that $\frac{d}{dt} v(t) = A(t)v(t) + b(t)$. We assume that for finite time $t \geq 0$, $-\infty < \text{Re}(A_0(t)) \leq 0$ as well as $\exists B > 0$, $\max_{0 \leq t' \leq t} \|b(t')\|_{\ell_2}$. The general solution to Problem 5 in this setup follows,*

$$v(t) = \mathcal{T} e^{\int_0^t ds A(s)} v(0) + \int_0^t ds \mathcal{T} e^{\int_s^t ds' A(s')} b(s). \quad (57)$$

This leads to an error in the infeasible space of at time $t \geq 0$

$$\|v(t)\|_{\ell_2, S_c}^2 \leq \varepsilon \quad (58)$$

for $\lambda \geq \frac{1}{\varepsilon} \left(v_{\max}^2 + v_{\max} B_{L^1} + B_{L^1}^2 \right) \frac{t^2}{2} \max_{0 \leq t' \leq t} \|\{P_c, A_0(t')\}_{\sim}\|$.

Proof. We can directly apply Proposition 6 in this setting. Recall that

$$\langle P(t) \rangle - \langle P \rangle_0 \approx \zeta \int_0^t dt' \frac{\text{tr} \left[\left\{ P, \bar{V}(t, t') \sigma(t', t) \right\} \right]}{\text{tr} [\sigma(t, t)]} \quad (59)$$

with $\{X, Y\}_\sim = XY + Y^\dagger X$, $\sigma(t', t) = T_{t'}(v(0)\delta(t') + b(t'))(T_t(v(0)\delta(t) + b(t)))^\dagger$ where $T_t(u) = \int_0^t ds \mathcal{T} \exp\left(\int_s^t dt' H(t')\right)u(s)$ and $\bar{V}(t, t') = \int_{t'}^t d\tau V(\tau)$. The expectation $\langle \cdot \rangle_0$ means expectation with respect to the solution of the unperturbed dynamics.

The quantity we are looking for is the unnormalized squared error, $|\langle v(t), P_c v(t) \rangle|$. Therefore, we bound

$$|\langle v(t), P_c v(t) \rangle| = \text{tr}[\sigma(t, t)] \cdot |\langle P(t) \rangle - \langle P \rangle_0|. \quad (60)$$

In our setting, we have that $H(t) = -iP_c$ and $\zeta V(t) = \frac{1}{\lambda} A_0(t)$. Then, $T_t(u) = \int_0^t ds e^{-iP_c(t-s)}u(s) = e^{-iP_c t} \left(\int_0^t ds e^{iP_c s} u(s) \right)$, which means that the unperturbed evolution is unitary and has a time-independent generator which simplifies the analysis. Furthermore, we also use P_c as the observable to measure the (ℓ_2, S_c) -error. As now, the unperturbed dynamics are unitary, $T_t^\dagger T_t = \mathbb{I}$, we get

$$\begin{aligned} \sigma(t', t) &= e^{-iP_c t'} \int_0^{t'} d\tau' \int_0^t d\tau e^{iP_c \tau'} (v(0) + b(\tau'))(v^\dagger(0) + b^\dagger(\tau)) e^{-iP_c \tau} e^{iP_c t} \\ &=: e^{-iP_c t'} \tilde{v}(t', t) e^{iP_c t}, \end{aligned} \quad (61)$$

and therefore we have that

$$\bar{V}(t, t') \sigma(t', t) = \int_{t'}^t ds A_0(s) e^{-iP_c t'} \tilde{v}(t', t) e^{iP_c t}. \quad (62)$$

Then, the anti-commutator $\{P_c, \bar{V}(t, t') v(t', t)\}_\sim$ becomes

$$\int_{t'}^t ds \left[P_c A_0(s) e^{-iP_c t'} \tilde{v}(t', t) e^{iP_c t} + e^{-iP_c t} \tilde{v}^\dagger(t', t) e^{iP_c t'} A_0^\dagger(s) P_c \right]. \quad (63)$$

Computing the trace of this expression, we get for the left term,

$$\int_{t'}^t ds \text{tr} \left[P_c A_0(s) e^{-iP_c t'} \tilde{v}(t', t) e^{iP_c t} \right] = \int_{t'}^t ds \int_0^t d\tau \int_0^{t'} d\tau' w^\dagger(\tau) e^{iP_c(t-\tau)} P_c A_0 e^{iP_c(\tau'-t')} w(\tau') \quad (64)$$

end for the right term

$$\int_{t'}^t ds \text{tr} \left[e^{-iP_c t} \tilde{v}^\dagger(t', t) e^{iP_c t'} A_0^\dagger(s) P_c \right] = \int_{t'}^t ds \int_0^t d\tau \int_0^{t'} d\tau' w^\dagger(\tau') e^{iP_c(\tau'-t')} A_0^\dagger(s) P_c e^{iP_c(t-\tau)} w(\tau) \quad (65)$$

When we add the two terms together, we can re-label $(\tau, t) \leftrightarrow (\tau', t')$ to add them directly and use that P_c

commutes with its time evolution,

$$\int_{t'}^t ds \int_0^t d\tau \int_0^{t'} d\tau' w^\dagger(\tau) \left(P_c e^{iP_c(t-\tau)} A_0(s) e^{-iP_c(t'-\tau')} + e^{-iP_c(t-\tau)} A_0^\dagger(s) e^{iP_c(t'-\tau')} P_c \right) w(\tau'). \quad (66)$$

Next, we additionally add the integral over t' ,

$$\int_0^t dt' \int_{t'}^t ds \int_0^t d\tau \int_0^{t'} d\tau' w^\dagger(\tau) \left(P_c e^{iP_c(t-\tau)} A_0(s) e^{-iP_c(t'-\tau')} + e^{-iP_c(t-\tau)} A_0^\dagger(s) e^{iP_c(t'-\tau')} P_c \right) w(\tau'). \quad (67)$$

We continue as follows: We apply the Cauchy-Schwartz-inequality to Eq. (67) after taking the absolute value. Then, for each summand, we commute the τ, τ' - P_c -evolutions ‘outwards’ to the $w^\dagger(\tau), w(\tau')$. The order here does not matter insofar as the ℓ_2 -norm that arises from the inner product is unitarily invariant. Indeed, if we have two terms $e^{iP_c\tau'} w(\tau')$ and $e^{-iP_c\tau'} w(\tau')$ (there are always \pm -opposite pairs) that are associated in the Cauchy-Schwartz inequality and are not directly compliant, the corresponding vectors are perfectly aligned except for a complex phase of $e^{\pm i\tau'}$ on the P_c -subspace. Hence this does not pose a complication in application of the Cauchy-Schwartz inequality as the obtained upper bound holds. Additionally, we use a similar argument regarding mis-aligned complex phases to re-express the matrix norm through the modified anti-commutator $\{X, Y\}_\sim = XY + Y^\dagger X$. Hence,

$$\begin{aligned} \text{Eq. (67)} &\leq \int_0^t dt' \left\| \int_0^t d\tau w(\tau) \right\|_{\ell_2} \left\| \int_0^{t'} d\tau' w(\tau') \right\|_{\ell_2} \left\| \int_{t'}^t ds \left(P_c e^{iP_c t} A_0(s) e^{-iP_c t'} + e^{-iP_c t} A_0^\dagger(s) e^{iP_c t'} P_c \right) \right\| \\ &\leq \int_0^t dt' \left\| \int_0^t d\tau w(\tau) \right\|_{\ell_2} \left\| \int_0^{t'} d\tau' w(\tau') \right\|_{\ell_2} \left\| \left\{ P_c, \int_{t'}^t ds A_0(s) \right\}_\sim \right\| \\ t' \leq t &\leq \left\| \int_0^t d\tau w(\tau) \right\|_{\ell_2}^2 \int_0^t ds \left\| \left\{ P_c, \int_0^s dt' A_0(s) \right\}_\sim \right\| \end{aligned} \quad (68)$$

Recall that $w(t) = v(0)\delta(t) + b(t)$. Thus, we want to estimate the norm of

$$\int_0^t ds w(s) = v(0) + \int_0^t ds b(s). \quad (69)$$

We obtain

$$\begin{aligned} \left\| \int_0^t ds w(s) \right\|_{\ell_2}^2 &= \langle v(0), v(0) \rangle + 2 \operatorname{Re} \left\langle v(0), \int_0^t ds b(s) \right\rangle + \left\| \int_0^t ds b(s) \right\|_{\ell_2}^2 \\ &\leq \|v(0)\|_{\ell_2}^2 + 2\|v(0)\|_{\ell_2} \|b(s)\|_{L^1([0,t])} + \|b(s)\|_{L^1([0,t])}^2, \end{aligned} \quad (70)$$

where $\|f\|_{L^1(W)} = \int_W ds |f(s)|$ for $W \subseteq \mathbb{R}$, which implies that $\left\| \int_W ds f(s) \right\|_{\ell_2}^2 \leq \|f(s)\|_{L^1(W)}^2$. To make notation shorter, we recall that $\|v(0)\|_{\ell_2} =: v_{\max}$ (by $\operatorname{Re}(A) \leq 0$) and define $\|b(s)\|_{L^1([0,t])} =: B_{L^1}$.

Therefore,

$$\begin{aligned}
 \text{Eq. (70)} \quad &\leq \left(v_{\max}^2 + v_{\max} B_{L^1} + B_{L^1}^2 \right) \int_0^t ds \, s \, \|\{P_c, A_0(s)\}_{\sim}\| \\
 &\leq \left(v_{\max}^2 + v_{\max} B_{L^1} + B_{L^1}^2 \right) \frac{t^2}{2} \max_{0 \leq t' \leq t} \|\{P_c, A_0(t')\}_{\sim}\|.
 \end{aligned} \tag{71}$$

To conclude, this means that

$$|\langle v(t), P_c v(t) \rangle| \leq \frac{1}{\lambda} \left(v_{\max}^2 + v_{\max} B_{L^1} + B_{L^1}^2 \right) \frac{t^2}{2} \max_{0 \leq t' \leq t} \|\{P_c, A_0(t')\}_{\sim}\|. \tag{72}$$

□

C. Application to Discretized Partial Differential Equations

The type of constraints we are mainly interested in in this work are constraints coming from boundary conditions in the discretization of linear, evolutionary partial differential equations. Namely, for \mathcal{L} a linear differential operator, then for $t \in \mathbb{R}_+$ and $r \in \Omega \subseteq \mathbb{R}^d$, and $v(t, r)$ comes from a function space so that the PDE with respect to \mathcal{L} is well-posed,

$$\begin{aligned}
 \partial_t v(t, r) - \mathcal{L} v(t, r) &= f(t, r), & r \in \Omega \\
 v(t, r) &= g(r, t), & r \in \Gamma_D
 \end{aligned} \tag{73}$$

$$\begin{aligned}
 \langle \partial_n, v(t, r) \rangle &= h(r, t), & r \in \Gamma_N \\
 v(0, r) &= v_0(r).
 \end{aligned} \tag{74}$$

The solution lives on a domain Ω and constrained to a specific value on the Dirichlet boundary Γ_D or a normal derivative on the Neumann boundary Γ_N . Robin boundary conditions, which specify a linear combination of derivative and value at the boundary can be obtained as a corollary, see Section II D 3.

In the context of Problem 7, we have that on a discretized version of $v(t, r)$, P_c^D projects onto the domain Γ_D , P_c^N applies a backwards difference stencil along the surface normal on Γ_N (for details see Section II C 2) and the differential operator \mathcal{L} becomes $A_0(t)$. There are no further assumptions beyond linearity on \mathcal{L} so far, though most of our error bounds in the previous section require that the for the discretized operator, $\text{Re}(A_0) \leq 0$.

The methodology we developed so far is able to enforce $g_c(t) = 0$ and $h(t) = 0$, assuming access to boundary projections P_c^D, P_c^N . Thus, we next consider how to deal with non-zero values as this is an essential aspect of the utility of our method.

1. Non-zero Dirichlet boundaries

We start by considering the problem in Eq. (73), assuming the condition on Γ_D . Let us further assume for simplicity that $\bar{\Omega} = [0, L]^d$. We will construct a function $u(r, t)$ that satisfies the constraint on Γ_D in (73).

For the one-dimensional case, $d = 1$, this can be found quite easily:

$$u(r, t) = \frac{1}{2} \frac{r}{L} g(L, t) + \frac{1}{2} \left(1 - \frac{r}{L}\right) g(-L, t). \quad (75)$$

Extending this to arbitrary dimension $d \geq 1$ follows naturally

$$u(r, t) = \frac{1}{2} \sum_{i=0}^{d-1} \frac{r_i}{L} g(r, t)|_{r_i=L} + \left(1 - \frac{r_i}{L}\right) g(r, t)|_{r_i=-L}. \quad (76)$$

Now, let us consider a new function

$$v'(r, t) = v(r, t) - u(r, t), \quad (77)$$

and compute the following,

$$\begin{aligned} \partial_t v'(r, t) - \mathcal{L} v'(r, t) &= \partial_t v(r, t) - \mathcal{L} v(r, t) - \partial_t u(r, t) + \mathcal{L} u(r, t) \\ &= f(r, t) + \mathcal{L} u(r, t) - \partial_t u(r, t) \end{aligned} \quad (78)$$

$$=: \tilde{f}(r, t) \quad (79)$$

where

$$\partial_t u(r, t) = \frac{1}{2} \sum_{i=0}^{d-1} \frac{r_i}{L} \partial_t g(r, t)|_{r_i=L} + \left(1 - \frac{r_i}{L}\right) \partial_t g(r, t)|_{r_i=-L}. \quad (80)$$

The initial condition becomes

$$v'(r, 0) = v(r, 0) - u(r, 0) = v_0(r) - u(r, 0) = v_0(r) \quad (81)$$

and the boundary condition

$$v'(r, t)|_{r \in \Gamma_D} = g(r, t) - \underbrace{v'(r, t)|_{x \in \Gamma_D}}_{=g(r, t)} = 0. \quad (82)$$

Therefore, the differential equation for v' is given by

$$\begin{aligned} \partial_t v'(r, t) - \mathcal{L}(t) v'(r, t) &= \tilde{f}(r, t), \quad r \in \Omega, t > 0 \\ v'(r, t) &= 0 \quad r \in \Gamma_D, t \geq 0, \\ v'(r, 0) &= v'_0(r) \quad r \in \overline{\Omega}, t = 0. \end{aligned} \quad (83)$$

That means that the PDE in $u(r, t)$ now has Dirichlet boundary conditions of value zero. The solution $v(r, t)$ to the original problem can then be obtained by

$$v(r, t) = v'(r, t) + u(r, t). \quad (84)$$

Therefore we easily obtain the following corollary to Lemma 10 and Lemma 13 for the case of a suitable discretization with error at most $O(\varepsilon)$, where then the differential operator \mathcal{L} has discrete representation A_0 .

Corollary 14 (Error in the infeasible space under stable dynamics with non-zero Dirichlet Boundary Conditions.). *We have the same assumptions as in Lemma 9 and additionally assume that the domain of interest is a regular box of length $L > 0$ in d dimensions, $\bar{\Omega} = [0, L]^d$. We are looking for a solution to non-zero value constraints as in*

$$\begin{aligned} \frac{d}{dt}v(t) &= A_0v(t) + b(t), \\ \mathbf{P}_c v(t) &= g_c(t) \in S_c, t \geq 0. \end{aligned} \quad (85)$$

Then, let $v'(t) = v(t) - g_c(t)$, which implies that for $v(t)|_{S_c} = g_c(t)$, the modified variable satisfies $v'(t)|_{S_c} = 0$. Then, with $b'(t) = -A_0g_c(t) - \frac{d}{dt}g_c(t) + b(t)$ we get an equivalent homogeneous system

$$\begin{aligned} \frac{d}{dt}v'(t) &= A_0(t)v'(t) + b'(t), \\ \mathbf{P}_c v'(t) &= 0, \quad t \geq 0. \end{aligned} \quad (86)$$

This means, the penalized form of Eq. (86), $\frac{d}{dt}v'(t) = (A_0(t) - i\lambda\mathbf{P}_c)v'(t) + b'(t)$, will satisfy the desired boundary condition from Eq. (85) as per Lemmas 10 and 13 using an inhomogeneous term $b'(t) = A_0(t)g_c(t) - \frac{d}{dt}g_c(t) + b(t)$. The necessary λ to achieve an error of at most ε is

$$A_0 \text{ time-indep.} \quad \lambda = \frac{2\|A_0\|}{\varepsilon} \left(v_{\max}^2 + 2tv_{\max}B' + t^2B'^2 \right) \quad (87)$$

$$A_0(t) \text{ time-dep.} \quad \lambda = \frac{\left(v_{\max}^2 + v_{\max}B'_{L^1} + (B'_{L^1})^2 \right) t^2}{\varepsilon} \max_{0 \leq t' \leq t} \|\{\mathbf{P}_c, A_0(t')\}_{\sim}\| \quad (88)$$

where $B' \geq \max_{0 \leq t' \leq t} \|A_0g_c(t') - \dot{g}_c(t') + b(t')\|_{\ell_2}$, $B'_{L^1} = \int_0^t dt' |A_0(t')g_c(t') - \dot{g}_c(t') + b(t')|$, and the modified anti-commutator as before $\{X, Y\}_{\sim} = XY + Y^\dagger X$.

Assuming a suitable discretization technique [44, 45] using a finite-dimensional basis of n basis functions per dimension, we obtain a semi-continuous solution vector $v(t) \in \mathbb{R}^{n^d}$. In alignment with Definitions 1 and 2 we call the discrete domain S , the value boundary S_c^D and the derivative boundary S_c^N . Then, we retrieve the formulation readily posed in Problem 7.

2. Neumann boundary conditions

Within this work, we will not worry about the approximation error with respect to the continuum limit and assume that we are provided with an ODE that follows from a sensible discretization, achieving a target discretization error $\varepsilon > 0$. Thus, we will continue only with bounding the error in representing a difference formula, denoted by D , using our projection method. The difference formula is implicitly defined by the sets ζ_j as given in Definition 1; a weighted combination of differences with neighbours which is then implemented through a SWAP network.

Errors from enforcing the constraint via the penalty projection follow similar as in the case for Dirichlet conditions. This is because fundamentally what we do is suppress the overlap on the subspace given by the penalty projection. Then, if the penalty projection approximates a derivative reasonably well, as in Eq. (103), the approximation of a derivative follows. We give an example using zero Neumann boundary conditions as the simplest case later in Section IID 2.

Moreover, the same approach of ‘shifting the data’ can be applied to the case of Neumann boundary conditions, i.e., constraints on the derivative such as $\langle \partial_{\mathbf{n}}, v(t, r) \rangle = h(r, t)$ for $r \in \Gamma_N$ in Eq. (73). Here, \mathbf{n} is the outward facing normal vector on the Neumann boundary of the domain, Γ_N . This problem has a solution only if the following consistency condition is satisfied,

$$\int_{\Gamma_N} \langle \partial_r v(r, t), \mathbf{n}(r) \rangle dS = \int_{\Gamma_N} h(r, t) dS \implies \int_{\Omega} \Delta v(r, t) dV = \int_{\Gamma_N} h(r, t) dS, \quad (89)$$

where the implication follows from the divergence theorem and dV and dS are volume and surface elements respectively. We assume this condition is satisfied so that the Neumann-value problem is well-posed.

Similar to the Dirichlet case, we seek a function $u(r, t)$ that complies with the constraint,

$$\langle \partial_r u(r, t), \mathbf{n}(r) \rangle = h(r, t) \quad \text{for any } r \in \Gamma_N. \quad (90)$$

This function $u(r, t)$ also should satisfy the consistency condition Eq. (89). Now, let

$$v'(r, t) = v(r, t) - u(r, t). \quad (91)$$

The respective PDE in v' then is

$$\begin{aligned} \partial_t v'(r, t) - \mathcal{L}v'(r, t) &= \partial_t v(r, t) - \mathcal{L}v(r, t) - \partial_t u(r, t) + \mathcal{L}u(r, t) \\ &= f(r, t) + \mathcal{L}u(r, t) - \partial_t u(r, t) =: \tilde{f}(r, t), \end{aligned} \quad (92)$$

with initial condition $v'(r, 0) = v_0(r) - u(r, 0) =: v_0'(r)$, and boundary condition $\langle \partial_r u(r, t), \mathbf{n}(r) \rangle = 0$. Therefore, in total, v' will satisfy the homogeneous Neumann problem

$$\begin{aligned} \partial_t v'(r, t) - \mathcal{L}v'(r, t) &= \tilde{f}(r, t), & r \in \Omega, t > 0 \\ v'(r, 0) &= v_0'(r), & r \in \bar{\Omega}, t = 0 \\ \langle \partial_r v'(r, t), \mathbf{n}(r) \rangle &= 0, & r \in \Gamma_N, t \geq 0. \end{aligned} \quad (93)$$

Analogous to the Dirichlet case, this gives rise to a means to solve (93) for v' and adding to it the function $u(r, t)$. Then, $v' + u$ satisfies the Neumann problem as in Eq. (73).

Notice that the consistency condition for v' implies

$$\int_{\Omega} \Delta v'(r, t) dV = 0. \quad (94)$$

An alternative approach to enforcing the derivative constraint that we do not follow within this work thus would be to express a penalty term in the modified ODE Eq. (11) so that \mathbf{P}_c^N projects onto second derivatives within the unconstrained domain S , corresponding to Eq. (94). The error can be quantified according to Corollary 14 by using the difference-projection \mathbf{P}_c^N instead of \mathbf{P}_c^D .

D. Input Model of Constraint Projections for Quantum Implementation

We continue by discussing constructing the relevant projections and their quantum implementations. The quantity we want to encode is the solution vector $v(t)$, which is expressed with n_l points per dimension $l \in [d]$; recall the definitions of $\mathcal{I}_{\Omega}, \mathcal{I}_{\Gamma_D}, \mathcal{I}_{\Gamma_N}$ from Definition 1. This vector is represented in terms of an

amplitude encoding:

$$|v(t)\rangle = \frac{1}{\|v(t)\|} \sum_{\mathbf{j} \in \mathcal{I}_{\Omega \cup \Gamma}} v_{\mathbf{j}}(t) |\mathbf{j}\rangle. \quad (95)$$

Here, $\mathbf{j} = (j_1, j_2, \dots, j_d)$ is a multi-index over d dimensions so that $j_l \in [n_l - 1]_0$ for all $l \in [d]$.

In order to specify boundaries, we assume access to an oracles O_{bdry} so that

$$O_{\text{bdry}} : |\mathbf{j}\rangle |0\rangle_{\text{bdry}} \rightarrow \begin{cases} |\mathbf{j}\rangle |0\rangle_{\text{bdry}}, & \mathbf{j} \in \mathcal{I}_{\Omega} : \text{internal point} \\ |\mathbf{j}\rangle |1\rangle_{\text{bdry}}, & \mathbf{j} \in \mathcal{I}_{\Gamma_D} : \text{Dirichlet condition} \\ |\mathbf{j}\rangle |2\rangle_{\text{bdry}}, & \mathbf{j} \in \mathcal{I}_{\Gamma_N} : \text{Neumann condition} \\ |\mathbf{j}\rangle |3\rangle_{\text{bdry}}, & \mathbf{j} \in \mathcal{I}_{\Gamma_R} : \text{Robin condition} \end{cases} \quad (96)$$

The algorithm we present in Section IV will consider the dynamics we study exclusively in an interaction picture with respect to P_c . Therefore, the type of access we require to a projection is through Hamiltonian simulation of it, which we study alongside. An important point then so that the interaction picture simulation algorithm in [46] is efficient is that the projection's Hamiltonian simulation can be fast-forwarded [47, Definition 1], so that the complexity of implementation depends at most logarithmically on λ .

1. Projections for Dirichlet conditions and value constraints

Dirichlet boundary conditions in PDEs are point-wise value constraints. On a grid, this naturally induces a projection matrix by projecting directly onto basis elements. We can define P_c^D to be

$$P_c^D = \sum_{\mathbf{j} \in \mathcal{I}_{\Gamma_D}} |\mathbf{j}\rangle\langle\mathbf{j}|, \quad (97)$$

which is equivalent to conditioning on the boundary flag from the boundary oracle O_{bdry} in Eq. (96) being in 1-state, so $\mathbf{j} \in \mathcal{I}_{\Gamma_D}$. Given this oracle O_{bdry} it is straightforward to construct a circuit for a value constraint projector,

$$U_{P_c^D} : |\mathbf{j}\rangle |0\rangle_{\text{bdry}} \mapsto O_{\text{bdry}}^\dagger \left(\mathbb{I} \otimes |1\rangle\langle 1|_{\text{bdry}} \right) O_{\text{bdry}} |\mathbf{j}\rangle |0\rangle_{\text{bdry}}. \quad (98)$$

In terms of LCU, we can see O_{bdry} as PREP and $\mathbb{I} \otimes |1\rangle\langle 1|_{\text{bdry}}$ as (a part of) SEL.

Hamiltonian simulation of the value constraint projection. From [47, Theorem 3], we have that for any commuting Hamiltonian H so that $\|H\|_\infty = 1$, $H \in \mathbb{C}^{2^n \times 2^n}$ and $\text{supp}(H) = k$ with $k \in O(\log n)$, Hamiltonian simulation of H can be (T, α) fast-forwarded with $T \in 2^{O(n)}$ and $\alpha > 0$. In the case of value constraints, locality is easy to show as $k = 1$ and as we deal with projections, it follows that $\|P_c^D\|_\infty = 1$.

We notice that $[|\mathbf{j}\rangle\langle\mathbf{j}|, |\mathbf{k}\rangle\langle\mathbf{k}|] = 0$ for any \mathbf{j}, \mathbf{k} in \mathcal{I}_{Ω} . This means for the evolution that

$$e^{-i\lambda t P_c^D} = \prod_{\mathbf{j} \in \mathcal{I}_{\Gamma_D}} e^{-i\lambda t |\mathbf{j}\rangle\langle\mathbf{j}|}. \quad (99)$$

So for time-independent constraints, this can be implemented simply by phase gates parametrized by the penalty λ , controlled on $|\mathbf{j}\rangle$.

$$\text{HamSim}(\mathbf{P}_c^D, \lambda t) |j\rangle |0\rangle_{\text{bdry}} = \mathbf{O}_{\text{bdry}}^\dagger \left(e^{-i\lambda t} \otimes |1\rangle\langle 1|_{\text{bdry}} \right) \mathbf{O}_{\text{bdry}} |j\rangle |0\rangle_{\text{bdry}} \quad (100)$$

Therefore, Eq. (100) is fast-forwarded by this construction as the implementation cost does not directly depend on the parameter λt .

2. Projectors for Neumann conditions and derivative constraints

To obtain a finite-dimensional approximation to a Neumann projection, we employ a discrete finite-difference derivative \mathbf{D} . As observed in the statement of Problem 5, a crucial ingredient for our method to work is that the projection \mathbf{P}_c^N for the approximate derivative condition is orthogonal to, and thereby commutes with, the projection onto the feasible region and the projection onto the value constraint region. We discuss next how these requirements are satisfied by a simple finite difference stencil evaluated on two points assuming a grid discretization. The motivation is that this allows us to enforce that the value on the boundary has the same value as the next-closest value within the domain in the direction of interest.

First, we look at a one-dimensional example. Take $v = \sum_{l=1}^L v_l e_l$ with the canonical basis $\{e_l\}_{l=1}^L$. Consider $\partial_n \cdot v|_L = 0$ and v representing a line split into L points, then v_L falls into the derivative constraint. Then, a ‘inward’ finite difference stencil would be $\frac{v_L - v_{L-1}}{h}$. For the sake of a projection, we only care about the difference, and may omit the scaling by the grid spacing h . Then, a discrete derivative is given by $\mathbf{D}v|_{\Gamma_N} = v_L - v_{L-1}$. Consequently, what we want to enforce is that $v_L = v_{L-1}$. The feasible and infeasible spaces then are

$$S = \text{span}\{v : v_L = v_{L-1}\}, \quad S_c^N = \text{span}\{v : v_L \neq v_{L-1}\}. \quad (101)$$

We will design an algorithm that allows to attain an approximate S_c^N via

$$\text{span}\{v : |v_L - v_{L-1}| < \varepsilon\} \quad (102)$$

for $\varepsilon > 0$. A swap operation \mathbf{S} so that $\mathbf{S}v = \sum_{l=1}^{L-2} v_l e_l + v_L e_{L-1} + v_{L-1} e_L$ has the property that it leaves S invariant. Then, the projection $\frac{1}{2}(\mathbb{I} - \mathbf{S}) \equiv \mathbf{P}$ has the desired properties that $\ker(\mathbf{P}) = S$ and $\text{image}(\mathbf{P}) = S_c^N$. Note that the canonical basis to S_c are not eigenvectors to \mathbf{P} but its image is closed in S_c^N . That means it will allow us to project onto elements that are unacceptable and we can annihilate them. As we want orthogonal projections as per assumptions in Definition 3, we need to choose Hermitian projections. The ‘bad’ space projection already satisfies this, for the ‘good’ projection we can use $\mathbf{P}^\perp = \frac{1}{2}(\mathbb{I} + \mathbf{S})$.

We continue by discussing how to create the projector for $|\mathcal{I}_{\Gamma_N}| > 1$. A general solution vector v represents a spatial discretization of the continuous solution over a domain $\Omega \subseteq \mathbb{R}^d$, with overall $n = \prod_{l=1}^d n_l$ basis elements. For every point $j \in \mathcal{I}_{\Gamma_N}$ within the computational domain that lies on the derivative constraint region or Neumann boundary Γ_N , we have a set of neighbours ζ_j that represent the set of basis elements that we use for the respective finite difference formula. This describes the set of mutual swaps that need to be done for every j on Γ_N . It is reasonable to assume this discretization is ζ -local in the sense that every neighbour set has at most $|\zeta_j| = \zeta \in \mathbb{N}$ elements. In fact, for a regular grid discretization, every node has at most $(n-1)^d < n^d - 1$ neighbours of which only a subset will be interesting for the derivative constraints. Therefore we only need to store information specifically what a node’s respective neighbours are rather than which others every node neighbours. This leads to the following as a formulation for the sought after

projector,

$$\mathbf{P}_c^N = \frac{1}{2} \left(\mathbb{I} - \prod_{j \in \mathcal{I}_{\Gamma_N}, k \in \zeta_j} \text{SWAP}(j, k) \right) = \frac{1}{2} (\mathbb{I} - \mathbf{S}). \quad (103)$$

Direct implementation by a linear combination of unitaries yields,

$$\begin{array}{c} |0\rangle \text{---} [X] \text{---} [\text{Had}] \text{---} \bullet \text{---} [\text{Had}] \text{---} [X] \text{---} \langle 0| \\ | \psi \rangle \text{---} \text{---} [S] \text{---} \text{---} \frac{1}{2} (\mathbb{I} - S) | \psi \rangle. \end{array} \quad (104)$$

Circuit constructions for the SWAP's \mathbf{S} are discussed in the upcoming paragraphs.

Later on, we will discuss fast-forwarded Hamiltonian simulation of the constraint projections. For this to be possible, we will require the following conditions on the problem setup:

- Any point that is neighbour to a constraint point for the sake of a derivative condition (i.e., part of the finite difference formula) cannot be affected by a derivative constraint itself.

$$\forall j \in \mathcal{I}_{\Gamma_N}, \zeta_j \cap \mathcal{I}_{\Gamma_N} = \emptyset \quad (105)$$

- Any point can be neighbour in a finite difference formula for a derivative constraint to at most one point on Γ_N .

$$\forall j, k \in \mathcal{I}_{\Gamma_N}, \zeta_j \cap \zeta_k = \emptyset \quad (106)$$

For discretized PDEs, this scenario can be realized easily. Suppose a grid discretization would not satisfy these conditions (see left-hand side of Fig. 4), then a refinement of the discretization is sufficient (right-hand side of Fig. 4) and comes at little cost in extra qubits. If the problem-at-hand is a more general constrained ODE, one can think of the same strategy together with introducing additional dummy variables that are trivially coupled with their neighbours instead of a global ‘refinement’.

Example 1 (Error on a derivative constraint for stable dynamics). *We consider a system as in Problem 5 with dynamics generated by $A = A_0 - i\lambda \mathbf{P}_c^N$, with \mathbf{P}_c^N from Eq. (103), A_0 and thus also A are normal and the real parts of the eigenvalues of A_0 are non-positive, $\lambda > 0$ and \mathbf{P}_c^N the projector on the infeasible space as defined in Definition 3. Then, the error at time $t > 0$ along the boundary with respect to the finite difference formula embodied by \mathbf{P}_c^N is bounded as follows,*

$$\|\mathbf{D}v(t)\|_{\ell_2, S_c^N}^2 \leq \epsilon \quad (107)$$

for $\lambda = \frac{2v_{\max}^2 \|A_0\|}{\epsilon}$.

Proof. Using Eq. (103), we have that $\mathbf{P}_c^{N^2} = \mathbf{P}_c^N = (\mathbf{P}_c^N)^\dagger$. We now determine the approximation error of the projective boundary conditions with respect to the finite-dimensional approximation of a derivative constraint through $\mathbf{D}v(t)$, $\|\mathbf{D}v(t) - h\|$, while we consider $h = 0$ in this Lemma. But this then allows us to

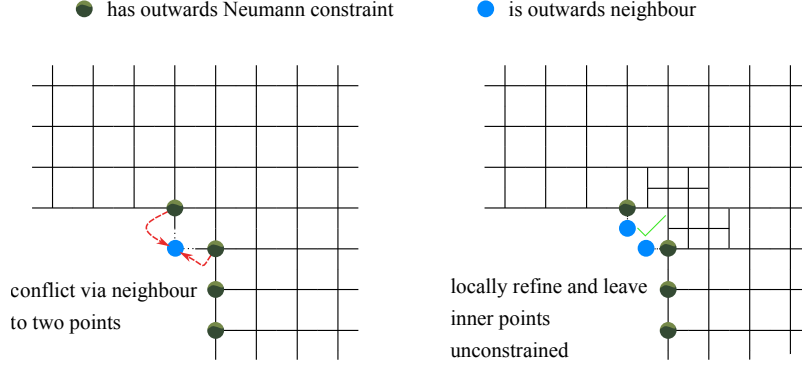


FIG. 4: Conflicts arising in derivative constraints on a regular grid (left). Mitigation is possible by either only allowing one of the constraints, or a local grid refinement and ignoring the constraint on the finer level (right).

say that

$$\|Dv(t)\|_{\ell_2, S_c^N}^2 = |\langle P_c^N v(t), P_c^N v(t) \rangle| = |\langle v(t), P_c^N v(t) \rangle|, \quad (108)$$

Now, we can bound $|\langle v(t), P_c^N v(t) \rangle|$ similar to the Dirichlet case. We recall that $v(t) = \exp(At)v(0)$, $A = A_0 - i\lambda P_c^N$, $\text{Re}(A_0) \leq 0$. First, observe that

$$|\langle v(0), Av(0) \rangle| = E_0 < \infty, \quad (109)$$

as we assume enough sufficient smoothness in the initial condition to satisfy the boundary condition. The rest of the proof then follows equivalently the proof of Lemma 9. Thus, to summarize, we can say that

$$|\langle v(t), P_c^N v(t) \rangle| \leq 2v_{\max}^2 \frac{\|A_0\|}{\lambda}. \quad (110)$$

□

Remark 5 (Alternative approach to Value Constraints: Example for time-independent case). *Derivative constraints provide an alternative to the implementation of non-zero value constraints compared to homogenizing the ODE as in Section II C. We can introduce dummy variables (similar to ‘ghost points’), which are not coupled with the other variables through $A_0(t)$, and store the desired values in them. Then, enforce a derivative constraint with the respective nodes, so that the effect of the constraint is that the affected boundary points will obtain the same value as stored in the dummy variables. That is,*

$$\tilde{v} = \begin{bmatrix} v \\ v_{\text{dummy}} \end{bmatrix}, \quad \widetilde{A_0} = \begin{bmatrix} A_0 & 0 \\ 0 & 0 \end{bmatrix}, \quad (111)$$

where $v_{\text{dummy}} \in \mathbb{C}^{|\mathcal{I}_{\Gamma_N}|}$. Then, adding the constraint projection

$$P_c^N = \frac{1}{2}(\mathbb{I} - \text{SWAP}(v|_{\Gamma_N}, v_{\text{dummy}})) \quad (112)$$

to the dynamics through $\frac{d}{dt}\tilde{v} = (\widetilde{A}_0 - i\mathbf{P}_c^N)\tilde{v}$ leads to $v = \mathbf{P}_{S \oplus S_c^N}\tilde{v}$ so that a value/Dirichlet constraint is enforced up to accuracy ε for λ chosen according to the example above.

Note that this approach leads to a lower bound on λ necessary for accuracy ε follows, as $v_{\max}^2 + B^2 > \tilde{v}_{\max}^2 = v_{\max}^2 + \|v_{\text{dummy}}\|_{\ell_2}^2$ with $B = \|A_0 g\|_{\ell_2}$ and $\|v_{\text{dummy}}\|_{\ell_2} = \|g\|_{\ell_2}$; see Corollary 14 vs. Lemma 9. On the other hand, the implementation cost for the derivative constraint is slightly higher due to the SWAP construction compared to the value constraints as we will observe in the following.

a. Input model for SWAP circuit. This section discusses a circuit construction for the swap circuit \mathbf{S} in Eq. (103). The first ingredient to that is an oracle \mathbf{O}_ζ that prepares a superposition encoding the distances $\mathbf{k} - \mathbf{j}$ over all neighbours \mathbf{k} from a neighbour set $\zeta_j \subseteq \mathcal{I}_{\Omega \cup \Gamma}$ that contains the neighbours to node \mathbf{j} . Then, we define the neighbour oracle by its action on a state $v_j |\mathbf{j}\rangle$ as

$$\begin{aligned} \mathbf{O}_\zeta : v_{j_1 \dots j_d} |j_1 \dots j_d\rangle |0\rangle \\ \rightarrow v_{j_1 \dots j_d} |j_1 \dots j_d\rangle \left(\frac{1}{\sqrt{|\mathcal{I}_{\Gamma_N}| |\zeta_j|}} \sum_{(k_1 \dots k_d) \in \zeta_j} |k_1 - j_1\rangle |k_2 - j_2\rangle \dots |k_d - j_d\rangle \right). \end{aligned} \quad (113)$$

The action of $\text{SWAP}(\mathbf{j}, \mathbf{k})$ for a set of neighbour shifts $(k_1 - j_1, \dots, k_d - j_d) \in \zeta_j$ is given as follows:

$$v_{j_1 \dots j_d} |j_1 \dots j_d\rangle \mapsto v_{j_1 \dots j_d} |k_1\rangle |k_2\rangle \dots |k_d\rangle. \quad (114)$$

Namely, it effects a shift by distances $k_w - j_w$, $w \in [d]$, where the distances are given by the neighbour oracle \mathbf{O}_ζ . Whenever the constraints are given by Neumann boundary conditions, we can also expect that most of these differences are zero. In the case of a two-point stencils to approximate the derivative, there is only one index k_w that needs to be shifted in d' dimensions, where $d' < d$ is the dimension of the boundary. Then, Eq. (114) becomes

$$v_{j_1 \dots j_d} |j_1 \dots j_d\rangle \mapsto v_{j_1 \dots j_d} |j_1\rangle |j_2\rangle \dots |k_w\rangle \dots |j_d\rangle \quad (115)$$

Therefore, these swaps can be implemented a sequence of controlled additions of j_w with the distances $k_w - j_w$ and call this subroutine. The arithmetic that needs to be done here is fairly simple as we only need to add bit-strings. Recall that CADD is defined as

$$\begin{aligned} \text{CADD} : |\mathbf{j}\rangle |\mathbf{k}\rangle &\rightarrow |\mathbf{j} + \mathbf{k}\rangle |\mathbf{k}\rangle \\ &\equiv |j_1\rangle |j_2\rangle \dots |j_d\rangle |k_1\rangle |k_2\rangle \dots |k_d\rangle \rightarrow |j_1 \oplus k_1\rangle |j_2 \oplus k_2\rangle \dots |j_d \oplus k_d\rangle |k_1\rangle |k_2\rangle \dots |k_d\rangle, \end{aligned} \quad (116)$$

where j_1, \dots are bitstrings with length $\lceil \log_2(n) \rceil$ and \oplus is addition modulo 2. Note that for the sake of our input model with added distances $\mathbf{k} - \mathbf{j}$, the addition will never exceed the representable range of grid point indices.

Moreover, for each $\mathbf{j} \in \mathcal{I}_{\Gamma_N}$, we have $|\zeta_j|$ neighbours with d dimensions. Thus, we need to do at most $O(d|\mathcal{I}_{\Gamma_N}| \cdot \max_j |\zeta_j|)$ additions. Assuming we have at most n basis elements per dimension to index and thereby each summand has at most $\lceil \log_2 n \rceil$ bits, then the overall cost to perform the additions will be

$O(d \lceil \log_2 n \rceil |\mathcal{I}_{\Gamma_N}| \cdot \max_j |\zeta_j|)$ [48]. Applying the CADD circuit to Eq. (113), we obtain

$$(113) \xrightarrow{\text{CADD}} \sum_{j_1 \dots j_d} v_{j_1 \dots j_d} |k_1(j_1)\rangle |k_2(j_2)\rangle \dots |k_d(j_d)\rangle \left(\frac{1}{\sqrt{|\mathcal{I}_{\Gamma_N}| |\zeta_j|}} \sum_{\mathbf{k} \in \zeta_j} |\mathbf{k} - \mathbf{j}\rangle \right) \quad (117)$$

$$\xrightarrow{\text{O}_\zeta^{-1}} \left(\sum_{j_1 \dots j_d} v_{j_1 \dots j_d} |k_1(j_1)\rangle |k_2(j_2)\rangle \dots |k_d(j_d)\rangle \right) |0\rangle, \quad (118)$$

where we also uncompute the register of boundary differences by O_ζ^{-1} . This means that $\prod_{j,k} \text{SWAP}(\mathbf{j}, \mathbf{k})$ is implemented by

$$U_{\text{SWAPS}} \left(v_{\mathbf{j}} |\mathbf{j}\rangle_{\mathbf{v}} |0\rangle_{\text{bdry}, \zeta} \right) = \text{O}_{\text{bdry}}^{-1} (\text{O}_\zeta^{-1} \otimes |2\rangle\langle 2|_{\text{bdry}}) \cdot \text{CADD} (\text{O}_\zeta \otimes |2\rangle\langle 2|_{\text{bdry}}) \text{O}_{\text{bdry}} \left(v_{\mathbf{j}} |\mathbf{j}\rangle_{\mathbf{v}} |0\rangle_{\text{bdry}, \zeta} \right). \quad (119)$$

Overall, we have the following registers,

- a state register $|\mathbf{j}\rangle_{\mathbf{v}}$, consisting of $d \lceil \log_2(n) \rceil$ qubits for n basis elements per dimension with binary representation;
- ancillas $|\cdot\rangle_{\text{bdry}}$ with 2 qubits to encode the type of basis element (inner, Dirichlet boundary, Neumann boundary);
- ancillas $|\cdot\rangle_\zeta$ to hold the neighbour set values coming from O_ζ , with $d \lceil \log_2(\max_j |\zeta_j|) \rceil$ qubits.

b. Hamiltonian simulation of the derivative constraint projection. In order to time-evolve a derivative constraint, we consider Lemma 15 that allow to avoid compiling $e^{i\lambda t \mathbf{P}_c^N}$ using Hamiltonian simulation techniques of the Hermitian projector \mathbf{P}_c^N . The following formula illustrates how this can be performed easily in the case of orthogonal projections.

Lemma 15 (Exponential of an orthogonal projection.). *Let \mathbf{P}, \mathbf{Q} be orthogonal and thus Hermitian projections on a vector space so that $\mathbf{P} + \mathbf{Q} = \mathbb{I}$. Then, for any $\xi \in \mathbb{C}$,*

$$e^{\xi \mathbf{P}} = \mathbf{Q} + e^{\xi} \mathbf{P}. \quad (120)$$

The case of $\xi \in i\mathbb{R}$ recovers Hamiltonian simulation of an orthogonal projection.

Hence, access to \mathbf{P}_c^N and its orthogonal complement is sufficient for simulation in this context as only the image of the penalty projection is meant to experience a phase. Recall that the situation was the same for value constraints before, however, the complement there was simply the identity on the unconstrained domain and thus does not require an additional circuit implementation. Then, Lemma 15 permits us to implement $\mathbf{P}_c^{N\perp} + \mathbf{P}_c^N e^{i\lambda t}$ rather than $e^{-i\lambda t \mathbf{P}_c^N}$. More specifically, this is

$$\text{HamSim}(\mathbf{P}_c^N, \lambda t) = \frac{1}{2}(\mathbb{I} + \mathbf{S}) + \frac{e^{-i\lambda t}}{2}(\mathbb{I} - \mathbf{S}). \quad (121)$$

Indeed, this form is now equivalent to the value constraints up to modified projectors, where in the former case we can identify \mathbf{Q} with $\sum_{\mathbf{j} \in \Omega \setminus \Gamma_D} |\mathbf{j}\rangle\langle \mathbf{j}|$ and \mathbf{P} with $\sum_{\mathbf{j} \in \Gamma_D} |\mathbf{j}\rangle\langle \mathbf{j}|$. A circuit construction for \mathbf{S} was given

above in Eq. (119). Then, constructing a circuit for Eq. (121) is simple. Instead of packing things into extra LCUs, which would come at a constant factor loss in the success probability, we can do the following:

$$(122)$$

For the ancilla qubit, instead of projecting onto one of the basis states as before, we measure and discard the result (i.e., there is no post-selection necessary). The controlled phase gate $e^{-i\lambda t}$ is the same as in the value constraint evolution in Eq. (100). This allows us to effectively fast-forward the evolution of P_c^N , as the complexity of the circuit in Eq. (122) is independent of λt . The ability to fast-forward also follows from [49, Theorem 3.1 and Fig. 2].

c. Interface conditions via ‘derivative projection’. The finite difference construction to approximate Neumann conditions is also useful to represent interface conditions, i.e., conditions between regimes that are governed by different PDEs. Suppose there are η subdomains which represent a different physical model (expressed by a different linear PDE)

$$(\partial_t - \mathcal{L}_1)u_1(x; t) = 0, \quad x \in \Omega_1, \quad \dots, \quad (\partial_t - \mathcal{L}_\eta)u_\eta(x; t) = 0, \quad x \in \Omega_\eta, \quad (123)$$

then one can define interface conditions describe relationships at any intersections of the domains $k \neq l \in [\eta]$,

$$u_k(x; t) = \gamma u_l(x; t), \quad x \in \Omega_k \cap \Omega_l, \quad (124)$$

with $\gamma \in \mathbb{C}$; one can also think of more general relationships. The numerical treatment of interface conditions in classical numerical methods is described e.g. in [50]. Our approach somewhat resembles the ‘penalty method’ described there, in the sense that it also introduces a notion virtual work that is minimized by admissible solutions.

In order to use ‘Neumann projections’ as in Eq. (103) we need an index set $\mathcal{I}_{\text{interface}}$ and neighbour sets $\bigcup_{j \in \mathcal{I}_{\text{interface}}} \zeta_j$. Using a grid discretization of the computational domain, then there are no more ‘true’ boundary points that are in $\Omega_k \cap \Omega_l$ but every point is in either k or l ; therefore, what we get are bipartite sets that give immediate rise to the necessary boundary point—neighbour relation. Upon proper definition of these sets and the according boundary oracles following Eq. (96), the treatment of interface conditions then follows immediately from how P_c^N is treated.

3. Input Model for Robin Boundary Conditions

The ability to implement value constraints and derivative constraints allows us to extend the applicability to another class of boundary conditions. Constraints described by a superposition of Dirichlet and Neumann conditions are called Robin boundary conditions [51]; they can be expressed as

$$\alpha v(x; t) + \beta \partial_n \cdot v(x; t) = f(x; t), \quad x \in \Gamma_R, \quad (125)$$

with constants α, β . Therefore, we can choose a projection

$$\mathbf{P}_c^R = \alpha \sum_{j \in \mathcal{I}_{\Gamma_R}} |j\rangle\langle j| + \frac{\beta}{2} \left(\mathbb{I} - \prod_{j \in \mathcal{I}_{\Gamma_R}, k \in \zeta_j} \text{SWAP}(j, k) \right), \quad (126)$$

and additionally assume that $\alpha, \beta \in \mathbb{R}$ so that \mathbf{P}_c^R is Hermitian. The point-wise projection $\sum_{j \in \mathcal{I}_R} |j\rangle\langle j|$ maps any bitstrings from $\mathcal{I}_{\Omega \cup \Gamma}$ to those inside the Robin-boundary \mathcal{I}_{Γ_R} , whereas the SWAP-circuit takes any from $\mathcal{I}_{\Omega \cup \Gamma}$ to those that are considered neighbours for the Robin boundary $\mathcal{I}_{\Gamma_R \cap \Omega} = \bigcup_{j \in \mathcal{I}_{\Gamma_R}} \zeta_j$. Therefore, the commutativity of these operations depends on how the sets are defined. One option is to use ‘outside’ ghost points for the finite differences in the Neumann projections for the rather than points inside the domain, and include these to the image of the Dirichlet projection. Then, the operations commute restricted to the domain of interest (that is, disregarding the ghost points) and one can compile $\exp(-i\lambda t \mathbf{P}_c^R)$ with a product formula

$$\exp(-i\lambda t \mathbf{P}_c^R) = \exp\left(-i\alpha\lambda t \sum_{j \in \mathcal{I}_{\Gamma_R}} |j\rangle\langle j|\right) \exp\left(-i\frac{\beta}{2}\lambda t (\mathbb{I} - \mathbf{S}_R)\right), \quad (127)$$

or equivalently

$$\text{HamSim}(\mathbf{P}_c^R, \lambda t) = \text{HamSim}(\mathbf{P}_c^D|_{\mathcal{I}_{\Gamma_R}}, \alpha\lambda t) \text{HamSim}(\mathbf{P}_c^N|_{\mathcal{I}_{\Gamma_R}}, \beta\lambda t), \quad (128)$$

where we know how to implement both from above, Eqs. (100) and (121).

E. Hamiltonian simulation of combined projections

Using the results from the previous two sections, we can express the Hamiltonian simulation of orthogonal value and derivative projections as follows,

$$\begin{aligned} \text{HamSim}(\mathbf{P}_c, \lambda t) = \mathbf{O}_{\text{bdry}}^{-1} & \left(\text{HamSim}(\mathbf{P}_c^D, \lambda t) \otimes |1\rangle\langle 1|_{\text{bdry}} \right. \\ & + \text{HamSim}(\mathbf{P}_c^N, \lambda t) \otimes |2\rangle\langle 2|_{\text{bdry}} \\ & \left. + \text{HamSim}(\mathbf{P}_c^D, \alpha\lambda t) \text{HamSim}(\mathbf{P}_c^N, \beta\lambda t) \otimes |3\rangle\langle 3|_{\text{bdry}} \right) \mathbf{O}_{\text{bdry}}, \end{aligned} \quad (129)$$

where $\text{HamSim}(\mathbf{P}_c^D, \lambda)$ requires a call to controlled $e^{-i\lambda t}$ and $\text{HamSim}(\mathbf{P}_c^N)$ needs additionally a controlled implementation of the swap \mathbf{S} . Recall that $|1\rangle_{\text{bdry}}$ marks Dirichlet points, $|2\rangle_{\text{bdry}}$ Neumann points and $|3\rangle_{\text{bdry}}$ Robin boundary points.

III. NUMERICAL EXPERIMENTS

In the following, we are presenting numerical experiments as proof-of-concept validation of the penalty projections method via interaction picture based on classical simulation of the dynamics. In addition, we are interested in tightness of our bounds on λ derived in Section II B. To that end, we consider the heat equation and the wave equation as two of the canonical examples for ‘simple’ PDEs. While for the heat equation, a quantum speedup beyond a quadratic one coming from amplitude amplification cannot be expected in general

when evaluating an expectation value with respect to the final state (see [52]), it still serves as an illustrative example. However, as shown in [19] and recovered as the isotropic case in [53], the wave equation, which in contrast to the heat equation is not dissipative and obeys conservation of energy, allows for an at least cubic speedup.

A. Setup

In the computations below, we restricted the possible range of λ to ‘small’ values (up to 10^6) to avoid aliasing in the numerical solution of the highly oscillatory system in interaction picture. Note that this is not as much of a problem in the quantum implementations, as we will outline below, as the necessary time discretization only grows with $\log(\lambda)$. For spatial discretization, we use a simple central three-point finite difference formula in periodic boundary conditions form to represent the Laplacian. We use the Runge-Kutta scheme RK23 [54] to simulate the time evolution. Even though this is not high-accuracy, it proves sufficient for the regimes we are looking at; in order to capture high-frequency effects of the interaction picture simulation of $A_I(t)$, a relatively small time-step is already required, hence the accuracy is sufficient here to ensure that the penalty error is the dominant source of error. We are solving the following discretized PDEs by time-stepping the interaction picture equations from Eq. (143) with respect to the discretized differential operators.

B. Simulation results

In what follows, we present numerical experiments for dimensionless heat and wave equations, discretized by finite differences.

1. Heat equation with Dirichlet and Neumann boundary conditions

We consider the following 2D-problem for the heat equation:

$$\partial_t u(x, y; t) = D \Delta u(x, y; t) + f(x, y; t) \quad (130)$$

$$u(x, y; t)|_{x, y \in \Gamma_D} = g(x, y; t) \quad (131)$$

$$\partial_n \cdot u(x, y; t)|_{x, y \in \Gamma_N} = h(x, y; t) \quad (132)$$

$$u(x, y; t = 0) = u_0(x, y). \quad (133)$$

with the temperature distribution $u(x, y; t)$ and diffusion coefficient $D > 0$; for the sake of simplicity, we choose isotropic diffusion here. The initial conditions are described by u_0 , f is a forcing term (heat source) and g describes the temperature along the boundary Γ_D , where h describes the temperature flux across the boundary Γ_N . Then, we introduce an equidistant uniform grid for space to obtain $\mathbf{u}_h(t) \in \mathbb{R}^{N^2}$ using N points to represent x and y , and a fourth-order finite difference stencil to approximate Δ via $\mathbf{L}_h \in \mathbb{R}^{N^2 \times N^2}$ with truncation error $O(N^{-4})$. Then, we have the discretized ODE system

$$\frac{d}{dt} \mathbf{u}_h(t) = D \mathbf{L}_h \mathbf{u}_h(t) + \mathbf{f}(t), \quad (134)$$

and use the constraint projections as defined earlier in Eqs. (97) and (103) and use the homogenization strategies outlined in Section II C for non-zero boundary conditions.

We examine the following choices of boundary conditions:

- Vanishing boundary conditions, $\mathbf{P}_c^D \mathbf{u}_h(t) = 0$. See Figs. 5 and 7.
- Non-zero boundary conditions, $\mathbf{P}_c^D \mathbf{u}_h(t) = g(\mathbf{x}, \mathbf{y})$

$$\mathbf{g} = (1 - \mathbf{y}) \odot \begin{cases} \mathbf{x}, & \mathbf{x} \leq \frac{1}{2} \\ (1 - \mathbf{x}), & \mathbf{x} > \frac{1}{2}, \end{cases} \quad (135)$$

where $\mathbf{x} = [0, \Delta x, 2\Delta x, \dots]^T$ and $\mathbf{y} = [0, \Delta y, 2\Delta y, \dots]^T$ are the grid representation of the x, y domain and \odot denotes element-wise multiplication. This is implemented via the approach outlined in Section II C 1. Results are shown in Fig. 6.

- No heat in/out-flux: $\mathbf{P}_c^N \mathbf{u}_h(t) = 0$. The boundary values are zero in compliance to the initial condition. If the initial condition is equal to zero on the boundary indices, then this scenario can test both the usage of the Neumann projectors to enforce a value as well as the gradient. The numerical results are depicted in Fig. 8.

All simulations are dimensionless, and as initial state we use a centred, isotropic Gaussian with height 1 and define a cut-off so that the initial condition respects the boundary constraints. Additionally, we use a point-source $\mathbf{f}(t) = 298$ at the centre element.

2. Wave equation with Dirichlet boundary conditions

The 2-D wave equation is defined as

$$\partial_{tt} u(x, y; t) = c^2 \Delta u(x, y; t), \quad (136)$$

with a speed-of-sound parameter $c^2 > 0$. In order to solve the wave equation, let $w(x, y; t) = \partial_t u(x, y; t)$. Then, Eq. (136) is equivalent to the system

$$\partial_t \mathbf{v}(t) = \partial_t \begin{bmatrix} u(t) \\ w(t) \end{bmatrix} = \begin{bmatrix} 0 & \mathbb{I} \\ c^2 \Delta & 0 \end{bmatrix} \begin{bmatrix} u(t) \\ w(t) \end{bmatrix} = \mathbf{A} \mathbf{v}(t), \quad (137)$$

with initial data $\mathbf{v}(t) = \begin{bmatrix} u(x, y; t=0) \\ \partial_t u(x, y; t=0) \end{bmatrix}$. Upon discretizing space on a uniform, regular grid with N points per spatial dimension, we obtain a matrix $\mathbf{L}_h \in \mathbb{R}^{N^2 \times N^2}$ and overall system matrix $\mathbf{A}_h \in \mathbb{R}^{2N^2 \times 2N^2}$, $\mathbf{v}_h(t) \in \mathbb{R}^{2N^2}$. For the constrained system,

$$\frac{d}{dt} \mathbf{v}_h(t) = (\mathbf{A}_h - i\lambda \mathbf{P}_c) \mathbf{v}_h(t)$$

we apply a penalty projection on both the original variable \mathbf{u} and $\mathbf{w} = \partial_t \mathbf{u}$, $\mathbf{P}_c = \begin{bmatrix} \mathbf{P}_c & 0 \\ 0 & \mathbf{P}_c \end{bmatrix}$. As the value of interest is only $\mathbf{u}(t)$, we measure the error via $\|\mathbf{u}\|_{\ell_2, S_c}^2 = \langle \mathbf{v}, \tilde{\mathbf{P}}_c \mathbf{v} \rangle$ so that $\tilde{\mathbf{P}}_c = \begin{bmatrix} \mathbf{P}_c & 0 \\ 0 & \mathbb{I} \end{bmatrix}$.

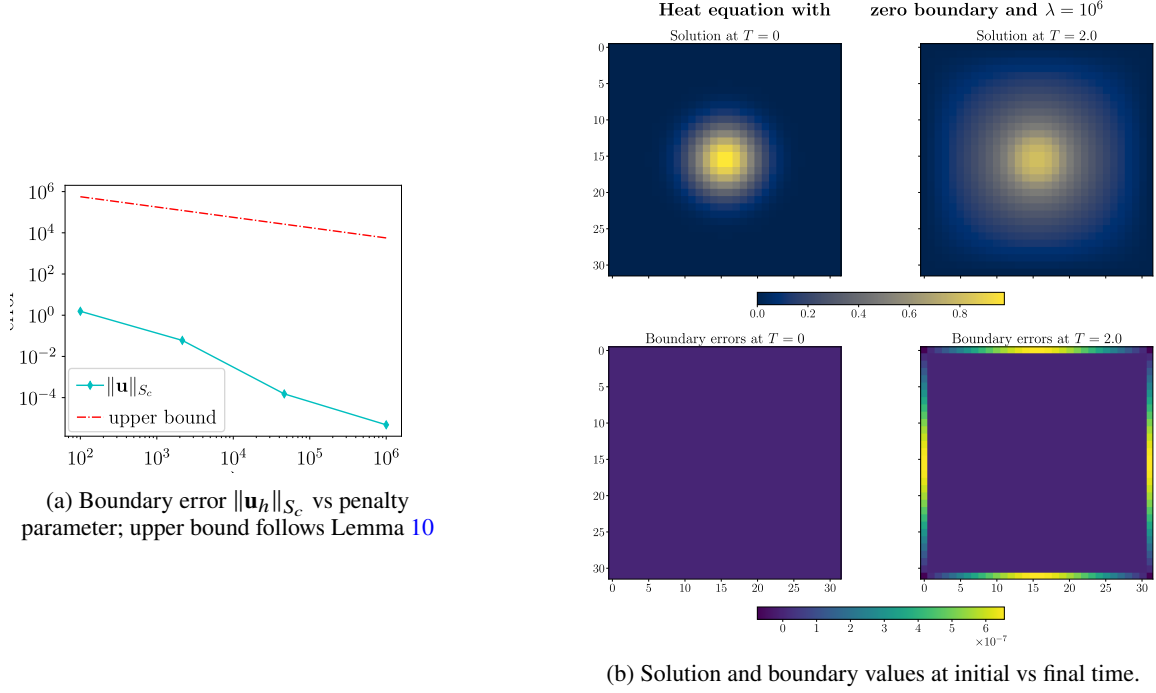


FIG. 5: Numerical simulations of heat equation with $\mathbf{P}_c^D \mathbf{u}_h = 0$, $D = 4$, $N = 2^5$, $t = 1$, and $\Delta t = 10^{-5}$. The boundary is defined as the outer grid points ('wall').

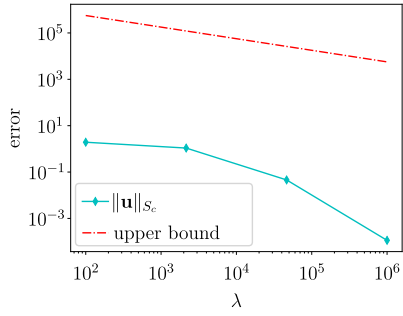
Recall that we generally assumed that $\text{Re}(A) \leq 0$. Looking for the eigenvalues χ of the discrete operator,

$$\begin{bmatrix} 0 & \mathbb{I} \\ c^2 \mathbf{L}_h & 0 \end{bmatrix} \begin{bmatrix} \mathbf{u} \\ \mathbf{w} \end{bmatrix} = \chi \begin{bmatrix} \mathbf{u} \\ \mathbf{w} \end{bmatrix}, \quad (138)$$

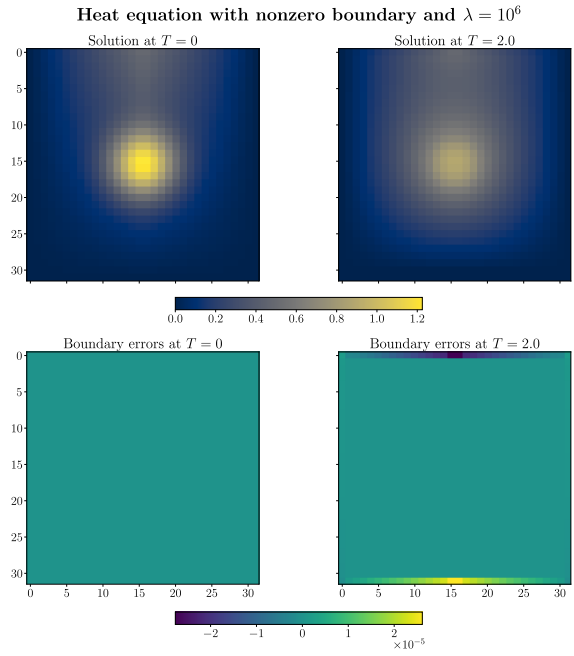
we obtain that $\mathbf{w} = \chi \mathbf{u}$ and $c^2 \mathbf{L}_h \mathbf{u} = \chi \mathbf{w}$. Therefore, $\mathbf{L}_h \mathbf{u} = (\chi/c)^2 \mathbf{u}$. Both the abstract Laplacian Δ as well as for the discretized $\mathbf{L}_h^{\text{per}}$ with periodic boundary conditions have a spectrum (contained in) $(-\infty, 0]$. Therefore, χ as in Eq. (138) is purely imaginary and $\text{Re} \left(\begin{bmatrix} 0 & \mathbb{I} \\ c^2 \mathbf{L}_h & 0 \end{bmatrix} \right) = 0$. Thus, as long as there is no interaction with an environment (i.e., periodic boundary conditions), there is no dissipation. The initial condition is given by

$$\begin{bmatrix} \mathbf{v}_0 \\ \mathbf{w}_0 \end{bmatrix} = \begin{bmatrix} 0.001 \sin(\mathbf{x}) \sin(\mathbf{y}) \\ 0.01 \cos(\mathbf{x}) \cos(\mathbf{y}) \end{bmatrix} \text{ if } \mathbf{x}^2 + \mathbf{y}^2 \leq 0.1, \text{ else } 0. \quad (139)$$

The simulation results are shown in Fig. 9.

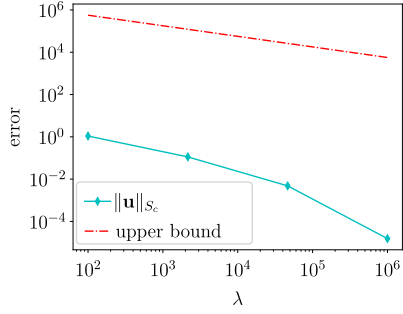


(a) Boundary error $\|\mathbf{u}_h\|_{S_c}$ for $N = 2^5$, $\Delta t = 10^{-5}$, $D = 4$ and boundary along the four walls upper bound follows Lemma 10.

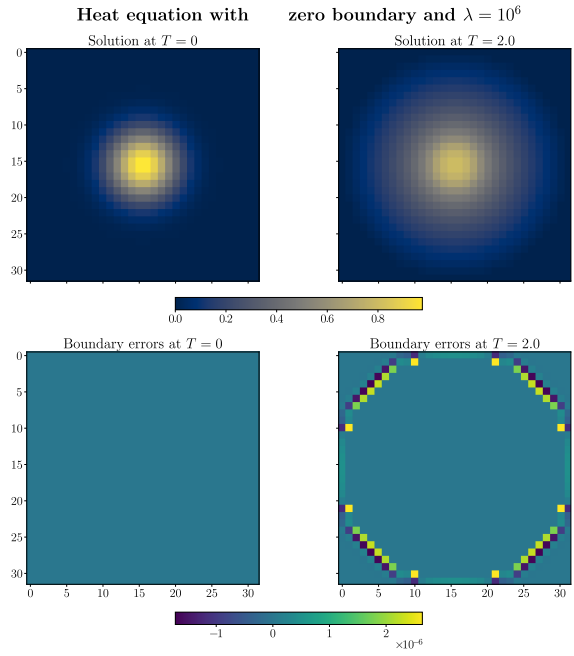


(b) Solution and boundary values at initial vs final time.

FIG. 6: Numerical simulations of heat equation with $\mathbf{P}_c^D \mathbf{u}_h = \mathbf{g}$ from Eq. (135), $D = 4$, $N = 2^5$, $t = 1$, and $\Delta t = 10^{-5}$. The boundary is defined to be the outer grid points ('wall').

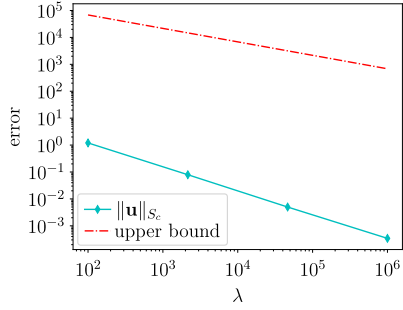


(a) Boundary error $\|\mathbf{u}_h\|_{S_c}$ for $N = 2^5$, $\Delta t = 10^{-5}$, $D = 4$ and boundary along a circle boundary Lemma 9

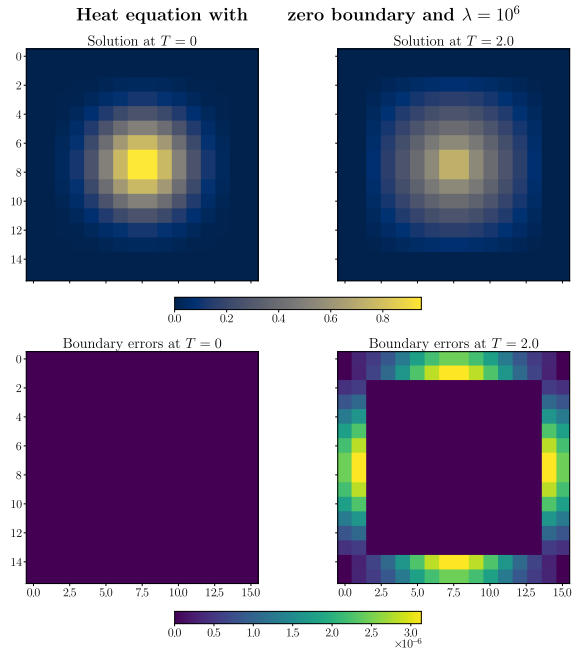


(b) Solution and boundary values at initial vs final time.

FIG. 7: Numerical simulation of heat equation with $\mathbf{P}_c^D \mathbf{u} = \mathbf{g}$ from Eq. (135), $D = 4$, $N = 2^5$, $t = 1$, and $\Delta t = 10^{-5}$. The boundary is defined to be on a circle of radius $\frac{1}{2}$.

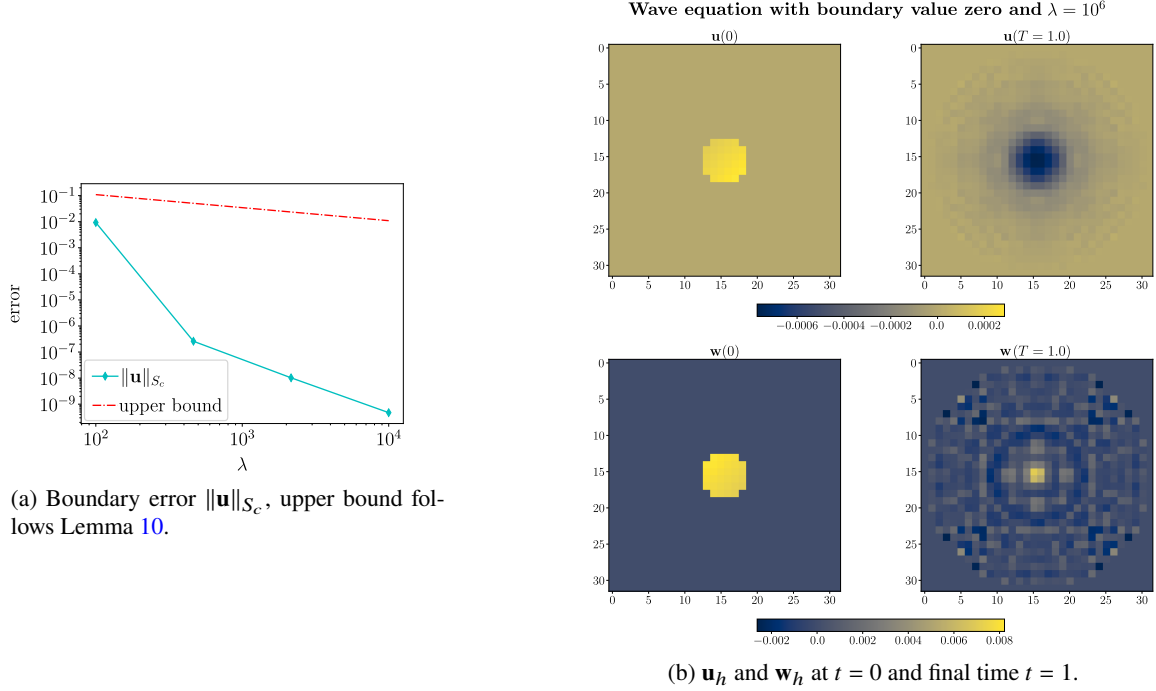


(a) Neumann boundary error $\|\mathbf{u}_h\|_{S_c}$ on wall boundary with respect to 'derivative constraint' \mathbf{P}_c^N



(b) Solution and boundary values at initial vs final time.

FIG. 8: Numerical simulations of heat equation with $\mathbf{P}_c^N \mathbf{u}_h = 0$ from Eq. (135), $D = 4$, $N = 2^4$, $t = 2$, and $\Delta t = 10^{-3}$. The constraint region is formed by the differences of the outer points ('wall') with their closest neighbours inwards. The corner points as well as one of the points next to the corner are skipped so that every inner point is only neighbour to at most one corner point.



(a) Boundary error $\|\mathbf{u}\|_{S_c}$, upper bound follows Lemma 10.

(b) \mathbf{u}_h and \mathbf{w}_h at $t = 0$ and final time $t = 1$.

FIG. 9: Numerical experiments for wave equation with zero boundary conditions at radius $\frac{1}{2}$. $N = 2^5$, $\Delta t = 10^{-4}$, $t = 1$, $c^2 = 1$.

3. Discussion

The results to our simulations are shown in Figs. 5 to 8 and Fig. 9. For all simulations, we can observe that the errors that we witness decrease quadratically, or slightly faster, with λ , i.e. $\|\mathbf{u}\|_{S_c} \in O(\lambda^{-1/2})$. This aligns very well with the upper bounds derived previously. The measured errors are several orders of magnitude smaller than the upper bounds that we derived. Even though the asymptotic behaviour seems to be well-captured in the bounds, they appear to be quite loose. This is not necessarily surprising as they rely on first-order perturbation theory, and within the regimes we studied numerically, the ratio of perturbation λ vs. ‘system energy’ $|\langle v, A_0 v \rangle|$ is not in a clearly perturbative regime yet.

The results in Fig. 6 validates the efficacy of the procedure of homogenizing/shifting the solution in order to solve for non-zero constraints. Moreover, we tested a circle boundary in Fig. 7 as a simple example for a non-trivial geometry. In particular, we notice that the solution does not penetrate further than two grid points into the constraint region within the chosen discretization. Additionally note that the constraint error decays faster in the case of the wave equation in Fig. 9; roughly linear if not including the first point at $\lambda = 100$. In the case of the heat equation, we observe that error performance is more reliable and more favourable in the case of derivative/Neumann constraints (Fig. 8). Therefore, using this setup in combination with ‘ghost points’ that store a desired value and are out of the range of the generator A_0 could be an interesting alternative to directly enforcing the value constraints.

IV. QUANTUM ALGORITHM VIA INTERACTION-PICTURE SIMULATION

Recall that the constrained ODEs we consider in this work have the form

$$\frac{d}{dt}v(t) = A_0(t)v(t) - i\lambda P_c v(t) + b(t) \equiv A(t)v(t) + b(t), \quad (140)$$

with initial data $v(t=0) = v_0$ and an orthogonal projection P_c . The general solution to this via the variation of parameters formula is

$$v(t) = \mathcal{T}e^{\int_0^t A(s)ds} v_0 + \int_0^t \mathcal{T}e^{\int_s^t A(s')ds'} b(s)ds. \quad (141)$$

There exist many quantum DE solvers that we could employ here; a common trait among all of them is that they depend (in the optimal case, linearly) on the block-encoding or subnormalization factor $\alpha_A \geq \sup_{0 \leq t \leq T} \|A(t)\|$, which itself, by Eq. (140), is linear in λ . As we saw before in Section II B, a necessary penalty factor is at least of the size $\lambda \gtrsim v_{\max}^2 \frac{\|A\|}{\epsilon}$, which would render implementations of the constraint projection impractical.

We can overcome this limitation by simulating Eq. (140) in the interaction frame of the projection. Then, the overhead in λ compared to unconstrained evolution is only logarithmic. The reason for this is that an interaction picture transformation is unitary, thereby $\alpha_{A_I} = \alpha_{A_0}$, where $A_I(t) = e^{-i\lambda P_c t} A_0(t) e^{i\lambda P_c t}$. The logarithmic overhead in the gate complexity is expected as the number of grid-points to simulate the interaction picture dynamics depends on the maximum frequency [46, Lemma 5], as $\|\partial_t A_I(t)\| = O(\lambda)$. A necessary condition of this to work efficiently is that the cost of the interaction picture transformation itself, i.e., $e^{-i\lambda P_c t}$, does not depend on λ . We know from Section II D that P_c is fast-forwardable by construction – which makes the setup suited for such an interaction picture implementation [46].

Therefore, let $v_I(t) = e^{i\lambda P_c t} v(t)$. A quick calculation shows that

$$\frac{d}{dt}e^{i\lambda P_c t} v(t) = e^{i\lambda P_c t} i\lambda P_c v(t) + e^{i\lambda P_c t} \frac{d}{dt}v(t) \quad (142)$$

$$\begin{aligned} &= e^{i\lambda P_c t} i\lambda P_c v(t) + e^{i\lambda P_c t} (A - i\lambda P_c) e^{-i\lambda P_c t} e^{i\lambda P_c t} v(t) \\ &= \underbrace{e^{i\lambda P_c t} A e^{-i\lambda P_c t}}_{=A_I(t)} e^{i\lambda P_c t} v(t) = A_I(t) v_I(t). \end{aligned} \quad (143)$$

This means that if we solve for

$$v_I(t) = \mathcal{T}e^{\int_0^t A_I(s)ds} v_0 + \int_0^t \mathcal{T}e^{\int_s^t A_I(s')ds'} b_I(s)ds =: S_I(t) v_I(0), \quad (144)$$

we can retrieve the sought-after solution $v(t)$ through implementing

$$\text{HamSim}(P_c, -\lambda) \underbrace{S_I(t)}_{\text{ODE solver}} \text{HamSim}(P_c, +\lambda). \quad (145)$$

A. Time Evolution by LCHS

We use the near-optimal Linear Combination of Hamiltonian simulations approach [11, 12] as a quantum ODE solver. For our purposes, this choice is more natural to tackle ODEs or discretized PDEs compared to Schrödingerisation [13, 55], has better complexity with respect to approximation error and time compared to time-marching approaches [7], and has better complexity with respect to state preparation compared to the linear-systems based approaches. The LCHS theorem in [11] allows to write the (time-ordered) exponential of a general matrix $A(t)$ as an integral of a unitary time evolution with a specific kernel function $\frac{f(k)}{1-ik}$, namely

$$\mathcal{T}e^{\int_0^t A(s)ds} = \int_{\mathbb{R}} \frac{f(k)}{1-ik} \mathcal{T}e^{\int_0^t i(kA_{\text{Re}}+A_{\text{Im}})(s)ds} dk, \quad (146)$$

where the real and imaginary part of a matrix A respectively are

$$A_{\text{Re}} = \frac{A + A^\dagger}{2}, \quad A_{\text{Im}} = \frac{A - A^\dagger}{2i}. \quad (147)$$

Duhamel's formula gives an extension to particular solutions given a source term [11]. In our case, the ODE system is defined by the interaction picture matrix

$$A_I(t) = e^{i\lambda P_c t} (A_0) e^{-i\lambda P_c t} = e^{i\lambda P_c t} (A_{0,\text{Re}} + A_{0,\text{Im}}) e^{-i\lambda P_c t}. \quad (148)$$

We note that [10] provides an algorithm of LCHS with interaction picture, however in a different setting. In our case, the operator for the interaction frame itself is a Hamiltonian simulation and does not require treatment by the LCHS formula. Furthermore, in [10], the authors are using LCHS with the non-optimal kernel function from [12] which does not achieve high accuracy. Choosing $\lambda \in i\mathbb{R}$ would recover the approach in [10, Lemma 17] which could easily be extended to the higher-order quadratures and improved kernel function of [12]. However, this would lead to higher simulation cost as we would need to simulate the linear combination $e^{-|\lambda|P_c t \cdot k_j}$ for all $k_j = -K, \dots, K$ with $[-K, K]$ the discretization of the Fourier domain in the LCHS formula Eq. (146).

The solution of ODEs using LCHS requires access to a HAM-T oracle (Hermitian block-encoding access 'HAM' with a time parameter 'T') for $A_I(t)$ and a fast-forwarded Hamiltonian simulation $e^{-i\lambda t P_c}$. For completeness, we briefly recall the LCHS algorithm from [12] applied to $\mathcal{T}e^{\int_0^t A_I(s)ds}$. Given $k \in \mathbb{R}$, consider the Hamiltonian simulation integrand in (146),

$$U(k; t) = \mathcal{T}e^{i \int_0^t k A_{I,\text{Re}} + A_{I,\text{Im}} ds}. \quad (149)$$

This unitary satisfies

$$\frac{d}{dt} U(k; t) = i(k A_{I,\text{Re}}(t) + A_{I,\text{Im}}(t)) U(k; t), \quad U(k; 0) = \mathbb{I}, \quad (150)$$

where

$$A_{I,\text{Re}}(t) = e^{i\lambda P_c t} A_{0,\text{Re}}(t) e^{-i\lambda P_c t}, \quad A_{I,\text{Im}}(t) = e^{i\lambda P_c t} A_{0,\text{Im}}(t) e^{-i\lambda P_c t}. \quad (151)$$

Simulating $U(k; t)$ is achieved by a truncated Dyson series algorithm [46]. Then, the integral over k in Eq. (146) is truncated to some finite interval $[-K; K]$ and evaluated with a higher-order quadrature; these steps amount to a linear combination the unitaries $U(k; t)$. These routines thus require HAM-T-access to

What this means is that we can trade off the error in overlap with success probability as we post-select on the \mathcal{P}_c -subspace, given by the 1-eigenvalue of $U_{\mathcal{P}_c}$. Then, this can be boosted using fixed-point amplitude amplification to cost $O(1/\varsigma)$ [56, Theorem 27]. \square

B. Complexity

In this section, we summarize the overall complexity. We first provide the final result and subsequently walk through the analysis.

1. Final Result

In Table Ia, we summarize the necessary strengths of the penalty through lower bounds on λ . Then, as we show in the subsequent section after stating the main complexity result, this allows us to derive the smoothness parameters Λ_I, Ξ_I as collected in Table Ib, which are part of the following theorem.

Theorem 17 (Complexity of linear constrained ODE solution using LCHS, adapted from Theorem 14 in [12]). *Consider the inhomogeneous ODE system in Problem 7. Suppose that $A_{I,\text{Re}}(\tau) \leq 0$ on $[0, t]$, and we are given the oracles described in Section IV A 1. Let $\|A(\tau)\| \leq \alpha_A$ and define $\Lambda_I = \sup_{p \geq 0, \tau \in [0, t]} \|(\partial_\tau)^p A_I(\tau)\|^{1/(p+1)}$*

TABLE I: Complexity-related parameters due to the constraint projection for different sets of assumptions

Result	Requirement on λ to achieve error $\varepsilon > 0$	Reformulation as $C \frac{v_{\max}^2 \ A_0\ }{\varepsilon} \cdot G$
Lemma 9	$2 \frac{v_{\max}^2 \ A_0\ }{\varepsilon}$	1
Lemma 10	$2 \frac{\ A_0\ }{\varepsilon} (v_{\max}^2 + 2v_{\max} t B + t^2 B^2)$	$1 + 2 \frac{tB}{v_{\max}} + \left(\frac{tB}{v_{\max}}\right)^2$
Lemma 11	$(1 + e^{2 \mu_{\max}(\text{Re}(A_0)) t}) \frac{v_{\max}^2 \ A_0\ }{\varepsilon}$	$1 + e^{2 \mu_{\max}(\text{Re}(A_0)) t}$
Lemma 12	$\frac{t v_{\max}^2}{\varepsilon} \max_{0 \leq t' \leq t} \ \{\mathcal{P}_c, A_0(t')\}_\sim\ $	$t \frac{\max_{0 \leq t' \leq t} \ \{\mathcal{P}_c, A_0(t')\}_\sim\ }{\ A_0\ }$
Lemma 13	$\frac{t^2}{2\varepsilon} (v_{\max}^2 + 2v_{\max} B_{L^1} + B_{L^1}^2) \max_{0 \leq t' \leq t} \ \{\mathcal{P}_c, A_0(t')\}_\sim\ $	$\frac{t^2}{2} \left(1 + 2 \frac{B_{L^1}}{v_{\max}} + \left(\frac{B_{L^1}}{v_{\max}}\right)^2\right) \frac{\max_{0 \leq t' \leq t} \ \{\mathcal{P}_c, A_0(t')\}_\sim\ }{\ A_0\ }$

(a) Asymptotic requirements on penalty factor per class of assumptions. Recall Lemma 9 assumes $\text{Re}(A_0) \leq 0, b = 0$, Lemma 10 has nonzero $b(t)$; Lemma 11 allows the spectrum of $\text{Re}(A_0)$ to be positive within finite time (with maximum eigenvalue μ_{\max}); Lemma 12 allows time-dependent $A_0(t)$ but no forcing and Lemma 13 allows time-dependency in $A_0(t)$ and non-zero $b(t)$.

Smoothness of dynamics Λ_I		Smoothness of forcing Ξ_I	
A_0 const.:	$\frac{v_{\max}^2 \ A_0\ }{\varepsilon}$	$b \neq 0$ const.:	$\frac{v_{\max}^2 \ A_0\ }{\varepsilon} \left(1 + 2 \frac{B}{v_{\max}} + \left(\frac{B}{v_{\max}}\right)^2\right)$
$A_0(t)$:	$\max_{0 \leq t' \leq t} \ A_0(t')\ _F \left(\frac{t v_{\max}^2}{\varepsilon} + \frac{ \mu_{\max}(\text{Im}(A_0(t))) }{ \mu_{\min}(\text{Re}(A_0(t))) }\right)$	$b(t)$:	$\frac{v_{\max}^2 \ A_0\ }{\varepsilon} \left(1 + 2 \frac{B}{v_{\max}} + \left(\frac{B}{v_{\max}}\right)^2\right) + \omega_{\max}$

(b) Asymptotic upper bounds for factors Λ_I, Ξ_I used in Theorem 17, with $\Gamma v_{\max}^2 \|A_0\|/\varepsilon = \Lambda_I + \Xi_I$. μ_{\max} and μ_{\min} denote the largest/smallest eigenvalues, and ω_{\max} the highest frequency component (in absolute value) of the forcing term that one aims to represent. Table entries as $O(\cdot)$.

and $\Xi_I = \sup_{p \geq 0, \tau \in [0, t]} \|(\partial_\tau)^p b_I(\tau)\|_{\frac{1}{p+1}}$. Then we can prepare an ε -approximation of the normalized solution $|v(t)\rangle$ with constant probability and a flag indicating success, by choosing

$$M \in O\left(\alpha_{At} \left(\log\left(\frac{\|v_0\| + B_{L^1}}{\|v(T)\|\varepsilon}\right)\right)^{1+1/\beta}\right), \quad M' \in \tilde{O}\left(t \frac{\Gamma \cdot v_{\max}^2 \|A_0\|}{\varepsilon} \left(\log\left(\frac{1 + B_{L^1}}{\|v(T)\|\varepsilon}\right)\right)^{1+1/\beta}\right), \quad (155)$$

where $\Gamma \frac{v_{\max}^2 \|A_0\|}{\varepsilon} = \Lambda_I + \Xi_I$. Different cases for Γ are summarized in Table [4b](#), and Λ_I, Ξ_I are at most $O\left(\frac{t^2}{\varepsilon}(v_{\max}^2 + B_{L^1}^2)\|A_0\|\right)$. Further, this requires

$$\tilde{O}\left(\frac{\|v(0)\| + B_{L^1}}{\|v(t)\|} \alpha_{A_0} t \left(\log\left(\frac{1}{\varepsilon}\right)\right)^{1+1/\beta}\right) \quad (156)$$

queries to the HAM-T oracle and

$$O\left(\frac{\|v(0)\| + B_{L^1}}{\|v(t)\|}\right) \quad (157)$$

queries to the state preparation oracles O_v and O_b .

Note that the penalty affects the complexity *only* through the number of discretization points necessary for the inhomogeneous solution, M' . Thereby, it does enter the final gate complexity and is not visible in the query complexity in Eq. (156).

2. Analysis of smoothness factors

Before we can do so, we look at the impact of the penalty projection. Intuitively, simulating $A_I(t)$ in the interaction picture with simulation parameter λt means that we simulate a highly oscillatory system, as λ is large. Therefore, this will have impact on the size of the time steps to avoid aliasing. To that end, consider the smoothness parameters $\Lambda_I \geq \sup_{p \geq 0, t \in [0, T]} \|(\partial_t)^p A_I(t)\|_{\frac{1}{p+1}}$, $\Xi_I \geq \sup_{p \geq 0, t \in [0, T]} \|(\partial_t)^p b_I(t)\|_{\frac{1}{p+1}}$ from [\[12\]](#), which need to be adjusted to the interaction picture simulation. Then, we obtain

$$(\partial_t)^p A_I(t) = (\partial_t)^p \left[e^{i\lambda P_c t} A(t) e^{-i\lambda P_c t} \right] \quad (158)$$

$$(\partial_t)^p b_I(t) = (\partial_t)^p \left[e^{-i\lambda P_c t} b(t) \right] \quad (159)$$

We can expand this as

$$\begin{aligned} (\partial_t)^p A_I(t) &= (\partial_t)^{p-1} \left((\dot{A}(t))_I + i\lambda [P_c, A_I(t)] \right) = (\partial_t)^{p-2} \left((i\lambda)^2 [P_c, [P_c, A_I]] + 2i\lambda [P_c, (\dot{A})_I] + (\ddot{A})_I \right) \\ &= \dots = \sum_{q \leq p} \binom{p}{q} \text{ad}_{i\lambda P_c}^q ((\partial_t^{p-q} A(t))_I) \end{aligned} \quad (160)$$

$$(\partial_t)^p b_I(t) = (\partial_t)^{p-1} (i\lambda P_c b_I(t) + (\dot{b})_I(t)) = \sum_{q \leq p} \binom{p}{q} (i\lambda)^q P_c (\partial_t^{p-q} b(t))_I \quad (161)$$

where we use the notation $\text{ad}_y(x) = [y, x]$, $\text{ad}_y^m(x) = \underbrace{[y, [y, \dots, [y, x]] \dots]}_{m \text{ times}} = \underbrace{\text{ad}_y \circ \dots \circ \text{ad}_y}_{m \text{ times}}(x)$ and ad^0 is identity. We motivate the derivation for the identities Eqs. (160) and (161) in Appendix B. Then, we get for the first quantity Λ_I ,

$$\Lambda_I = \sup_{p \geq 0, t \in [0, T]} \|(\partial_t)^p A_I(t)\|^{\frac{1}{p+1}} = \sup_{p \geq 0, t} \left\| \sum_{q \leq p} \binom{p}{q} \text{ad}_{i\mathbf{P}_c}^q ((\partial_t^{p-q} A(t))_I) \right\|^{1/p+1}. \quad (162)$$

Moving along, we look time-independent and time-dependent A separately. For the case of A being constant in time,

$$\Lambda_I = \sup_{p \geq 0, t} \lambda^{\frac{p}{p+1}} \|A\|^{\frac{1}{p+1}}. \quad (163)$$

Then, note from Lemma 9 that we can take from before that $\lambda = 2 \frac{v_{\max}^2 \|A\|}{\varepsilon}$ for target error $\varepsilon > 0$. This means that, up to the constant $2^{1-o(1)}$,

$$\Lambda_I \approx \sup_{p \geq 0} (v_{\max}^2)^{\frac{p}{p+1}} \|A\|^{\frac{p}{p+1}} \frac{1}{\varepsilon^{\frac{p}{p+1}}} = \frac{v_{\max}^{2(1-o(1))} \|A\|}{\varepsilon^{1-o(1)}}. \quad (164)$$

Next, we look at the situation when $A(t)$ is time-dependent, as treated in Lemma 12 and Lemma 13. We start this by simplifying the expression for Λ_I further using that the spectral norm stays invariant under interaction picture transformations and that $\|\mathbf{P}_c\| = 1$.

$$\begin{aligned} \sup_{p \geq 0, t} \left\| \sum_{q \leq p} \binom{p}{q} \text{ad}_{i\mathbf{P}_c}^q ((\partial_t^{p-q} A(t))_I) \right\|^{1/p+1} &= \sup_{p \geq 0, t} \left\| \sum_{q \leq p} \binom{p}{q} \lambda^q \text{ad}_{\mathbf{P}_c}^q (\partial_t^{p-q} A(t)) \right\|^{1/p+1} \\ &\leq \sup_{p \geq 0, t} \left(\sum_{q \leq p} \binom{p}{q} \lambda^q \|(\partial_t^{p-q} A(t))\| \right)^{1/p+1} \end{aligned} \quad (165)$$

We continue by first identifying that the spectral norm is upper-bounded by the Frobenius norm and then that Plancherel's theorem holds on matrix-valued functions under the Frobenius norm. Then, we can use that in Fourier-space, derivatives correspond to multiplication and we can introduce another bound with the maximum occurring frequency in A – this is valid as we assume that $A(t)$ is smooth and all its derivatives

are bounded.

$$\begin{aligned}
\text{Eq. (165)} &\leq \sup_{p \geq 0, t} \left(\sum_{q \leq p} \binom{p}{q} \lambda^q \|(\partial_t^{p-q} A(t))\|_F \right)^{1/p+1} \\
&= \sup_{p \geq 0, t} \left(\sum_{q \leq p} \binom{p}{q} \lambda^q \|\omega^{p-q} \hat{A}(\omega)\|_F \right)^{1/p+1} \\
&\leq \sup_{p \geq 0, t} \left(\sum_{q \leq p} \binom{p}{q} \lambda^q \omega_{\max}^{p-q} \|\hat{A}(\omega)\|_F \right)^{1/p+1} \\
&\leq \sup_{p \geq 0, t} \|A(t)\|_F^{1/p+1} \left(\sum_{q \leq p} \binom{p}{q} \lambda^q \omega_{\max}^{p-q} \right)^{1/p+1}
\end{aligned} \tag{166}$$

This expression already suggests, aligning with what one would expect, that the smoothness factor Λ_I is related to the maximum frequency of the constraint and the original dynamics. By the binomial theorem, we can conclude

$$\Lambda_I \lesssim \sup_{p \geq 0, t} \|A(t)\|_F^{1/p+1} (\lambda + \omega_{\max})^{\frac{p}{p+1}} = \max_{t'} \|A(t')\|_F^{o(1)} (\lambda + \omega_{\max})^{1-o(1)}. \tag{167}$$

Moreover, by Lemma 12, we have that we need $\lambda \approx \frac{tv_{\max}^2}{\varepsilon} \max_{t'} \|\mathbf{P}_c, A(t')\| \sim \frac{tv_{\max}^2}{\varepsilon} \max_{t'} \|A(t')\|$. Using this in our expression above,

$$\begin{aligned}
\sup_{p \geq 0, t} \|A(t)\|_F^{1/p+1} (\lambda + \omega_{\max})^{\frac{p}{p+1}} &\leq \sup_{p \geq 0, t} \|A(t)\|_F \left(\frac{tv_{\max}^2}{\varepsilon} \|A(t)\| + \frac{\omega_{\max}}{\|A(t)\|} \right)^{\frac{p}{p+1}} \\
&\leq \sup_{p \geq 0, t} \|A(t)\|_F \left(\frac{tv_{\max}^2}{\varepsilon} + \frac{|\mu_{\max}[\text{Im}(A)]|}{|\mu_{\min}[\text{Re}(A)]|} \right)^{\frac{p}{p+1}} \\
&= \|A(t)\|_F \left(\frac{tv_{\max}^2}{\varepsilon} + \frac{|\mu_{\max}[\text{Im}(A)]|}{|\mu_{\min}[\text{Re}(A)]|} \right)^{(1-o(1))}
\end{aligned} \tag{168}$$

With $\mu[\cdot]$, we denote eigenvalues. Thus, the ratio $\frac{|\mu_{\max}[\text{Im}(A(t))]|}{|\mu_{\min}[\text{Re}(A(t))]|}$ describes a notion of oscillation strength versus dissipation and is sometimes also called ‘stiffness ratio’ [57]. This term is a consequence of time-dependent simulation, whereas tv_{\max}^2/ε is due to the additional interaction picture simulation of the constraint.

The remaining term that needs to be discussed is the smoothness parameter due to the inhomogeneous solution, Ξ_I ,

$$\Xi_I = \sup_{p \geq 0, t} \|(\partial_t)^p b_I(t)\|_F^{\frac{1}{p+1}} = \sup_{p \geq 0, t} \left\| \sum_{q \leq p} \binom{p}{q} \lambda^q \mathbf{P}_c(\partial_t^{p-q} b(t))_I \right\|_F^{\frac{1}{p+1}} \tag{169}$$

Then, we consider the two cases whether b depends on time or not – for both, we have a time-independent

generator A . If $b(t)$ is constant, then

$$\Xi_I = \sup_{p \geq 0, t} \lambda^{\frac{p}{p+1}} \|b\|_{\ell_2}^{\frac{1}{p+1}} = \sup_{p \geq 0, t} \lambda^{\frac{p}{p+1}} B^{\frac{1}{p+1}}, \quad (170)$$

where in alignment with Lemma 10 we introduced $B = \max_{t'} \|b(t')\|_{\ell_2} = \|b\|_{\ell_2}$. Further, we have that Table Ia $\lambda = 2 \frac{\|A\|}{\varepsilon} (v_{\max}^2 + 2v_{\max}B + B^2)$. We can insert this into Eq. (170) to obtain, again up to a factor $2^{1-o(1)}$,

$$\Xi_I \simeq \frac{\|A\|^{1-o(1)}}{\varepsilon^{1-o(1)}} \left(v_{\max}^{2(1-o(1))} B^{o(1)} + v_{\max}^{1-o(1)} B + B^{1+o(1)} \right). \quad (171)$$

Now if we can say that B is within the convex hull of v_{\max} and $\|A\|$, then we know that Ξ_I is within the convex hull of $O(\frac{\|A\|}{\varepsilon} v_{\max}^2)$ and $O(\frac{\|A\|^2}{\varepsilon} v_{\max}^2)$. That is to say, we can simplify the expression for the complexity this way if the forcing term grows with the size of the initial data or the system matrix. For time-dependent $b(t)$, we can use a similar approach via the binomial theorem as previously for Λ_I . That is,

$$\begin{aligned} \sup_{p \geq 0, t} \left\| \sum_{q \leq p} \binom{p}{q} \lambda^q \mathbf{P}_c(\partial_t^{p-q} b(t))_I \right\|_{\ell_2}^{\frac{1}{p+1}} &\leq \sup_{p \geq 0, t} \left(\sum_{q \leq p} \binom{p}{q} \lambda^q \|\partial_t^{p-q} b(t)\|_{\ell_2} \right)^{\frac{1}{p+1}} \\ &= \sup_{p \geq 0, t} \left(\sum_{q \leq p} \binom{p}{q} \lambda^q \|\omega^{p-q} \hat{b}(\omega)\|_{\ell_2} \right)^{\frac{1}{p+1}} \\ &\leq \sup_{p \geq 0, t} B^{1/p+1} \left(\sum_{q \leq p} \binom{p}{q} \lambda^q \omega_{\max}^{p-q} \right)^{\frac{1}{p+1}} \\ &= \sup_{p \geq 0, t} B^{1/p+1} (\lambda + \omega_{\max})^{\frac{p}{p+1}}. \end{aligned} \quad (172)$$

Now we can again use substitute λ with $2 \frac{\|A\|}{\varepsilon} (v_{\max}^2 + 2v_{\max}B + B^2)$,

$$\begin{aligned} &\leq B \sup_{p \geq 0, t} \left(\frac{\|A\| v_{\max}^2}{\varepsilon} \left(\frac{1}{B} + \frac{2}{v_{\max}} + \frac{B}{v_{\max}^2} \right) + \frac{\omega_{\max}}{B} \right)^{p/p+1} \\ &= B \left(\frac{\|A\| v_{\max}^2}{\varepsilon} \left(\frac{1}{B} + \frac{2}{v_{\max}} + \frac{B}{v_{\max}^2} \right) + \frac{\omega_{\max}}{B} \right)^{1-o(1)} \\ &\leq \frac{\|A\| v_{\max}^2}{\varepsilon} \left(1 + 2 \frac{B}{v_{\max}} + \left(\frac{B}{v_{\max}} \right)^2 \right) + \omega_{\max}. \end{aligned} \quad (173)$$

What all of these expressions have in common is the following – similar to the pattern that we have some case-specific term, G times $v_{\max}^2 \|A\|/\varepsilon$ for λ as showcased in Table Ia: Both Λ_I, Ξ_I end up roughly linear in λ (more precisely, $\lambda^{1-o(1)}$), and sublinearly in $\|A\|$ through $\|A\|^{o(1)}$. Replacing λ with expressions from Table Ia, we can conclude that it is typically $O(\tilde{G} \cdot \frac{\|A\| v_{\max}^2}{\varepsilon})$, with \tilde{G} a modified case-specific factor as in Table Ib.

3. Implications for the solution of discretized PDEs with boundary conditions

Typically, when quantifying the cost of numerical methods, we are interested in the effect of the particular choice of discretization given a target error on the final cost (with a ‘finer’ discretization meaning more basis functions and thus more accurate representation). In our work, this ‘refinement’ is expressed by a number of grid points n^d . Upon choosing a suitable numerical method, there is also a relationship of approximation error with respect to the discretization. The example below estimates the complexity through the number of discretization points M' for the case of inhomogeneous solutions in Theorem 17

Example 2 (Overhead due to constraint for discrete heat equation). *As an example, we take the three-point finite difference stencil as was used in Section III. Then, the approximation error for the second derivative here goes as $O(n^{-d/2})$ [6, 58], which we can take as a rudimentary estimate for the time-evolved error.*

By Theorem 17, overhead due to the constraint arises from M' , through a gate complexity $O(\log(M'))$, and $M' \in \tilde{O}\left(\frac{t^3}{\varepsilon}(v_{\max}^2 + B_{L^1}^2)\|A_0\|\left(\log\left(\frac{1+B_{L^1}}{\|v(t)\|_{\ell_2}\varepsilon}\right)\right)^{1+1/\beta}\right)$, by Eq. (155) and Table Ib, where $v_{\max} = \|v(0)\|_{\ell_2}$ and $B_{L^1} = \|b\|_{L^1([0;t])}$. We know that the vector norms grow according to $O(n^{d/2})$ and $B_{L^1} \in O(tn^{d/2})$. Furthermore, the spectral norm of the discrete Laplacian with a three-point stencil follows $\|A_0\| = \|D\mathbf{L}_h\| \in O(n^{2d})$, taking the diffusion coefficient D as a constant. For the discrete Laplacian, this also means that $-\infty < \mu_{\min} \leq \mathbf{L}_h$, where $-\mu_{\min} \in O(n^{2d})$. By negative-semidefiniteness of \mathbf{L}_h , $\|v(t)\|_{\ell_2} \leq v_{\max} + B_{L^1} \in O(tn^{d/2})$. From Appendix D, Lemma 19, we have that $\frac{1}{\|v(t)\|_{\ell_2}^2} \leq e^{-D\mu_{\min}t} \frac{1}{2\|v(0)\|_{\ell_2}\|b\|_{L^1([0;t])}}$.

Then, together with $\varepsilon \in O(n^{-d/2})$, we get that

$$\begin{aligned} M' &\in \tilde{O}\left((t^3 n^{7d/2} + t^4 n^{3d}) \left(d \log\left(\frac{n^2(1+B_{L^1})}{\|v(0)\|_{\ell_2} B_{L^1}}\right)\right)^{1+1/\beta}\right) \\ &\in \tilde{O}\left((t^3 n^{7d/2} + t^4 n^{3d}) \left(d \log\left(\frac{n^2}{\|v(0)\|_{\ell_2}}\right)\right)^{1+1/\beta}\right), \end{aligned} \quad (174)$$

and note that $\text{const.} \lesssim \|v(0)\|_{\ell_2} \lesssim n^{d/2}$. Finally, the overhead in terms of gate complexity through $\log(M')$ becomes

$$\tilde{O}(d \log(n) + \log(t)), \quad (175)$$

if the discretization is chosen to have n^d grid-points. Moreover, note that an overhead using the penalty projections is only present for inhomogeneous solutions Eq. (155) when using the quadrature presented in [12]. However, we expect this to be the more likely case in practice, as non-zero boundary conditions expressed through the penalty method via value constraints lead to forcing terms in the ODE following the homogenization techniques outlined in Section II C. It is not immediately obvious whether introducing ghost points for the non-zero constraint values and using the derivative constraint projections (see Remark 5) would be more efficient here and we leave this for further study.

V. CONCLUSION AND OUTLOOK

We present a quantum algorithm that uses a penalty projection to enforce constraints such as boundary conditions in evolutionary discretized partial differential equations. Particularly, our approach enables

arbitrary constraints and boundary conditions for solving differential equations via the LCHS algorithm. The penalty projections have the advantage that they do not rely on adjustments of the block-encoding of the system matrix, which have the potential to make the algorithm more complicated when compiled to gates. Moreover, our approach is able to tackle a very general class of constraints and boundary conditions, as well as interface conditions. Assuming that the constraint projections are orthogonal, our approach only requires a few steps of fast-forwardable Hamiltonian simulation in addition to the usual ODE solution and interaction picture simulation of the constraint comes at a modest logarithmic overhead in the gate complexity when using the LCHS algorithm [11, 12] as ODE solver. The necessary penalty strength goes at most as $O\left(\frac{t^2}{\varepsilon}(\max_{t'} \|v(t')\|_{\ell_2}^2 + \|b\|_{L^1}^2)\right)$; for the example of the heat equation, we can show that the final gate complexity overhead grows at most as $\tilde{O}(d \log n + \log t)$ for n^d degrees of freedom. In a simple scenario of a uniform grid, directly enforcing constraints in the system matrix also attains a simple form for linear-systems based and time marching DE solvers. Yet, the algorithmic consequences, especially for LCHS, are not immediately obvious.

Looking ahead, it would be interesting to work out specific costings involving also constant factors of the presented method as compared to other approaches to enforce constraints presented in the literature. Beyond this, extensions to other constraints that admit decomposition into orthogonal subspaces, such as more general symmetries, seem like a straightforward extension. Less obvious but even more interesting are symmetries with non-local support or situations that lead to non-orthogonal projections, where it is not clear if fast-forwarding in the interaction frame is possible. One could envision this within the framework of scattering theory and build on, e.g., [59]. Furthermore, evaluating the performance on numerical examples of higher practical relevance would be an interesting subject of study. In particular, we found that our analytical error bounds were somewhat loose compared to the witnessed error in the simulation results of the heat and wave equations. Hence, one could look into exploring analytical methods that would enable tighter bounds, or perform a more thorough analysis of constant factors involved.

CODE AND DATA AVAILABILITY

For the simulations in Section III, we used Python with NumPy and SciPy as well as the `findiff` [60] package for finite difference discretization. The code used to generate the results below is available at <https://github.com/philipp-q/q-abs>.

ACKNOWLEDGEMENTS

PS thanks Lasse B. Kristensen and Mohsen Bagherimehrab for helpful discussions in early stages of the project. PS further thanks Stephen P. Jordan for useful comments through his thesis appraisal report. XYL and NW acknowledge the support from DOE, Office of Science, National Quantum Information Science Research Centers, Co-design Center for Quantum Advantage (C2QA) under Contract No. DE-SC0012704 (Basic Energy Sciences, PNNL FWP 76274). This research was also supported by Pacific Northwest National Laboratory’s Quantum Algorithms and Architecture for Domain Science (QuAADS) Laboratory Directed Research and Development (LDRD) Initiative. The Pacific Northwest National Laboratory is operated by Battelle for the U.S. Department of Energy under Contract DE-AC05-76RL01830. AAG thanks Anders G. Frøseth for his generous support as well as the NSERC Industrial Research Chair and the Canada 150 Research Chairs programs. This work is part of the University of Toronto’s Acceleration Consortium, which receives funding from the CFREF-2022-00042 Canada First Research Excellence Fund. This work is

supported by the Novo Nordisk Foundation, Grant number NNF22SA0081175, NNF Quantum Computing Programme. Resources used in preparing this research were provided, in part, by the Province of Ontario, the Government of Canada through CIFAR, and companies sponsoring the Vector Institute <https://vectorinstitute.ai/partnerships/current-partners/>. JPL acknowledges support from Tsinghua University and Beijing Institute of Mathematical Sciences and Applications.

-
- [1] D. W. Berry, High-order quantum algorithm for solving linear differential equations, *Journal of Physics A: Mathematical and Theoretical* **47**, 105301 (2014).
 - [2] D. W. Berry, A. M. Childs, A. Ostrander, and G. Wang, Quantum algorithm for linear differential equations with exponentially improved dependence on precision, *Communications in Mathematical Physics* **356**, 1057 (2017).
 - [3] D. W. Berry and P. Costa, Quantum algorithm for time-dependent differential equations using dyson series, *arXiv preprint arXiv:2212.03544* (2022).
 - [4] H. Krovi, Improved quantum algorithms for linear and nonlinear differential equations, *Quantum* **7**, 913 (2023).
 - [5] A. M. Childs and J.-P. Liu, Quantum spectral methods for differential equations, *Communications in Mathematical Physics* **375**, 1427–1457 (2020).
 - [6] A. M. Childs, J.-P. Liu, and A. Ostrander, High-precision quantum algorithms for partial differential equations, *Quantum* **5**, 574 (2021).
 - [7] D. Fang, L. Lin, and Y. Tong, Time-marching based quantum solvers for time-dependent linear differential equations, *Quantum* **7**, 955 (2023).
 - [8] S. S. Bharadwaj and K. R. Sreenivasan, Compact quantum algorithms for time-dependent differential equations, *arXiv preprint arXiv:2405.09767* (2024).
 - [9] D. An, J.-P. Liu, D. Wang, and Q. Zhao, A theory of quantum differential equation solvers: limitations and fast-forwarding, *arXiv preprint arXiv:2211.05246* (2022).
 - [10] D. An and K. Trivisa, Quantum algorithms for linear and non-linear fractional reaction-diffusion equations, *preprint* (2023), *arXiv:2310.18900* [quant-ph].
 - [11] D. An, J.-P. Liu, and L. Lin, Linear combination of hamiltonian simulation for non-unitary dynamics with optimal state preparation cost, *Physical Review Letters* **131**, 150603 (2023).
 - [12] D. An, A. M. Childs, and L. Lin, Quantum algorithm for linear non-unitary dynamics with near-optimal dependence on all parameters, *arXiv preprint arXiv:2312.03916* (2023).
 - [13] S. Jin, N. Liu, and Y. Yu, Quantum simulation of partial differential equations via schrödingerization, *Physical Review Letters* **133**, 230602 (2024).
 - [14] R. Lu, H.-E. Li, Z. Liu, and J.-P. Liu, Infinite-dimensional extension of the linear combination of hamiltonian simulation: Theorems and applications, *arXiv preprint arXiv:2502.19688* (2025).
 - [15] Z.-X. Shang, N. Guo, D. An, and Q. Zhao, Design nearly optimal quantum algorithm for linear differential equations via lindbladians, *arXiv preprint arXiv:2410.19628* (2024).
 - [16] Y. Cao, A. Papageorgiou, I. Petras, J. Traub, and S. Kais, Quantum algorithm and circuit design solving the poisson equation, *New Journal of Physics* **15**, 013021 (2013).
 - [17] M. Bagherimehrab, K. Nakaji, N. Wiebe, and A. Aspuru-Guzik, Fast quantum algorithm for differential equations, *arXiv preprint arXiv:2306.11802* (2023).
 - [18] I. Novikau and I. Joseph, Quantum algorithm for the advection-diffusion equation and the koopman-von neumann approach to nonlinear dynamical systems, *Computer Physics Communications* **309**, 109498 (2025).
 - [19] P. C. Costa, S. Jordan, and A. Ostrander, Quantum algorithm for simulating the wave equation, *Physical Review A* **99**, 012323 (2019).
 - [20] S. Jin, N. Liu, and C. Ma, Quantum simulation of maxwell’s equations via schrödingerisation, *ESAIM: Mathematical Modelling and Numerical Analysis* **58**, 1853 (2024).
 - [21] J.-P. Liu, H. Ø. Kolden, H. K. Krovi, N. F. Loureiro, K. Trivisa, and A. M. Childs, Efficient quantum algorithm for dissipative nonlinear differential equations, *Proceedings of the National Academy of Sciences* **118**, e2026805118 (2021).

- [22] J.-P. Liu, D. An, D. Fang, J. Wang, G. H. Low, and S. Jordan, Efficient quantum algorithm for nonlinear reaction–diffusion equations and energy estimation, *Communications in Mathematical Physics* **404**, 963 (2023).
- [23] P. Costa, P. Schleich, M. E. Morales, and D. W. Berry, Further improving quantum algorithms for nonlinear differential equations via higher-order methods and rescaling, *arXiv preprint arXiv:2312.09518* (2023).
- [24] X. Li, X. Yin, N. Wiebe, J. Chun, G. K. Schenter, M. S. Cheung, and J. Mülmenstädt, Potential quantum advantage for simulation of fluid dynamics, *Phys. Rev. Res.* **7**, 013036 (2025).
- [25] S. S. Bharadwaj and K. R. Sreenivasan, Towards simulating fluid flows with quantum computing, *Sādhana* **50**, 1 (2025).
- [26] J. Penuel, A. Katabarwa, P. D. Johnson, C. Farquhar, Y. Cao, and M. C. Garrett, Feasibility of accelerating incompressible computational fluid dynamics simulations with fault-tolerant quantum computers, *arXiv preprint arXiv:2406.06323* (2024).
- [27] I. Novikau, I. Dodin, and E. Startsev, Simulation of linear non-hermitian boundary-value problems with quantum singular-value transformation, *Physical Review Applied* **19** (2023).
- [28] S. Jin, X. Li, N. Liu, and Y. Yu, Quantum simulation for partial differential equations with physical boundary or interface conditions, *Journal of Computational Physics* **498**, 112707 (2024).
- [29] S. Jin, X. Li, N. Liu, and Y. Yu, Quantum simulation for quantum dynamics with artificial boundary conditions, *SIAM Journal on Scientific Computing* **46**, B403 (2024).
- [30] T. Kharazi, A. M. Alkadri, J.-P. Liu, K. K. Mandadapu, and K. B. Whaley, Explicit block encodings of boundary value problems for many-body elliptic operators, *Quantum* **9**, 1764 (2025).
- [31] M. Mangin-Brinet, J. Zhang, D. Lacroix, and E. A. R. Guzman, Efficient solution of the non-unitary time-dependent schrodinger equation on a quantum computer with complex absorbing potential, *Quantum* **8**, 1311 (2024).
- [32] D. G. Luenberger, Y. Ye, D. G. Luenberger, and Y. Ye, Penalty and barrier methods, *Linear and Nonlinear Programming*, 397 (2016).
- [33] J. Muga, J. Palao, B. Navarro, and I. Egusquiza, Complex absorbing potentials, *Physics Reports* **395**, 357 (2004).
- [34] M. Mangin-Brinet, J. Zhang, D. Lacroix, and E. A. Ruiz Guzman, Efficient solution of the non-unitary time-dependent Schrodinger equation on a quantum computer with complex absorbing potential, *Quantum* **8**, 1311 (2024).
- [35] S. V. Tsynkov, Artificial boundary conditions for the numerical simulation of unsteady acoustic waves, *Journal of Computational Physics* **189**, 626 (2003).
- [36] D. Burgarth, P. Facchi, H. Nakazato, S. Pascazio, and K. Yuasa, Generalized adiabatic theorem and strong-coupling limits, *Quantum* **3**, 152 (2019).
- [37] D. Burgarth, P. Facchi, G. Gramegna, and K. Yuasa, One bound to rule them all: from adiabatic to zeno, *Quantum* **6**, 737 (2022).
- [38] A. Van der Sluis, Perturbations of eigenvalues of non-normal matrices, *Communications of the ACM* **18**, 30 (1975).
- [39] A. B. Catli, S. Simon, and N. Wiebe, Exponentially better bounds for quantum optimization via dynamical simulation, *arXiv preprint arXiv:2502.04285* (2025).
- [40] R. Kubo, Statistical-mechanical theory of irreversible processes. i. general theory and simple applications to magnetic and conduction problems, *Journal of the physical society of Japan* **12**, 570 (1957).
- [41] D. Sticlet, B. Dóra, and C. P. Moca, Kubo formula for non-hermitian systems and tachyon optical conductivity, *Physical Review Letters* **128**, 016802 (2022).
- [42] K. T. Geier and P. Hauke, From non-hermitian linear response to dynamical correlations and fluctuation-dissipation relations in quantum many-body systems, *PRX Quantum* **3**, 030308 (2022).
- [43] L. Pan, X. Chen, Y. Chen, and H. Zhai, Non-hermitian linear response theory, *Nature Physics* **16**, 767 (2020).
- [44] W. Ames, *Numerical Methods for Partial Differential Equations*, Computer Science and Scientific Computing (Elsevier Science, 2014).
- [45] G. Evans, J. Blackledge, and P. Yardley, *Numerical Methods for Partial Differential Equations*, Springer Undergraduate Mathematics Series (Springer London, 2012).
- [46] G. H. Low and N. Wiebe, Hamiltonian simulation in the interaction picture, *arXiv preprint arXiv:1805.00675* (2018).
- [47] Y. Atia and D. Aharonov, Fast-forwarding of hamiltonians and exponentially precise measurements, *Nature communications* **8**, 1572 (2017).
- [48] C. Gidney, Halving the cost of quantum addition, *Quantum* **2**, 74 (2018).
- [49] S. Gu, R. D. Somma, and B. Şahinoğlu, Fast-forwarding quantum evolution, *Quantum* **5**, 577 (2021).

- [50] S. Cen and Q. Zhang, *Multiphysics Modeling: Numerical Methods and Engineering Applications* (Academic Press, 2015).
- [51] K. Gustafson and T. Abe, The third boundary condition—was it robin’s?, *Mathematical Intelligencer* **20** (1998).
- [52] N. Linden, A. Montanaro, and C. Shao, Quantum vs. classical algorithms for solving the heat equation, *Communications in Mathematical Physics* **395**, 601 (2022).
- [53] R. Babbush, D. W. Berry, R. Kothari, R. D. Somma, and N. Wiebe, Exponential quantum speedup in simulating coupled classical oscillators, *Physical Review X* **13**, 041041 (2023).
- [54] P. Bogacki and L. F. Shampine, A 3 (2) pair of runge-kutta formulas, *Applied Mathematics Letters* **2**, 321 (1989).
- [55] S. Jin, N. Liu, C. Ma, and Y. Yu, On the schrödingerization method for linear non-unitary dynamics with optimal dependence on matrix queries, *arXiv preprint arXiv:2505.00370* (2025).
- [56] A. Gilyén, Y. Su, G. H. Low, and N. Wiebe, Quantum singular value transformation and beyond: exponential improvements for quantum matrix arithmetics, in *Proceedings of the 51st Annual ACM SIGACT Symposium on Theory of Computing* (2019) pp. 193–204.
- [57] J. D. Lambert, *Numerical methods for ordinary differential systems: the initial value problem* (John Wiley & Sons, Inc., 1991).
- [58] I. D. Kivlichan, N. Wiebe, R. Babbush, and A. Aspuru-Guzik, Bounding the costs of quantum simulation of many-body physics in real space, *Journal of Physics A: Mathematical and Theoretical* **50**, 305301 (2017), publisher: {IOP} Publishing.
- [59] U. Riss and H.-D. Meyer, Calculation of resonance energies and widths using the complex absorbing potential method, *Journal of Physics B: Atomic, Molecular and Optical Physics* **26**, 4503 (1993).
- [60] M. Baer, *findiff software package* (2018), <https://github.com/maroba/findiff>.
- [61] G. Dattoli, A. Torre, and R. Mignani, Non-hermitian evolution of two-level quantum systems, *Physical Review A* **42**, 1467 (1990).
- [62] D. C. Brody, Biorthogonal quantum mechanics, *Journal of Physics A: Mathematical and Theoretical* **47**, 035305 (2013).
- [63] A. M. Childs, Y. Su, M. C. Tran, N. Wiebe, and S. Zhu, Theory of trotter error with commutator scaling, *Physical Review X* **11**, 011020 (2021).
- [64] G. H. Hardy, J. E. Littlewood, and G. Pólya, *Inequalities (Cambridge mathematical library)* (Cambridge university press, 1934).

Appendix A: Proof of Lemma 15

Lemma (Parametrized exponential of an orthogonal projection; Lemma 15 in main text). *Let P, Q be orthogonal projections on a vector space so that $P + Q = \mathbb{I}$. Then, for any $\xi \in \mathbb{C}$,*

$$e^{\xi P} = Q + e^{\xi} P. \quad (\text{A1})$$

For $\xi \in i\mathbb{R}$, we retrieve Hamiltonian simulation.

Proof. We start by using the Taylor series of the operator exponential,

$$\begin{aligned} e^{\xi P} &= \sum_{k \geq 0} \frac{\xi^k}{k!} (P)^k \\ &= \mathbb{I} + \sum_{k \geq 1} \frac{\xi^k}{k!} (P)^k \quad ; P^k = P \quad \forall k \geq 1 \\ &= \mathbb{I} \pm P + P \sum_{k \geq 1} \frac{\xi^k}{k!} \\ &= Q + e^{\xi} P. \end{aligned} \quad (\text{A2})$$

□

Appendix B: Derivatives for conjugated generators

Here we derive the identities in Eq. (161), recalling that

$$\begin{aligned} \text{ad}_y(x) &= [y, x] \\ \text{ad}_y^m(x) &= \underbrace{[y, [y, \dots, [y, x]] \dots]}_{m \text{ times}} = \underbrace{\text{ad}_y \circ \dots \circ \text{ad}_y}_{m \text{ times}}(x) \\ \text{ad}^0(x) &= x. \end{aligned} \quad (\text{B1})$$

Let the conjugated operator be

$$A_C(t) = e^{Bt} A(t) e^{-Bt}, \quad (\text{B2})$$

with $A(t)$ smooth in time $t \in \mathbb{R}$. In the main text, we use $B = iP_c$ and thus call this interaction picture $(\cdot)_I$. Similarly, $b_C(t) = e^{Bt} b(t)$ and smooth $b(t)$. We assume here that B is constant in time. Therefore, the final expressions rely on a conjugation operation T_t so that $T_t A(T_t)^{-1}$ satisfies $\partial_t T_t = B T_t$ and $[B, T_t] = 0$, which restricts us to e^{Bt} with constant B . Then, we consider an arbitrary p th, $p \in \mathbb{N}$, partial derivative with respect to time

$$(\partial_t)^p A_C(t) = (\partial_t)^{p-1} ((\dot{A}(t))_C + [B, A_C(t)]) = (\partial_t)^{p-2} ([B, [B, A_C]] + 2[B, (\dot{A})_C] + (\ddot{A})_C) = \dots$$

Using the ad-notation introduced above,

$$(\partial_t)^p A_C(t) = (\partial_t)^{p-1} ((\dot{A}(t))_C + \text{ad}_B(A_C(t))) = (\partial_t)^{p-2} \left(\text{ad}^2(A_C(t)) + 2\text{ad}_B((\dot{A})_C) + (\ddot{A})_C \right) = \dots$$

Then, as a direct consequence of the product rule of differentiation and the aforementioned condition that $\partial_t e^{Bt} = B e^{Bt} = e^{Bt} B$, we can recognize a binomial structure of

$$\partial_t^p (A_C(t)) = ((\partial_t + \text{ad}_B)^p (A(t)))_C, \quad p \in \mathbb{N}. \quad (\text{B3})$$

For binomials, we have the well-known identity that $(x + y)^p = \sum_{0 \leq q \leq p} \binom{p}{q} x^q y^{p-q}$, hence

$$((\partial_t + \text{ad}_B)^p (A(t)))_C = \left(\sum_{0 \leq q \leq p} \binom{p}{q} \text{ad}_B^q \partial_t^{(p-q)} A(t) \right)_C = \sum_{0 \leq q \leq p} \binom{p}{q} \text{ad}_B^q \left(\partial_t^{(p-q)} A(t) \right)_C \quad (\text{B4})$$

The same approach can be used for vectors $b(t)$, where the interaction picture rotation is only a left-multiplication by e^{Bt} rather than a conjugation. This means, simply replace $A(t)$ with $b(t)$ in Eq. (B4) and replace $\text{ad}_y^p(x)$ with left-multiplication instead of commutators, $y^p x$.

Appendix C: Proof of Proposition 6

Proposition 18 (Restatement of Proposition 6). *Let $A(t) = H(t) + \zeta V(t)$ be a perturbed dynamical generator with $\zeta \|V(t')\| \ll \|H(t')\|$ for any $t \geq t' \geq 0$ and $A(t), H(t), V(t)$ complex matrices. Let $v(t)$ be the solution to $\frac{d}{dt}v(t) = A(t)v(t) + b(t)$ with initial data $v(0)$. Further, suppose we are interested in measuring the expectation value of a matrix P . Then, the effect due to perturbation $\zeta V(t)$ on the expectation of P up to first order in the strength of the perturbation*

$$\langle P(t) \rangle - \langle P \rangle_0 = \zeta \int_0^t dt' \frac{\text{tr} \left[\left\{ P, \bar{V}(t, t') \sigma(t', t) \right\}_\sim \right]}{\text{tr} [\sigma(t, t)]} + O(\zeta^2) \quad (\text{C1})$$

where $\langle P(t) \rangle$ is the perturbed expectation and $\langle P \rangle_0$ is the expectation due to the unperturbed dynamics generated by $H(t)$. Further, there is the modified anticommutator $\{X, Y\}_\sim = XY + Y^\dagger X$, a density augmented by the forcing term $b(t)$ through $\sigma(t', t) = T_{t'}(v(0)\delta(t') + b(t'))(T_t(v(0)\delta(t) + b(t)))^\dagger$ where $T_t(u) = \int_0^t ds \mathcal{T} \exp\left(\int_s^t dt' H(t')\right)u(s)$ and $\bar{V}(t, t') = \int_{t'}^t d\tau V(\tau)$.

Proof. Given dynamics

$$\frac{d}{dt}v(t) = A(t)v(t) + b(t) = (H(t) + \zeta V(t))v(t) + b(t), \quad (\text{C2})$$

we seek to find a first-order estimate to the difference in an expectation of an operator P with respect to the perturbed evolution $v_{H+\zeta V}(t)$ compared to the unperturbed evolution $v_H(t)$:

$$\frac{\langle v_{H+\zeta V}(t), P v_{H+\zeta V}(t) \rangle - \langle v_H(t), P v_H(t) \rangle}{\langle v_H(t), v_H(t) \rangle} =: \langle P(t) \rangle - \langle P \rangle_0 = \delta \langle P(t) \rangle, \quad (\text{C3})$$

This covers, beyond non-Hermitian operators, also a time-dependency in the original dynamics and a forcing term in the differential equation and thus goes beyond formulas provided in [41, 42]. As a reference on non-Hermitian dynamics, e.g. see [61, 62]. We may express the solution, according to Eq. (57) in terms of homogeneous and particular solution as follows using Green's functions,

$$v(t) = v_h(t) + v_p(t) = (G \star v_0)(t) + (G \star b)(t) \quad (\text{C4})$$

where $v_0(t) = \delta(t)v(0)$ (where $\delta(t)$ is the delta distribution) and

$$(G \star x)(t) = (G \star x)(t, 0) = \int_0^t ds G(t, s)x(s). \quad (\text{C5})$$

Note that we restrict ourselves to finite-dimensional, matrix-values $A(t)$, and thus also $G(t, s)$. This means that all convolutions will go across the time degree of freedom and the space degree of freedom follows matrix-matrix and matrix-vector multiplication. Of course one could think of generalizing this approach to infinite-dimensional objects, which we leave up for further research. For time-propagation according to Eq. (C2), we can identify

$$G(t, s) = G_A(t, s) = \mathcal{T} e^{\int_s^t ds' A(s')}. \quad (\text{C6})$$

In the case of the homogeneous solution, the convolution simplifies to a matrix-vector product of the time-

ordered exponential with the initial vector, and similarly for a constant forcing term. The reason we choose this unconventional form for the homogeneous solution is that it allows us to treat the homogeneous $v_h(t)$ and particular solution $v_p(t)$ simultaneously. We denote $G = G_A$ with generator A , and G_H and G_V with the respective generators in the subscript. If we drop one of the time arguments, then $G(t) = G(t, 0)$.

The composition of multiple convolutions follows

$$(G_1 \star G_2 \star x)(t, 0) = \int_0^t dt_1 \int_0^{t_1} dt_2 G_1(t, t_1) G_2(t_1, t_2) x(t_2), \quad (\text{C7})$$

and similar for more than two kernel functions; this combination preserves time-ordering. To make notation simpler, let us introduce $w(t) = v_0(t) + b(t) = \delta(t)v(0) + b(t)$ to collect homogeneous and inhomogeneous terms.

In order to analyze perturbative problems, the notion of interaction picture is often convenient in physics to isolate the effects due to perturbation in the analysis – this will also be the case here. Initially, let us assume that $H(t) \neq H^\dagger(t)$. Then, we define T_t as evolution generated by $H(t)$ (‘forward’) and \bar{T}_{-t} is generated by $-H^\dagger(t)$ (‘backward’, defined on the adjoints $u^\dagger(t)$), so that $T_t(u) = (G_H \star u)(t)$ and $\bar{T}_{-t}(u^\dagger) = (u^\dagger \star G_{-H^\dagger})(t)$. While these are *not* unitary and $\{T_t\}_t, \{\bar{T}_t\}_t$ form separate dynamical semigroups (over the right and left half-line respectively), the inverse elements for $\{T_t\}$ are in the adjoint elements from $\{\bar{T}_{-t}\}$ and vice versa, i.e., $T_t \bar{T}_{-t}^\dagger = \bar{T}_{-t}^\dagger T_t = \bar{T}_{-t} T_t^\dagger = \mathbb{I}$. This is a consequence of bi-orthogonality of the bases of the non-Hermitian generator [61]. Then, T_t, \bar{T}_t give us a means to introduce a non-Hermitian interaction picture transformation similar to what was done in [41] where H was chosen to be constant in time; then, such an interaction picture transformation does not change the expectation based on the (not necessarily unique) definitions,

$$\begin{aligned} v_I(t) &:= \bar{T}_{-t}^\dagger v(t) = (G_{-H^\dagger}^\dagger \star v)(t) \\ v_I^\dagger(t) &:= v^\dagger(t) \bar{T}_{-t} = (v^\dagger \star G_{-H^\dagger})(t) \\ P_I(t) &:= T_t^\dagger P T_t. \end{aligned} \quad (\text{C8})$$

Intuitively, observables experience forward evolution and states undergo the backward evolution. We verify by inserting into the expectation,

$$\begin{aligned} \langle P(t) \rangle &:= \frac{\langle v(t), \mathbb{I} P \mathbb{I} v(t) \rangle}{\langle v(t), v(t) \rangle} = \frac{\langle v(t), \bar{T}_{-t} T_t^\dagger P T_t \bar{T}_{-t}^\dagger v(t) \rangle}{\langle v(t), v(t) \rangle} = \frac{\langle \bar{T}_{-t}^\dagger v(t), (T_t^\dagger P T_t) (\bar{T}_{-t}^\dagger v(t)) \rangle}{\langle v(t), v(t) \rangle} \\ &\equiv \frac{\langle v_I(t), P_I(t) v_I(t) \rangle}{\langle v(t), v(t) \rangle}. \end{aligned} \quad (\text{C9})$$

Notice that we need to be careful with the normalization term, as $\langle v(t), v(t) \rangle = \langle v(t), T_t \bar{T}_{-t}^\dagger v(t) \rangle \neq \langle v_I(t), v_I(t) \rangle$.

Now, Eq. (C9) gives us a good starting point for the perturbative analysis. We start by looking at the nominator. First, express v_I^\dagger, P_I, v_I up to first order in the perturbation, i.e., first order in ζ . Then, upon inserting this into Eq. (C9), we again continue by only keeping linear order. Finally, the denominator will receive similar treatment, to estimate impact of the perturbation onto the normalization.

We use notation $\mathcal{T} \exp\left(\int_0^\tau d\tau' A(\tau')\right) =: T_\tau[A]$, where we add the generator in square brackets. Then, our goal now is to simplify the evolutions $\bar{T}_{-t}^\dagger T_t[A] = (G_{-H^\dagger} \star G_A \star \delta)(t)$ that is used to express $v_I(t)$. Here it

proves useful to consider [63, Lemma A.2]. Given $A(\tau) = H(\tau) + V(\tau)$, it holds that

$$T_\tau[A] = T_\tau[H] T_\tau[T_\tau^\dagger[-H^\dagger] V T_\tau[H]], \quad (\text{C10})$$

since we recall from above that the inverse to $T_\tau[H]$ is $\bar{T}_{-\tau}^\dagger = T_\tau^\dagger[-H^\dagger]$. Using notation as before, $T_\tau = T_\tau[H]$ and $\bar{T}_{-\tau} = T_\tau[-H^\dagger]$ and using a ‘test function’ u , Eq. (C10) becomes

$$T_\tau[A] u = (G \star u)(\tau) = T_\tau T_\tau[\bar{T}_{-\tau}^\dagger V T_\tau] u = T_\tau T_\tau[V_I] u \quad (\text{C11})$$

Then,

$$\bar{T}_{-\tau}^\dagger T_\tau[A] = \underbrace{\bar{T}_{-\tau}^\dagger T_\tau T_\tau[V_I]}_{=I} = T_\tau[V_I] \quad (\text{C12})$$

and consequently $v_I(t) = (G_{V_I} \star w)(t)$. The expression for the adjoint element, $v_I^\dagger(t) = (w^\dagger \star G_{V_I}^\dagger)(t)$, follows immediately thanks to Eq. (C8). Furthermore,

$$G_{V_I}(t, s) = \mathcal{T} e^{\int_s^t d\tau \zeta V_I(\tau)}. \quad (\text{C13})$$

We continue by approximating this propagator to linear order in ζ by expanding the time-ordered exponential,

$$\begin{aligned} G_{V_I}(t, s) &= \sum_{n=0}^{\infty} \zeta^n \int_s^t d\tau_1 \int_s^{\tau_1} d\tau_2 \cdots \int_s^{\tau_{n-1}} d\tau_n V_I(\tau_1) V_I(\tau_2) \cdots V_I(\tau_n) \\ &= \delta(t-s) + \zeta \int_s^t d\tau_1 V_I(\tau_1) + O(\zeta^2). \end{aligned} \quad (\text{C14})$$

Moreover,

$$(G_{V_I} \star w)(t) = \int_0^t ds G_{V_I}(t, s) w(s) \approx \int_0^t d\tau_1 \left(\delta(t-\tau_1) + \zeta \int_{\tau_1}^t d\tau_2 V_I(\tau_2) \right) w(\tau_1) \quad (\text{C15})$$

$$= \underbrace{w(t)}_{=:w_0(t)} + \zeta \underbrace{\int_0^t d\tau_1 \int_{\tau_1}^t d\tau_2 V_I(\tau_2) w(\tau_1)}_{=: \zeta w_1(t)}. \quad (\text{C16})$$

We remember that $w(t) = v_0 \delta(t) + b(t)$. Now we can insert this in the expectation value $\langle v_I(t), P_I(t) v_I(t) \rangle$ as in Eq. (C9),

$$\begin{aligned} &\langle (G_{V_I} \star w)(t), P_I(t) (G_{V_I} \star w)(t) \rangle \stackrel{\text{Eq. (C16)}}{\approx} \langle w_0(t) + \zeta w_1(t), P_I(t) (w_0(t) + \zeta w_1(t)) \rangle \\ &= \underbrace{\langle w_0(t), P_I(t) w_0(t) \rangle}_{=:(\square)} + \zeta \underbrace{\langle w_0(t), P_I(t) w_1(t) \rangle + \langle w_1(t), P_I(t) w_0(t) \rangle}_{=:(\#)} + \zeta^2 \langle w_1(t), P_I(t) w_1(t) \rangle. \end{aligned} \quad (\text{C17})$$

Up to normalization, we identify the unperturbed expectation and recall that $T_t w_0(t) = (G_H \star w)(t)$ is the

unperturbed evolution,

$$\langle P \rangle_0 := \frac{\langle w_0(t), P_I(t) w_0(t) \rangle}{\langle (G_H \star w)(t), (G_H \star w)(t) \rangle} = \frac{\langle T_t w_0(t), P T_t w_0(t) \rangle}{\langle T_t w_0(t), T_t w_0(t) \rangle}, \quad (\square) = \langle P \rangle_0 \|T_t w_0(t)\|^2. \quad (\text{C18})$$

The linear-order terms lead to the following expression, where we use notation $\bar{V}_I(t, s) = \int_s^t d\tau V_I(\tau)$.

$$\begin{aligned} (\#) = & \zeta \left(\left\langle \int_0^t d\tau_1 \bar{V}_I(t, \tau_1) w(\tau_1), P_I(t) \int_0^t d\tau_2 \delta(t - \tau_2) w(\tau_2) \right\rangle \right. \\ & \left. + \left\langle \int_0^t d\tau_1 \delta(t - \tau_1) w(\tau_1), P_I(t) \int_0^t d\tau_2 \bar{V}_I(t, \tau_2) w(\tau_2) \right\rangle \right) \end{aligned} \quad (\text{C19})$$

The following relation will be convenient: $V_I(t) = \bar{T}_{-t}^\dagger V(t) T_t$. Consequently,

$$\begin{aligned} \bar{V}_I(t, s) &= \left(\int_s^t d\tau \bar{T}_{-\tau}^\dagger V(\tau) \right) T_\tau = \bar{T}_{-s}^\dagger \left(\int_0^{t-s} d\tau \bar{T}_{-\tau}^\dagger V(\tau + s) T_\tau \right) T_s \\ &= \bar{T}_{-s}^\dagger \left(\int_s^t d\tau \bar{T}_{-(\tau-s)}^\dagger V(\tau) T_{\tau-s} \right) T_s = \bar{T}_{-s}^\dagger \bar{V}(t, s) T_s \end{aligned} \quad (\text{C20})$$

Then, we may conclude that

$$\begin{aligned} (\#) &= \dots = \zeta \left(\int_0^t d\tau \left\langle w(\tau), \bar{V}_I^\dagger(t, \tau) T_t^\dagger P T_t w(\tau) \right\rangle + \int_0^t d\tau \left\langle w(t), T_t^\dagger P T_t \bar{V}_I(t, \tau) w(\tau) \right\rangle \right) \\ &= \zeta \left(\int_0^t d\tau \left\langle T_\tau w(\tau), \bar{V}^\dagger(t, \tau) T_{t-\tau}^\dagger P (T_t w(t)) \right\rangle + \left\langle T_t w(t), P T_{t-\tau} \bar{V}(t, \tau) (T_\tau w(\tau)) \right\rangle \right) \end{aligned} \quad (\text{C21})$$

Moving along, we define a ‘density’

$$v[A](t, \tau) := (T_t[A]v(t)) (T_\tau[A]v(\tau))^\dagger. \quad (\text{C22})$$

If we omit the generator in square brackets of $v[H] = v$, we assume the unperturbed evolution through $H(t)$. That means that Eq. (C21) becomes

$$\begin{aligned} & \zeta \int_0^t d\tau \text{tr} \left[v(\tau, t)^\dagger \bar{V}^\dagger(t, \tau) T_{t-\tau}^\dagger P + P T_{t-\tau} \bar{V}(t, \tau) v(\tau, t) \right] \\ &= \zeta \int_0^t d\tau \text{tr} \left[\left\{ P, T_{t-\tau} \bar{V}(t, \tau) v(\tau, t) \right\}_\sim \right] =: \zeta \mathbb{P}(t) \end{aligned} \quad (\text{C23})$$

with the modified anti-commutator $\{X, Y\}_\sim := XY + Y^\dagger X$.

Next, we consider the normalization term in Eq. (C9), up to first order. Here it also proves useful to use Eq. (C11) which implies that $v(t) = T_t v_I(t)$. Then,

$$\langle T_t v_I(t), T_t v_I(t) \rangle = \left\langle v_I(t), T_t^\dagger T_t v_I(t) \right\rangle \quad (\text{C24})$$

Thus, we can treat Eq. (C24) analogously to the nominator $\langle v_I(t), P_I(t) v_I(t) \rangle$ but replacing $P_I(t)$ with $T_t^\dagger T_t$, up to keeping in mind that we have to divide by this term:

$$\begin{aligned}
& \left\langle w_0(t) + \zeta w_1(t), T_t^\dagger T_t (w_0(t) + \zeta w_1(t)) \right\rangle \\
&= \left\langle w_0(t), T_t^\dagger T_t w_0(t) \right\rangle + \zeta \left(\left\langle w_1(t), T_t^\dagger T_t w_0(t) \right\rangle + \left\langle w_0(t), T_t^\dagger T_t w_1(t) \right\rangle \right) + O(\zeta^2) \\
&= \|T_t w_0(t)\|_{\ell_2}^2 \left(1 + \zeta \frac{\left\langle w_1(t), T_t^\dagger T_t w_0(t) \right\rangle + \left\langle w_0(t), T_t^\dagger T_t w_1(t) \right\rangle}{\|T_t w_0(t)\|_{\ell_2}^2} + O(\zeta^2) \right) \\
&= \|T_t w_0(t)\|_{\ell_2}^2 \left(1 + \zeta \frac{\mathbb{T}(t)}{\|T_t w_0(t)\|_{\ell_2}^2} + O(\zeta^2) \right)
\end{aligned} \tag{C25}$$

where $\mathbb{T}(t) = \int_0^t d\tau \operatorname{tr} \left[\left\{ \mathbb{I}, \bar{V}(t, \tau) \sigma(\tau, t) \right\}_\sim \right]$ by Eqs. (C19) and (C21) to (C23). To find the inverse of the parentheses term in Eq. (C25), consider the Taylor series of $\frac{1}{1+x}$ at $x = 0$ given by $\sum_{k=0}^{\infty} (-x)^k$. Then if we have small $x \ll 1$, we can use the approximation $\frac{1}{1+x} = 1 - x + O(x^2)$. This allows us to express the normalization factor in first order as

$$\frac{1}{\langle v(t), v(t) \rangle} = \frac{1}{\|T_t w_0(t)\|_{\ell_2}^2} \left(1 - \zeta \frac{\mathbb{T}(t)}{\|T_t w_0(t)\|_{\ell_2}^2} + O(\zeta^2) \right). \tag{C26}$$

The final step now is to assemble Eq. (C9) based on previous results,

$$\begin{aligned}
\langle P(t) \rangle &= \frac{\langle v_I(t), P_I(t) v_I(t) \rangle}{1} \cdot \frac{1}{\langle v(t), v(t) \rangle} \\
&= \left(\langle P \rangle_0 \cdot \|T_t w_0(t)\|^2 + \zeta \mathbb{P}(t) + O(\zeta^2) \right) \cdot \left(\frac{1}{\|T_t w_0(t)\|^2} \left(1 - \zeta \frac{\mathbb{T}(t)}{\|T_t w_0(t)\|^2} + O(\zeta^2) \right) \right) \\
&\approx \langle P \rangle_0 + \zeta \frac{\mathbb{P}(t)}{\|T_t w_0(t)\|_{\ell_2}^2} - \zeta \langle P \rangle_0 \mathbb{T}(t) + O(\zeta^2)
\end{aligned} \tag{C27}$$

And hence,

$$\langle P(t) \rangle - \langle P \rangle_0 = \zeta \frac{\mathbb{P}(t) - \langle P \rangle_0 \mathbb{T}(t) + O(\zeta)}{\|T_t w_0(t)\|^2} \tag{C28}$$

Let us continue by expanding the definitions of $\mathbb{P}(t)$, $\mathbb{W}(t)$,

$$\langle P(t) \rangle - \langle P \rangle_0 = \frac{\zeta}{\operatorname{tr}[v(t, t)]} \left(\int_0^t d\tau \operatorname{tr} \left[\left\{ (P - \langle P \rangle_0), \bar{V}(t, \tau) \sigma(\tau, t) \right\}_\sim \right] + O(\zeta) \right) \tag{C29}$$

Here, we can identify a transfer or response function $\chi(t, t')$ similar to [41, Eq. (1)] and [42, Eq. (2)]

$$\chi(t, t') = \mathbf{1}_{[t \geq t']} \frac{\operatorname{tr} \left[\left\{ (P - \langle P \rangle_0), \bar{V}(t, t') \sigma(t', t) \right\}_\sim \right] + O(\zeta)}{\operatorname{tr}[\sigma(t, t)]} \tag{C30}$$

so that $\delta\langle P(t) \rangle = \zeta \int_0^t dt' \chi(t, t')$. \square

Appendix D: A lower bound on the final solution norm for the discrete heat equation

Lemma 19. *Given $\frac{d}{dt}v(t) = D\mathbf{L}_h v(t) + b(t)$ with $v, b \in \mathbb{R}^{n^d}$ and $\mathbf{L}_h \in \mathbb{R}^{n^d \times n^d}$ a discrete Laplacian in periodic boundary conditions. Thus we also have that $\exists \mu_{\min} < 0$ so that $-\infty < \mu_{\min} \mathbb{I} \leq \mathbf{L}_h \leq 0$. Additionally, this means that $\|v(s)\|_{\ell_2} \leq \|v(0)\|_{\ell_2}$ for any $0 \leq s \leq t$. Furthermore, in this Lemma, we assume that $b(s) \geq 0$ for $0 \leq s \leq t$. Then,*

$$\|v(t)\|_{\ell_2}^2 \geq \|v(0)\|_{\ell_2}^2 \geq 2e^{D\mu_{\min}t} \|v(0)\|_{\ell_2} \|b\|_{L^1[0;t]} \quad (\text{D1})$$

Proof. By the governing equation, we have

$$\begin{aligned} \|v(t)\|_{\ell_2}^2 &= \left\| e^{D\mathbf{L}_h t} v(0) + \int_0^t ds e^{D\mathbf{L}_h s} b(s) \right\|_{\ell_2}^2 \\ &= \langle v(0), e^{2D\mathbf{L}_h t} v(0) \rangle + 2 \int_0^t ds \langle v(0), e^{D\mathbf{L}_h s} b(s) \rangle + \int_0^t ds \int_0^t ds' \langle b(s'), e^{D\mathbf{L}_h(s+s')} b(s) \rangle \\ &:= (\text{I}) + (\text{II}) + (\text{III}) \end{aligned} \quad (\text{D2})$$

We can obtain a lower bound using a reverse Cauchy-Schwartz-type inequality due to Pólya and Szegő [64, p. 62, §71], which says that for bounded vectors x, y with positive entries,

$$\langle x, y \rangle^2 \geq C \langle x, x \rangle \langle y, y \rangle \quad (\text{D3})$$

with a constant

$$C = \frac{1}{4} \left(\sqrt{\frac{\max\{x\} \max\{y\}}{\min\{x\} \min\{y\}}} + \sqrt{\frac{\min\{x\} \min\{y\}}{\max\{x\} \max\{y\}}} \right)^2. \quad (\text{D4})$$

For the case of the discretized heat equation here with the solution signifying temperature, the positivity assumption on $v(t)$ holds, for the forcing term we invoke a positivity assumption for the sake of this argument. This is physically reasonable when we think of a heat source. In the case of strong heat sinks, we may expect the solution to fully decay to zero (and not become negative to remain physical); we can ensure non-negativity by shifting the solution by $\|b\|_{L^1[0;t]}$. Then, applying the inequality on term (II),

$$\left\langle e^{D\mathbf{L}_h t} v(0), \int_0^t ds e^{D\mathbf{L}_h s} b(s) \right\rangle^2 \geq C \langle v(0), e^{2D\mathbf{L}_h t} v(0) \rangle \int_0^t ds \int_0^t ds' \langle b(s'), e^{D\mathbf{L}_h(s+s')} b(s) \rangle. \quad (\text{D5})$$

Using this expression in Eq. (D2),

$$\|v(t)\|_{\ell_2}^2 \geq (\text{I}) + C\sqrt{(\text{I})}\sqrt{(\text{III})} + (\text{III}) \quad (\text{D6})$$

In addition,

$$e^{\mu_{\min} t} \min_j [v(0)]_j \leq [e^{D\mathbf{L}_h t} v(0)]_j \leq \max_j [v(0)]_j \quad \forall j \in [n^d] \quad (\text{D7})$$

$$e^{\mu_{\min} t} \cdot t \min_{j, 0 \leq s \leq t} [b(s)]_j \leq \int_0^t ds e^{D\mathbf{L}_h s} b(s) \leq t \max_{j, 0 \leq s \leq t} [b(s)]_j \quad \forall j \in [n^d]. \quad (\text{D8})$$

For convenience, we define the amplification factor $Q := \frac{\max_j [v(0)]_j \max_{k,s} [b(s)]_k}{\min_j [v(0)]_j \min_{k,s} [b(s)]_k}$, noting that $Q \geq 1$, and obtain for the constant (where $\mu_{\min} < 0$)

$$C = \frac{1}{4} \left(\underbrace{e^{-\mu_{\min} t} \sqrt{Q}}_{>1} + \underbrace{e^{\mu_{\min} t} \sqrt{Q^{-1}}}_{<1} \right)^2 \geq \frac{e^{2\mu_{\min} t}}{4Q}. \quad (\text{D9})$$

Now,

$$\begin{aligned} \|v(t)\|_{\ell_2}^2 &\geq (\text{I}) + \sqrt{\frac{e^{2\mu_{\min} t}}{4Q}} (\text{I}) (\text{III}) + (\text{III}) \\ &\geq e^{2D\mu_{\min} t} \left(\|v_0\|_{\ell_2}^2 + \|b\|_{L^1[0;t]}^2 \right) + \sqrt{\frac{e^{2D\mu_{\min} t} \|v_0\|_{\ell_2}^2 \|b\|_{L^1[0;t]}^2}{4Q}} \\ &\geq e^{D\mu_{\min} t} \left(2 + \frac{1}{\sqrt{Q}} \right) \|v_0\|_{\ell_2} \|b\|_{L^1[0;t]} \end{aligned} \quad (\text{D10})$$

In the second inequality, we use the bounds $(\text{I}) \geq e^{2D\mu_{\min} t} \|v(0)\|_{\ell_2}^2$ and $(\text{III}) \geq e^{2D\mu_{\min} t} \|b\|_{L^1[0;t]}^2$. The third inequality follows from bounding the arithmetic with the geometric mean, $\frac{x+y}{2} \geq \sqrt{xy}$. Recall that $Q \geq 1$ to obtain

$$\|v(t)\|_{\ell_2}^2 \geq 2e^{D\mu_{\min} t} \|v(0)\|_{\ell_2} \|b\|_{L^1[0;t]}. \quad (\text{D11})$$

□